Active Distribution Network Operation Incorporating Distributed Generations and Compressed Air Energy Storage

by Mojtaba Jabbari Ghadi

Thesis submitted in fulfilment of the requirements for the degree of

Doctor of Philosophy

under the supervision of Li Li and Jiangfeng Zhang

University of Technology Sydney
Faculty of Engineering and Information Technology

October 2020

Faculty of Engineering and Information Technology
School of Electrical and Data Engineering

Active Distribution Network Operation Incorporating Distributed Generations and Compressed Air Energy Storage

Done by: Mojtaba Jabbari Ghadi

Email: Mojtaba.jabbarighadi@student.uts.edu.au

Supervisor: A/Prof. Li Li

E-mail: Li.Li@uts.edu.au

Co-supervisor: Dr. Jiangfeng Zhang

E-mail: Jiangfz@clemson.edu

Course code: C02018

Subject Number: Doctor of Philosophy (Ph.D.)

Dates: 10/04/2017 to 10/10/2020

University of Technology Sydney (UTS)
School of Electrical and Data Engineering,
P.O. Box 123, Broadway, Ultimo, N.S.W. 2007
Australia

Certificate of Original Authorship

I, *Mojtaba Jabbari Ghadi* declare that this thesis, is submitted in fulfilment of the requirements for the award of *PhD*, in the *SEDE/FEIT* at the University of Technology Sydney.

This thesis is wholly my own work unless otherwise referenced or acknowledged. In addition, I certify that all information sources and literature used are indicated in the thesis.

This document has not been submitted for qualifications at any other academic institution.

This research is supported by the Australian Government Research Training Program.

Signature of Student:

Mojtaba Jabbari Ghadi

Production Note:
Signature removed prior to publication.

Date: 27/07/2020

Acknowledgments

I would like to take this opportunity to thank the following people and organizations for their assistance and support during my candidature.

First, I would like to express my deep gratitude to my principal supervisor Dr. Li Li and my co-supervisor Dr. Jiangfeng Zhang for their guidance, encouragement, and belief in my abilities. Their constructive comments contributed significantly to the quality of this research.

I thank all my colleagues and friends, especially Amin Rajabi, Sahand Ghavidel, and Ali Azizivahed, with whom I have shared significant knowledge and experience during the course of my student life.

Finally, none of this would be made possible without the endless love and unconditional support of my wife and family.

Abstract

Restructuring of power systems, along with the integration of renewable energy resources in electricity networks, have transformed traditional power distribution networks (DNs) into new active distribution systems (ADSs). In addition, the rapid advancement of technology has enabled the bulk utilization of power generation units and energy storage (ES) systems in DNs. The next step in this trend is to decentralize ADSs to microgrids.

After presenting an introduction to the objectives and scope of the research in the first chapter, the second chapter aims to present a review of recent advancements in the development of ADSs. In this respect, the regulatory requirements and economic concepts, by which the traditional passive DNs have evolved into ADSs, are categorized and illustrated first. Then, the state-of-the-art of ADS formation is detailed based on the novel standpoint of grid operation factors that are involved in deregulated electricity markets at the distribution level. Additionally, this chapter presents a comprehensive review of recent advancements in the operation of ADSs. To be more specific, after some literature about the market participation of distribution system operator (DSO), distribution companies (DISCOs), and aggregated agents from economic perspectives, the impacts of energy storage systems (specifically, compressed air energy storage (CAES) and electric vehicle charging station (EVCS)) at the distribution level have been investigated. Then, technical factors suited for the secure operation of ADSs and their corresponding indices and required tools are studied.

In the third chapter, the application of CAES at the distribution level is investigated. This chapter presents the participation of an ADS equipped with a small-scale CAES (SCAES) in the day-ahead (DA) wholesale market. To make CAES applicable to DNs, the thermal-electrical setting design of the SCAES coupled with a packed-bed heat exchanger is adopted in the operation of the grid, where SCAES performs as ES for DNs to surpass existing deficiencies of battery banks. The

electrical/thermal conversion rate has been modeled for the SCAES operation. Moreover, the operation strategy of the SCAES is optimally coordinated with an electrical vehicle charging station (EVCS) as an alternative ES technology in deregulated DNs. To make EVCS simulation more realistic, the Gaussian Copula probability distribution function is used to model the behavior of the EVCS. The results obtained from different case studies confirm the value of SCAES as a reliable ES technology for DNs.

Chapter four proposes the application of SCAESs as a new potential ES technology in the daily operation of an ADS, to join the DSO for the participation in a day-ahead wholesale market. A two-agent modeling approach is formulated. The first agent is responsible for aggregating SCAES units and profit maximization of the aggregator based on the distribution local marginal price. The DSO, as the second agent, receives day-ahead scheduling from the independent SCAES aggregator and is responsible for the secure operation of the ADS utilizing solar and dispatchable distributed generations as well as purchasing power from the day-ahead wholesale market. Linear programming is used for the formulation and optimization of the SCAES aggregator, while a bi-objective optimization model (with the objectives of minimum operating cost as well as minimum power loss and emissions in different scenarios) is built for DSO scheduling.

Chapter five proposes a novel concept of mobile CAES in an electric DN to improve grid operation. The proposed configuration models transportable air storage tanks carrying stored energy among the locations motor-generators placed on some distribution nodes/buses. Employing several storage tanks, a higher dispatchability and storage capacity are obtained. To overcome routing challenges for trucks, using Google Maps Application Programming Interface, the configuration of the grid is mapped on the urban region of the city of Sydney, Australia, to accurately model distances between current and targeted locations, unavailability of tanks during traveling, route congestion, and fuel consumption. To solve the obtained CAES operation problem, a new heuristic mathematical method is proposed to

convert constraints of the mobile CAES (MCAES) model into feasible search spaces, which significantly improves the convergence quality and speed. Additionally, this method offers a technique for coding solutions to use the same solution vector for both commitment and dispatch of MCAES, which reduces the solution dimension and computational burden. Since the proposed solution method is applicable to both stationary and mobile CAESs, operating results for both cases are presented and compared. The methodology is applied to IEEE 136 bus DN in addition to IEEE 33-bus DN to demonstrate the competence of MCAES when dealing with larger-scale grids to efficiently assist the DN's operator in optimizing total operating profit, active power loss, energy not supplied (ENS), and voltage stability index of the grid. The generation of fuel-based generators is also optimized to maintain the secure operation of the grid.

Finally, the last chapter presents a summary of research done in this thesis along with future reserch plan.

Keywords:

Active distribution systems, Microgrids, Distributed energy resources, Energy storage systems, Electric vehicles, Network management, ADS planning, Distribution system operator, Distribution aggregator, Day-ahead wholesale market, Locational marginal price, Small-scale compressed air energy storage, mobile storage technology, grid operation.

Publications and Conference Contributions

The following publications are part of the thesis.

Journal publications

[1] Ghadi, M. Jabbari, et al. "A review on economic and technical operation of active distribution systems." Renewable and Sustainable Energy Reviews 104 (2019): 38-53.

[2] Ghadi, Mojtaba Jabbari, et al. "From active distribution systems to decentralized microgrids: A review on regulations and planning approaches based on operational factors." Applied Energy, 253 (2019): 113543.

[3] Ghadi, Mojtaba Jabbari, et al. "Day-Ahead Market Participation of an Active Distribution Network Equipped with Small-Scale Compressed Air Energy Storage Systems." IEEE Transactions on Smart Grid, 11, 04 (2020).

[4] Ghadi, Mojtaba Jabbari, et al. "Application of Small-Scale Compressed Air Energy Storage in the Daily Operation of an Active Distribution System." Energy (2021): 120961.

[5] Ghadi, Mojtaba Jabbari, et al. "Mobile Compressed Air Energy Storage for Active Distribution Systems." IEEE Transactions on Smart Grid [*Ready to submit*]

Table of contents

List of Tables

List of Figures

List of Abbreviations

Active distribution system planning	ADSP
Active distribution system	ADS
Advance metering infrastructure	AMI
Application Programming Interface	API
Compressed air energy storage	CAES
Copula distribution function	CDF
Day-ahead	DA
Demand response	DR
Distributed energy resource	DER
Distributed generation	DG
Distributed generation owner	DGO
Distribution company	DISCO
Distribution network	DN
Distribution system operator	DSO
Distribution locational marginal price	DLMP
Electric power system	EPS
Electric vehicle charging station	EVCS
Energy management system	EMS
Energy storage	ES
Energy not supplied	ENS
Finite step method	FDM
Geographic information system	GIS
Independent system operator	ISO
Loop power controller	LPC
Microgrid central controller	MGCC
Mobile CAES	MCAES
Momentary average interruption frequency index	MAIFI

On-load tap changer	OLTC
Packed bed heat-exchanger	PBHE
Photovoltaic	PV
Plug-in electric vehicle	PEV
Pumped-storage hydropower	PSH
Renewable energy sources	RESs
Small-scale CAES	SCAES
Soft open point	SOP
Static synchronous compensator	STATCOM
Static VAR compensator	SVC
Swarm robotics search & rescue	SRSR
System average interruption duration index	SAIDI
System average interruption frequency index	SAIFI
Transmission system operator	TSO
Transportable energy storage system	TESS
Wind turbine	WT

Chapter 1 Introduction

1.1 Background and research question

Traditional distribution networks (DNs) have been managed with specified management systems for many years. In traditional DNs, the main contents of planning and operation are mainly based on the grid reconfiguration, construction of new transmission lines and transformers, and also the allocation of reactive power sources [1, 2]. In traditional DNs, distribution system operators (DSOs) are responsible for employing operation methods to simultaneously improve the operating indices of the grid (e.g., active power losses and voltage profile) as well as minimizing the total cost.

However, the integration of distributed energy resources (DERs), as well as emerging new market concepts in the active distribution systems (ADSs), has significantly changed these principles in terms of both objective functions and implementation methods [3]. Environmental concerns besides the tendency for maximizing the profit of individual distribution companies have made the concept of ADS to be considered as an efficient approach for high penetration of DERs in DNs [4]. The concept of ADS encompawsses various aspects in which the capability of real-time monitoring of the network and the flexibility of DERs are of great importance to increase the hosting capacity of low-voltage grids [5, 6] for the deployment of renewable energy.

Restructuring of traditional DNs toward ADSs has provided some potential platforms for emergence and development of novel types of distribution-size energy storage (ES) technologies. Energy storage systems can help in creating a more resilient energy

infrastructure and decreasing the costs of utilities and consumers. CAES and electric vehicle charging stations (EVCS) are two potential energy storage technologies to maximally exploit renewable energy resources since they can compensate for the fluctuating nature of renewables [7]. Although difficulties associated with uncertainties of plug-in electric vehicles (PEVs) and the development of power-electronic inverters suitable for PEV batteries have made the advance of EVCS challenging, CAES technology benefits from low construction costs and longer life-cycle. Therefore, small-scale CAESs (SCAES) are growing rapidly for the improvement of the grid operating factors, tackling uncertainties of DERs, and participating in the wholesale, retail, and reserve markets.

Another potential benefit of ADS development is in the case of aggregated management of some parts of the grid, distributed generators, and energy storage units. Accordingly, in some countries, some aggregators in the form of distribution companies (DISCOs) have got the managing responsibility of a section of the grid by constructing a microgrid and have played more critical roles in energy markets. Subsequently, based on their own objectives, operation methods of a part of the grid owned by DISCO have also been changed. In this respect, some small-scale storage and power generating units may form an aggregator as well to maximize their own profit while benefiting a DSO to improve the grid operating factors. In fact, small-scale DERs or energy storages can participate in the retail or wholesale energy markets with the assistance of aggregators [8]. Besides, some bulk renewable producers may opt to participate in the wholesale market through the aggregators to enjoy the benefits of joining with storage units.

The concepts related to the reliability and resilience of DNs are from other operating factors that have emerged or been significantly changed after the development of ADSs. To

deal with such advances, novel concepts and tools have been developed during the recent decade. Mobile CAES technology is a novel and potential energy storage system which can significantly improve operating grid factors in terms of profit, active power losses, expected energy not supplied (ENS), and voltage stability, due to its high transportability and low construction costs.

In sum, this thesis has provided three novel concepts for distribution grids. The first novelty is in the case of small-scale CAESs is proposed in Chapter 3. As opposed to previous literature, this work has presented a model for CAESs incorporating their mechanical thermodynamics. In this respect, two new charging/discharging efficiencies are proposed for distribution-size CAESs. Then, an EVCS has been modeled, and its performances has been compared with those of the proposed CAES. On the other side, the involvement of different storages, including CAESs, in ADSs is increasing. The concept of aggregators for several small-scale CAESs considering their unique operating characteristics is another novel concept presented in Chapter 4. Even though this thesis demonstrates that stationary CAES units are significantly game-changing elements for the future of restructured ADSs, their abilities can be significantly improved by considering them as mobile units. For the first time, the new concept of mobile CAESs is modeled in Chapter 5 Overall, this thesis shows how small-scale CAESs in their different forms can improve the operating factors of ADSs.

1.2 Research objectives and scope

The aims and scopes of this thesis are as follows:

- A day-ahead market participation framework will be offered for ADS equipped with a SCAES and PEVs to maximize net profit while maintaining the secure

operation of the network.

- A coordinated strategy for the joint operation of EVCS and SCAES will be determined to optimally schedule sells/buys energy from/to the market, PEVs, and SCAES units, after getting power forecast from solar units to meet load demand and operating constraints.
- A model will be produced for the detailed electrical and thermodynamic models of SCAES to assist DSO and DISCOs to reach a more accurate model for the grid operation.
- A double agent aggregation model will be proposed to provide the maximum profit of day-ahead market participation for private SCAES owners based on the locational marginal price received from the DSO.
- A novel concept is formulated for the modeling of mobile CAESs, which have capabilities of improving operating profit, reliability and resilience factors, power loss reduction, and voltage profile improvements.

1.3 Dataset

In this thesis, the preliminary intention was to utilize the data of the Australian electricity market. However, the data related to distribution grids was not available. Therefore, the IEEE 33 bus and IEEE 136 bus are considered as the test systems in the case studies which have been used in numerous studies. The data related to the generation of solar units and the price of energy in the day-ahead wholesale market are based on the dataset provided by the Australian energy market operator [9]. The price of diesel fuel and the fuel consumption of rigid trucks carrying mobile air storage tanks are assumed based on the Survey of Motor

Vehicle Use, Australia [10]. Additionally, the actual distances between buses for the modeling of mobile storage units are calculated using the Google Maps Application Programming Interface (API).

1.4 Contributions and organization of the thesis

1.4.1 Intellectual contributions

The key contributions of this thesis can be summarized as follows:

- In the first study, a new outline for the participation of a DSO equipped with a SCAES in the day-ahead market is proposed. Then, a coordinated strategy for the joint operation of SCAES and EVCS is proposed. DSO, as the owner of ADS, is responsible for the scheduling of PEVs and SCAES, and transactions with day-ahead market using forecast data of solar distributed generators load demand while considering operating constraints. The proposed CAES model is specifically designed to be suitable for the distribution grids where SCAES is equipped with a packed-bed heat exchanger to increase efficiency and reduce the size of the on-land reservoir tank. Considering the thermal modeling of SCAES is different from the large-scale CAES in the sense of efficiency, thermal modeling of heat exchanger unit, and loss destruction during compression and expansion procedures, this study evaluates actual thermal-electrical conversion rate for SCAES for DN applications based on several thermodynamic simulations. In the case of EVCS, highly uncertain behaviors of PEVs are modeled using the Gaussian copula distribution function (CDF) when EVCS is optimally matched with SCAES as a potential alternative ES in DN.
- The next study focuses on the aggregation of storage units at the distribution level.

The aggregation of privately owned SCAES units is a new concept presented in this thesis, which makes secure participation of distribution-size energy storage units in the different markets possible. In this respect, a two-agent policy applicable to restructured distribution power markets is proposed for the daily operation of the ADS. The scheduling is optimized for the profit maximization of the SCAES aggregator based on the locational energy price received from the DSO. Then, the DSO schedules diesel generators and transactions in the day-ahead market to maximize its own profit on the other side while maintaining the security of the grid. A linearized model is developed for the profit maximization problem of the CAES aggregator, which is solved using a linear optimization toolbox. Employing a bi-objective solution approach, Pareto front solutions for simultaneous minimization of power loss and emissions, as well as maximizing net profit, are obtained in different scenarios.

- In the last chapter, a novel concept of mobile CAES (MCAES) is presented that is superior to the battery technology in terms of lifespan and capital costs. This type of mobile energy storage can pave the way for the widespread development and utilization of transportable storage units. In this regard, a new formulation well-matched to the projected framework is provided in which the number of low construction cost mobile air tanks is much higher than the number of motor-generators. Besides, a novel heuristic-based technique based on a forward-backward sweep scheme is proposed, which tackles deficiencies of traditional constraint handling by converting constraints related to MCAESs into feasible ranges. Hence, the convergence speed and quality of the algorithm is significantly increased. Besides, a new solution coding is defined in which a single matrix will represent both dispatch

and commitment matrices. As opposed to previous literature, instead of the mathematical modeling of the traveling approach of mobile using non-linear formulations, this study firstly maps the IEEE test systems on the map of Sydney. Then Google Maps Application Programming Interface (API) is employed to solve complications related to route modeling.

1.4.2 Thesis organization

The rest of the thesis is organized as follows. Chapter 2 reviews the background, literature, and concepts related to operation of ADSs. Chapter 3 studies day-ahead market participation of an ADS equipped with SCAES considering the charging/discharging thermodynamics of the storage unit. The cooperation of EVCS and CAES is also studied in this chapter to diminish uncertainties associated with PEVs. The joint operation of a CAES aggregator and a DSO for participation in the day-ahead electricity market is studied in Chapter 4. A multi-objective optimization-based approach is adopted to optimally schedule private CAES units and DSO owned diesel units at a double-agent restructured power market with high penetration of solar generations. Chapter 5 proposes a novel concept of mobile CAES for ADS as significantly efficient equipment for profit maximization, ENS and power loss minimization, and voltage stability improvement of the DNs. Finally, Chapter 6 concludes the thesis, along with suggestions for future works.

Chapter 2 Background and Literature Review

2.1 Active distribution systems (ADSs)

The integration of DERs into DNs and utilization of various types of energy storage technologies and responsive loads have led to the emergence of new grids, which are usually known as ADSs [11, 12]. As depicted in Fig. 2-1, the concept of ADSs encompasses various notions in which the capability of real-time monitoring of the network and employing the flexibility of DERs, to increase the hosting capacity of low-voltage grids, is of great importance.

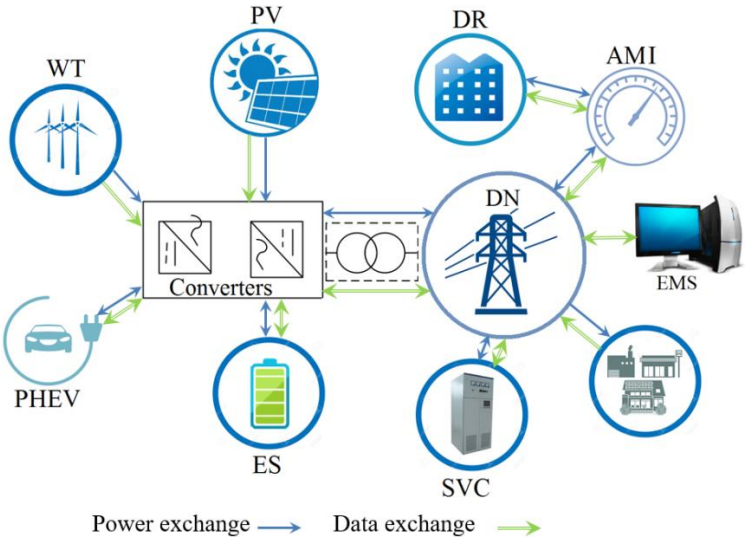

Fig. 2-1. Comprehensive structure of ADS

In this figure, the energy management system (EMS) provides DSO with a greater insight into different units of the distribution grid, and it has the ability to supervise and partially control distributed generations (DGs), energy storage, and demand response (DR) units as well as the network configuration. With possible applications in the state estimation, voltage stability performance indices, optimal topology change, fault calculation, contingency

analysis, load flow, and optimal power flow, EMS provides utilities with the opportunity for better visualization, operation, optimization, and maintenance of the network. However, in practice, the development of ADSs faces various challenges [13, 14]. The fluctuating nature of renewable units, the assumption of unidirectional power flow in the design of traditional DNs, and the need for a novel approach to ensure the expected profits for the providers and operators of various equipment and technologies like DERs, ESs, and demand response resources are among the main challenges. Therefore, extensive studies are needed to ensure the appropriate planning as well as the optimal operation of ADSs [15]. Besides, the high integration of renewable energy resources, which are involved with the development of novel components, new grid configurations, new strategies of grid operation, and new models for business and incentives, has given rise to different concerns about security, efficiency, and organization of ADSs [16]. To this end, considering the integration of different types of renewable energy sources (RESs) as well as challenges to the legacy system, microgrids have been emerged as effective solutions to improve the quality of energy service. The incorporation of microgrids is developing the interactions and couplings between DG sources and between suppliers and end-users as well [17].

Noteworthy, optimal operation of DNs plays a vital role for the appropriate integration of RESs, power provision to consumers as well as economic energy management. Power loss reduction, reliability and power quality improvement, competence for greater penetration of DGs, and energy consumers' satisfaction are among other advantages of the optimal operation of ADS. These facts confirm the value of the effective utilization of these facilities to support and improve ADSs operation [18]. In such an environment, the optimal operation of these new smart DNs has turned into a major concern for power system managers from different

technical and economic perspectives.

In this regard, [19] introduces ADS management as a key means for the smooth incorporation of DERs into power systems, and it considers DSOs as the agents for the integration of DERs into the European electricity market that can maximize the share of RESs in overall energy consumption. Moreover, [19] states that a major part of these resources is comprised of intermittent wind and solar, which are connected to medium and low voltage DNs instead of having large-scale wind or solar farms. Besides, [19] investigates the current situation of several European countries that have already been enjoying a high DER penetration like Spain, Germany, and Ireland. It also mentions some regions in these countries where the installed capacity of RESs connected to the DNs already exceeds the peak load-demand of the area. Finally, it summarizes the EURELECTRIC findings and recommendations of ADSs management. Another research in the case of ADSs operation is presented in [20], where potentials of DERs are referred to dispatchable units for effective scheduling in order to reach definite operating objectives, for example, voltage regulation and costs minimization. Accordingly, it highlights the necessity for DSOs to alter DNs from the traditional passive operation to an active operation approach. It also mentions that a challenging task is to formulate the operation characteristics of various types of DERs and incorporate them into the scheduling approaches of ADSs. This issue is extensively investigated in the study. After discussing the challenges of traditional DNs to accommodate the high penetration of DERs, [21] proposes ADSs as one of the alternative solutions based on advanced metering infrastructure and the application of information/communication technology. In [21], the effects of DERs on the traditional DNs are examined, and thus the inevitability of developing ADSs is clarified; the fundamental concept of ADSs, the need for

research, the different aspects of traditional DNs and ADSs, and corresponding study outcomes are introduced. Finally, some cost-effective enabling technologies which are for the transitions from the existing DNs to the ADS are discussed.

A common perspective in the review papers, especially in the context of ADSs planning, is to explore recent researches based on the effects of network components (i.e., generating, ES, and regulation units) on different objectives. However, referring to the time interval of their applications, the potential applications of these components will change significantly, and this has been neglected in most of the studies. In this regard, [22] firstly provides an overview of the formulation of ADSs operation, objectives, control architecture, and analysis of ADS components; then numerical and heuristic methods of solving the optimization problem of ADS operation as well as challenges and future research are detailed.

2.1.1 Technical/regulatory requirements of ADSs

The advent of ADS can provide several advantages for DN operators. However, DSOs have faced several problems by the emergence of ADSs, including volt/VAR variations and congestion management, increasing costs and complexity of maintenance scheduling, grid extension, reversed power flows and protection challenges, harmonics, and flickers of power electronic converters [23, 24]. Therefore, specific communication and technical requirements for the design of EMS of ADSs should be provided. In this regard, recent technical publications have addressed the development of EMS for ADSs. An EMS framework consisting of four layers, is presented in [25]. The first layer is responsible for gathering information from RESs, loads, and network parts. The second layer implements cloud-based computation and provides the data storage platform. The third layer performs the current state

estimation of the ADS, line currents, and voltages. The fourth layer provides a decision-making process with the purpose of improving the ratio of the asset utilization, reducing outage time, and providing high-reliability services. Authors in [26, 27] present new methods for real-time control of the ADS with explicit power set-points. In [26], two major EMS approaches, one based on centralized stochastic optimization control and the other utilizing multi-agent techniques, are investigated and then a composable method is proposed which overcomes the problems of previous EMS. A consensus-based distributed computational intelligence technique is utilized in [27] for the real-time optimal control in smart ADSs. The main assumption for forming a smart grid in this paper is that each DG or controllable load is a separate entity and can participate privately in this market.

Besides the technical aspects of EMS, some studies have focused on the regulation and market barriers for the formation of ADSs. In this regard, authors in [28] present the fundamentals of an adjustment approach to regulating the European electricity market. The proposed method calculates the maximum incentive for the DERs participating in the market as well as the maximum possible usage of local resources. Another attempt for providing an efficient concept of market regulation is presented in [29] with a case study of demand response participation in European distribution markets, where it firstly investigates the value of demand response for both the electric power markets in the higher level and operation of ADSs in the lower level to boost the economic efficiency of electricity markets across Europe, followed by the discussions on the market barriers of demand response implementations in ADSs. Valles et al. [30] provide a quantitative study on potential economic advantages of demand response by two case studies of rural and urban areas of Spain. Potential mechanisms that permit DSOs to incorporate demand response into procedures of DN planning are

investigated in this paper. Authors in [31] pay attention to some technical as well as managerial challenges for providing demand response from residential customers, PEVs, and other small-scale shift-able loads. After a brief review of the main concepts of demand response programs and demand response aggregation, a detailed review of various literature related to demand response aggregations is reported, and consequently, the most important challenges for procuring demand response aggregations are illustrated. Considering the fact that procuring the demand response from residential households is much more complicated in comparison with industrial or commercial sectors, authors in [32] propose the use of proper clustering techniques to categorize different residential customers based on their daily consumption patterns into a limited number of clusters and then apply suitable demand response programs to each of them. Authors in [33] examine the aggregation of PEVs for offering energy and price bids in electricity markets. The problem is formulated as non-linear stochastic programming, and a risk-averse approach is selected by adding the conditional value at risk measure to the final formulation. A summary of technical and regulatory barriers and their corresponding solutions for the implementation of ADS are detailed in Table 2-1 [34].

2.1.2 Impacts of DERs and energy storages on ADS

The incorporation of new supply sources of electricity like small-scale DGs, wind-based generators [35, 36], solar power units [37, 38], and combined cooling, heat, and power in the power network affects various stakeholders and market participants, especially the operators and owners of the DG units, network companies (both transmission and distribution), and even end-users of the grid (including different types of consumers) [39]. In addition to

Table 2-1. Technical and regularity barriers of ADS development

Type	Barrier	Description
Regulatory	Transmission system operator (TSO)/DSO communications with DERs	As a regulatory option, distributed generation owners (DGOs) can choose to send their measurements to either DSO or TSO. It prevents the full access of DSO to generation measurements which are needed for the network state estimation.
	Inadequate regulations on DERs	DERs are not allowed to take part in ancillary service for voltage management. Regulations set a fixed power factor set-point for DER, which is not coordinated with the optimal grid operation.
	TSO control over DERs	DER should respond to instructions and set-points from TSO. As a consequence, the connected medium-voltage generators cannot be controlled by DSO.
Technical and economic	Voltage management by power electronic devices	Voltage control using power electronic devices is a relatively novel technology for DSO. Lack of experience imposes additional costs on DSO within the operation procedure.
	Lack of a uniform standardization	Due to embedding several communication standards, adding a new device (for example, smart secondary substations) may face several technical challenges.
	ICT dependence	New frameworks necessitate the development of telecommunication architectures, which are mostly expensive and complicated to implement.

economic aspects, there are a large number of situations in which DERs and energy storages have effects on the operation of the power grid. Therefore, some studies have presented the technical and economic impacts of the presence of DERs and energy storages in ADSs. In [40], a comprehensive list of new quantification indices (i.e., voltage quality, economics, and

host capacity) for ADSs is provided at the first step. Then, based on the presented indices, the system is analyzed employing time-series power flow with an interval of 10 minutes to evaluate the effects of the presence of DERs in ADS. In [41], the daily operation of low-voltage ADSs in renewable-based microgrids are analyzed.

As it can be seen in Fig. 2-2, a microgrid is a manifestation of a distinct energy system involving the DERs (including generating systems, storage, and demand management) and electrical/thermal loads with the capability of operating in grid-connected or islanded modes [42].

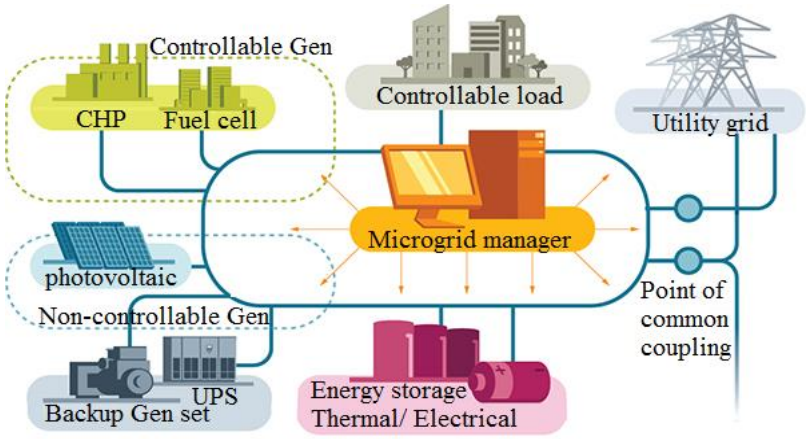

Fig. 2-2. A typical microgrid configuration [43]

The primary purpose for microgrid formation is to guarantee the provision of local, affordable, and reliable energy for both rural and urban consumers. Seasonal outputs of DERs and profiles of residential loads during a day are considered in [41] to find out the worst case scenarios for line losses and steady-state voltage variations. In [44], the environmental, technical, and economic impacts of DERs and energy storages on the network are presented after providing a detailed explanation about the technology of different types of DERs, ESs, and the mutual effects of energy storages on DERs using some case studies in the US.

Alongside with the aforementioned study on DERs and ESs, there are some studies that

present a deeper insight into the technology and application of energy storage systems in electric grids. Ref. [45] reviews the potential benefits of energy storage systems for ADSs. In addition, some key features for the allocation of these technologies based on four proposed classifications of energy storages (i.e., mechanical, electrical, thermal, and chemical) are described. In [46], the authors implement a conceptual cost-benefit analysis for the presence of compressed air energy storage (CAES) with a high penetration of DERs. Similar to the approach in [45], an extensive overview of various available types of energy storage systems in six categories is presented in [47]. Moreover, some specific energy storage potentials are proposed in [47] based on the operation value, technical aspect, and economic feature.

A detailed analysis of the application of energy storages to enhance the islanded operation of microgrids, i.e., when the microgrid is disconnected from the main grid due to the contingency, is presented in [48]. The required features of ESs, to be best suited for this mode of microgrid operation, and also some experiences from existing energy storages in real islanded microgrids are explained in this paper. Moreover, some specific communication and technical requirements for designing EMS of ADSs, including microgrids, are provided for DISCOs and also DSO. It should be mentioned that DSO can participate in the market like a DISCO if it possesses a part of or the entire DN. The structure of data and information exchange between DISCOs and microgrids and the corresponding requirements are shown in Fig. 2-3 [49]. As can be seen in Fig. 2-3, three main agents including DISCO, microgrids and ISO/TSO are involved in the operation of a DN in a restructured power market. From this figure, two different operating periods between a DISCO and microgrids can be observed.

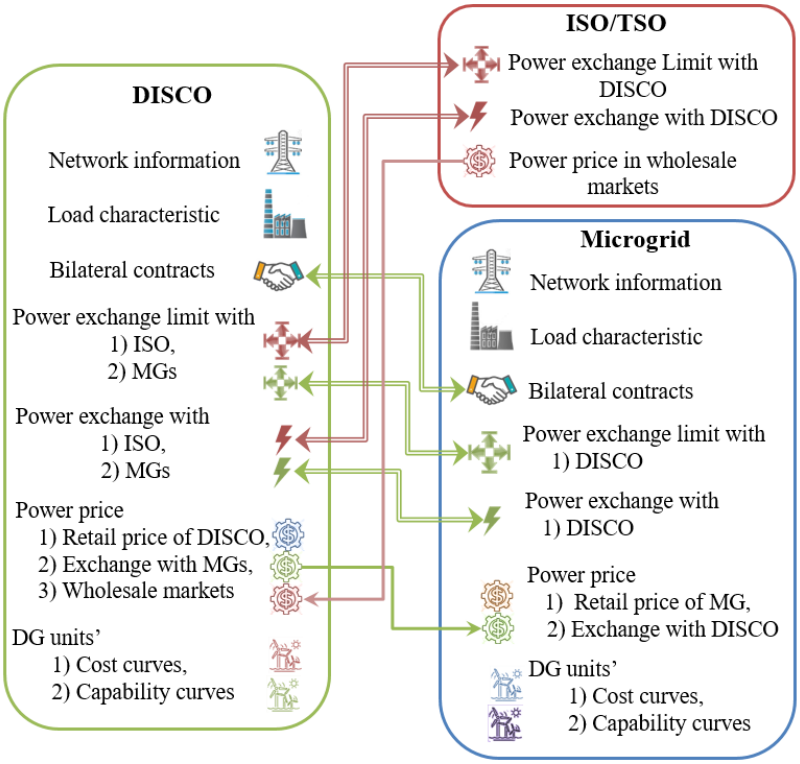

Fig. 2-3. Links between a DISCO and a microgrid in an ISO-supervised restructured power market

The first period happens when DISCO receives the operational and market data (e.g., energy clearing price of wholesale market and limitations of power exchange with the upstream grid) from ISO/TSO as the source of data exchange for microgrids. After a local process on the received information, DISCO determines operational and market parameters of DN (e.g., information of bilateral contracts and energy price for buying from /selling to the microgrids), and the corresponding information will be sent to the microgrids. The second period is when the received data from the Disco is processed in a microgrid, and the information on bilateral contracts and power exchange will be returned back to the DISCO or other microgrids. However, in both periods, some detailed data such as information related to loads, network, and generation units are not shared with other agents. When local distribution locational marginal price (DLMP) for different buses and microgrids are cleared, and

transactions between the DISCO and microgrids are finalized, power exchange and technical limitations are referred to as the upstream agents.

Combining two or more types of energy storage systems can create new operation features for ADSs and thus improve the network operation efficiency. Determination of the appropriate combination of ESs, as well as the optimal energy storage allocation, is investigated in [50]. The operational characteristics of ESs, such as capacity, maximum charge, and discharge rates, efficiency, self-discharge rate, cycle lifetime, energy density, power density, and power ramp time, are firstly ranked, and an optimization model is offered to create an optimal combination of ESs. Then this model, along with the data gathered from the smart meters of 5000 local demands, is used for the cost-benefit analysis of different storage configurations.

Along with the related literature on the concepts of planning, regulation, and operation of ADSs, some other publications provide valuable information for future directions. For example, an overview of the activities of the CIGRE C6.19 Working Group, focusing on the development and operation of ADSs, is presented in [51]. This group is involved in various tasks, including the literature review on the planning of ADSs, the study of the requirements for planning procedures, recognition of the suitable models for ADS planning in different time horizons, reliability models, and methods of ADS planning and expansion (for example, integration of energy storage systems and demand-side management).

Another piece of work on real practices, considering the sustainability assessment in power systems with ADSs, is provided in [52], where some indices for ADS sustainability improvement of microgrids and also several objectives for planning and management of ADSs based on the experiences of real projects are presented. In [53], three real DNs in Italy

as the representatives of urban, industrial, and rural sectors are examined as the ADS test systems. Based on the presented concepts, the process in which the passive DN is evolved into the active one is briefly described in Table 2-2 [54].

Table 2-2. Recent changes in different layers of DNs from passive to active

Feature	**Passive DN**	**ADS management**
Planning & Operation	1. Mostly based on fit and forget methodology. 2. Considering major reliability aspects at the planning stage. 3. No or limited tools for the active daily operation of the grid.	1. Based on the combination of operation and planning in most cases. 2. Capability for the active management of power loss and voltage profile. 3. Interactions of ADS with market participants as the result of flexible services for selling energy. 4. The necessity to have the active access for the management of DER 5. Capability to provide new ancillary services in commercial scales
Communication and information exchange	Limited exchange of information between TSO, DSO, and DERs	Real-time information sharing with standard interfaces
Network monitoring	1. Limited control and monitoring capabilities 2. Conventional supervisory control and data acquisition	1. Advanced monitoring, simulation, and control over low-voltage grids via telecommunication facilities 2. Advanced EMS through the integration of high-tech supervisory control and data acquisition
DERs participation	1. ESs, PEV, and demand response are not considered 2. Often, both the active and reactive power of DGs are not controlled.	Reaching a configurable setting for grid operation by involving DERs, into the network

Based on the literature, there are some existing studies on the CAES applications in DNs. However, the thermal modeling of SCAES is different from the large-scale CAES in the sense of efficiency, thermal modeling of the heat exchanger unit, and loss destruction during compression and expansion procedures. Such differences have not been extensively noted in

the literature, and most of the existing studies still use the conversion rates of large-scale CAESs for small-scale ones, which will cause non-negligible inaccuracies. Indeed, the scale of an energy storage based on mechanical procedures has a significant impact on the total efficiency of the unit. Therefore, there is a need for the development of a detailed SCAES model to cover both the thermal and electrical processes rather than the simple electrical-only formulations in the literature. However, some model simplifications are required to make the models more convenient and less complicated for future applications. Using some practical results of SCAES can be beneficial in this regard. Finally, some comparisons with other emerging types of charging units like EVCS can demonstrate the quality of the potential models.

2.1.3 Microgrid applications in ADSs

In recent years, research on resilient microgrid has gained substantial attention [55]. This is mainly due to the great interest of power system operators in the formation of microgrids to encourage the private sector investments, facilitate the integration of DERs into low-voltage DNs, and improve network reliability. A microgrid is a local energy grid with control capability, meaning that it can be disconnected from the main grid and operate autonomously. A microgrid is connected to the power grid at a point of common coupling. This assures that the voltage remains at the same level as the main grid unless there is some sort of problem on the grid or other reasons cause the microgrid to disconnect from the network. The disconnection of the microgrid from the main grid can happen automatically or manually. After the disconnection, the microgrid will function in the islanding operation mode. Considering the potential benefits of smart microgrids/grids, initiatives for the formation of

these grids are of high importance. Some of these aspects are shared with ADSP and, therefore, are not repeated here. In the following sections, the current practice of the utilization of microgrids is briefly reviewed, and consequently, the motives for moving toward microgrids are detailed.

a) Decentralized management of ADS

Microgrids can effectively help in the economic management of ADSs [56]. The high penetration of DGs in distribution systems, as the main challenge for DSOs, is addressed in [41]. This paper studies the daily operation of radial networks and analyses the effects of the intermittent nature of renewable generation resources and the existence of bi-directional power flow on the DN. As can be seen in Fig. 2-4, the DN is segmented into several microgrids. Most of these microgrids belong to DISCOs, and DSO only manages a limited number of them. In this settlement, each DISCO can participate in electricity markets, and the DSO maintains the security of the grid. This framework is also utilized in [49], in which the interactions of several connected microgrids are modeled to maximize the benefit of each

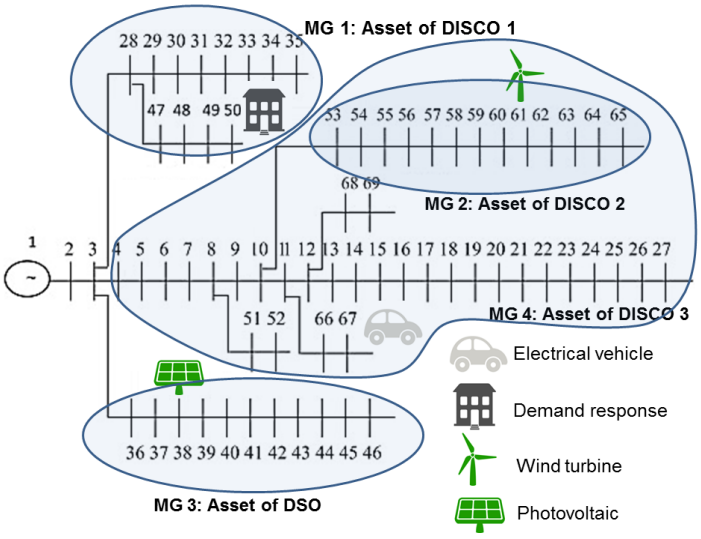

Fig. 2-4. Clustering of the network to several microgrids as DSO or DISCO assets

involved entity. The proposed approach, which is based on the "system of system" model, considers the DISCO and microgrids as individual agents that exchange information under a hierarchical optimization procedure.

Based on a microgrid management procedure, [42] proposes an EMS for ADSs. The remaining capacity of energy storage units and controllable DGs are utilized as an extended energy storage system, and an interactive energy game matrix is suggested to maximize the profit of each participant. Kargarian *et al.* [57] investigate the cooperation of ISO and DSOs in managing the generation and distribution systems simultaneously. A system of systems model is employed to ensure the secure operation of ISO and DISCOs and minimize the participants' costs. In the proposed model, thermal generating units and microgrids are scheduled from the ISO and DISCOs' perspectives, respectively.

As it can be inferred from the literature, storage units at the distribution level are conventionally operated as an asset of the DSO. However, this consideration is not valid anymore, along with restructuring distribution markets in which the private sector tends to invest and operate renewable sources and energy storage units based on financial factors. In such a situation, owners of these units aim to maximize their profit separate from the security of the grid operation. To this end, the formation of an aggregator for privately owned storage units in ADSs that can cooperate with DSO seems to be a potential concept for restructured DNs. In other words, storage aggregator and DSO should be modeled as two separate agents that aim to maximize their own objectives based on distribution power market structure while increasing the incorporation of private owners of storage units.

b) Microgrid for market participation

In the restructured power markets, microgrids have the option to participate in both markets of energy and ancillary services. However, the current available markets for microgrids are mostly in an oligopolistic form [58], which are structured by the participation of microgrid central controller (MGCC) agent, power system agent, consumption agents, and power production agents [59]. The role of MGCC is to control the microgrid as a market operator as well as system manager by matching the generation of DERs (production agents) to the load demand of consumers (consumption agents with shedable/non-shedable loads). The participation of load and DERs in the matching procedure is implemented through their relevant load and generator controllers. The power system agent only defines and publicizes buying/selling prices for all participants without any further involvement in the operation of the market. Finally, the energy provided by a microgrid could be traded in the market if the benefits obtained as the result of optimal energy management and a strategic DER deployment are considerable [60].

MGCC runs software platforms for automatic and intelligent management of both the system operation and market with the aim of satisfying the local heat/electricity load-demand. To reach this target, it determines an optimum allocation of its local generation units through the power exchange with or without the participation of the grid. Moreover, there is an autonomous control system in all DER units, which produces the optimum level of energy corresponding to an hourly given price in the market. This price is determined through MGCC by the system operator, market operator, or DSO. Therefore, the congestion issues of nearby feeders and microgrids during the peak hours, in which the energy price is high, or the islanding operation of microgrid is totally/partially mitigated through the flexible operation

of DER units. It is worth noting, the energy price in the market also has an influence on the responses of the controllable/shedable consumers during peak hours [61]. The operator of the distribution system should guarantee the power supply of consumers by buying energy from the wholesale markets, either by having bilateral forward contracts with brokers and generating units (long-term contracts), or participating in spot electricity markets [62]. Generators in the market are normally dispatched based on their operating cost from the most economic to the most expensive until meeting the total load demand of the market. While a major part of the total load demand is provided by the settlement of long-term contracts with reliable suppliers, the remaining part is cleared in the spot market [62]. Due to the uncertain nature of renewable generations of wind and PV, they are allowed to participate in the market only if they are equipped with storage facilities, which can mitigate the chaotic features of renewable DERs and provide a smoother production profile. Moreover, there is an opportunity for DERs to participate in the market of emission trading in which, both data of emission and energy price are sent to MGCC through a communication service. The final CO_2 remuneration of DERs in the grid is paid based on the data gathered by this communication service [58, 63].

In the case of the reserve market, there are two short-term markets of spinning/non-spinning reserve with a start-up duration of 10-30 minutes. Besides, there is one long-term market of standby reserve with a start-up duration of less than 30 minutes. Considering the current regulatory framework of reserve markets in the world and having the present technology of renewable DGs, it is challenging for DGOs to participate in the short-time reserve markets [62]. Such a challenge is less intricate in terms of diesel and gas DGs due to their capability to be dispatched and remotely controlled. In most of the reserve markets, a

single price is calculated daily and will remain unchanged during the day [62].

In the restructured power market, EMS is responsible for selling reserve capacities for the day-ahead (DA) market through clearing reserve bids. Finally, the optimal bidding strategies are applied to the short/long-term ancillary market to reach the optimum planning for the operation of DERs in microgrids [64]. As it is not easy to store the electric power, the spot price of electricity may fluctuate significantly when the supply and demand are not balanced. In such conditions, when the spot price is high, selling contingency reserve to the grid may provide a microgrid with more profits.

c) Reliability/resiliency enhancement

Some reliability concepts like resiliency of distribution grid, which have emerged with high penetration of chaotic renewable DERs, are only applicable by means of decentralized control of DN. Efficient approaches for optimal construction of virtual self-adequate microgrids are explored in [65]. In the next step, the effects of adding reactive power resources and energy storages to the network on the self-adequacy of microgrids are studied. A similar microgrid formation and allocation approach is presented in [66] using a new probabilistic index based on both the active/reactive power supply-adequacy and reliability aspects of microgrids. This study constructs a reliability index by combining the system average interruption duration index, momentary average interruption frequency index, and system average interruption frequency index.

2.2 Operation approaches of ADSs

Economic aspects of the DNs operation in the new structure of the electric power system (EPS) management can be considered as the most important objective for DSOs and DISCOs.

However, several different structures of scheduling can be observed in various studies, and there are a considerable number of papers in which different objectives have been transformed into economic indices.

2.2.1 Day-ahead scheduling

The day-ahead scheduling and optimal operation of developed infrastructures in a restructured power market need more investigations from researchers and system operators. The day-ahead operation of ADSs can be divided into (1) scheduled operation of the grid, mostly one-day ahead (or more days) schedule, which is planned based on the forecasts of RESs generations and load demand. These scheduling programs are mostly based on economic factors and also adding some other objectives like emission minimization, power loss improvement or voltage regulation; (2) real-time operation of the network, modification commands to change DN working point and their corresponding actions occurring in short-time periods employing communication signals and state-estimation algorithms. This chapter aims to provide a taxonomy for the operation of ADSs in two different time-scales for days-ahead and technical management. In this respect, the main contributions of the chapter can be concluded as follows. Firstly, compared to a large number of review papers on DN planning, only a limited number of papers have been presented on the economic and technical operation of ADSs. To this end, this chapter aims to present a comprehensive review of recent advancements regarding ADS operation with a broader perspective. Secondly, under a new time-hierarchy viewpoint, this chapter categorizes existing studies into two sections of the economic and technical management of DNs based on operational time-intervals. The first operational time-interval refers to the days-ahead (i.e., 1-3 days) management of the grid,

which necessitates economic scheduling of the system. Four major tendencies and their respective implementation approaches for the economic ADSs operation are detailed. The second operational time-interval refers to the daily operation of the DN in terms of technical management and power quality correction, which includes three sub-conditions of static, dynamic, and transient. In fact, set-points provided in the first interval are reference points for the second interval. Finally, the last part of the chapter investigates studies related to modeling and control requirements for the implementation of approaches detailed in the previously mentioned two intervals. In other words, this chapter highlights the potential applications of DSO's properties in respect to the time-interval of their applications during operating procedures. Independent system operator (ISO) merely has the responsibility of verifying the reliability of energy across the transmission network regardless of market transactions. Subsequently, DSO will need to meet the obligation of ensuring the reliability of retail transactions within the DN. This procedure for DER providers in retail and wholesale power markets is shown in Fig. 2-5.

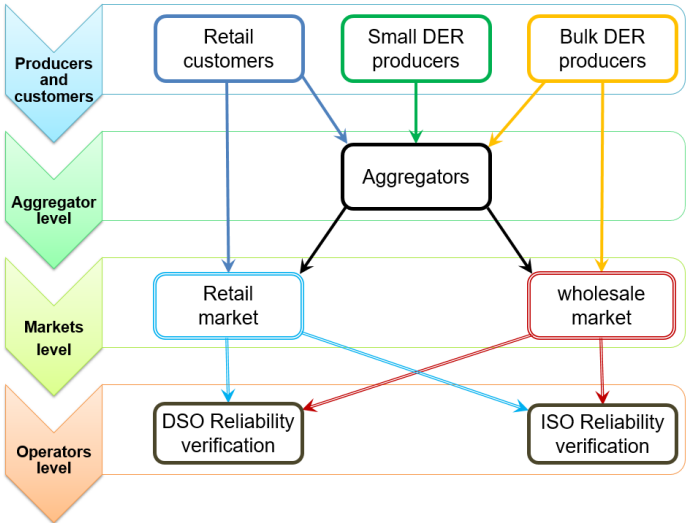

Fig. 2-5. Participation of DERs in the electricity markets

This figure illustrates the participation of DERs in the markets. As can be seen in the figure, there are four major players, including small DER producers, bulk DER producers, retail customers, and aggregators who can participate in the retail and wholesale markets; while the reliability of these two markets should be verified by DSO and ISO respectively. Considering that small DER units are not allowed to individually participate in the markets, several small producers should form an aggregator. Through the aggregators, they can participate in either of the markets. The same situation is valid for retail customers to participate in the retail market. Finally, the reliability of wholesale and retail markets should be verified by both DSO and ISO [56].

Along with the formation of the deregulated power market and participation of DISCOs in the energy market, the economic management of ADSs has attained more attention. This procedure is shown in Fig. 2-6.

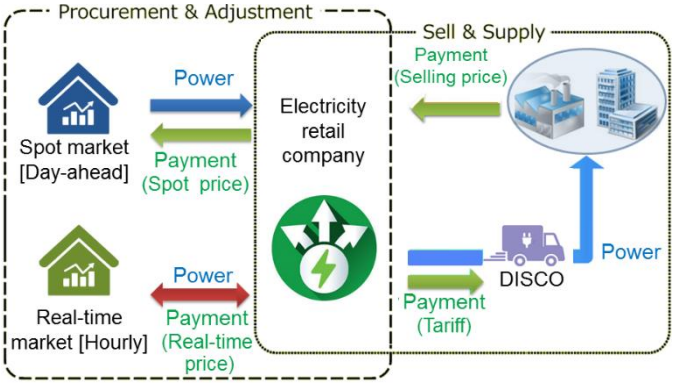

Fig. 2-6. Participation of DISCOs in the energy market

As can be seen, the retail company trades with both spot and real-time markets. In this respect, a scheduling method for active/reactive powers of the upstream bus, DERs, ESs, and controllable loads is presented in [67] to minimize the operating cost of ADS. The study with the objective of minimizing DN power losses in addition to operating costs is carried out

in [68, 69] using power flow control and rapid reconfiguration of the DN. Back-to-back voltage source converters are employed to guarantee power flow control. Moreover, the setting of an on-load tap changer (OLTC), power imported from the

upstream grid, and the level of DG curtailment are regarded as controlling tools for ADSs. In addition to daily scheduling, two marginal scenarios, including *a*) no generation/high demand and *b*) high generation/low demand, are investigated. In [68], the minimization of power curtailment for renewable-based DERs is added to the objectives of [67] by using a multi-objective methodology. Interruptible loads and energy storages are also incorporated in this study to provide a set of compromised solutions among different objectives. The proposed concept is applied on a DN with two sub-regions and an inter-regional tie line to reach the maximum exploitation of renewable energy. A robust optimization problem for active/reactive power is proposed in [70] to minimize the power losses, cost for electricity imported from the main-grid, wind power curtailment, and operational costs caused by OLTC, capacitor bank, static VAR compensator (SVCs), and ESs. Based on a weighting technique, network voltage deviation and operating expenditures are combined and used as an objective in [71] to obtain an operating time-table for active/reactive power of wind turbine, PV and energy storage units.

The formation of an intraday market for DNs besides the day-ahead wholesale market has provided a new environment for the market participants to schedule their facilities more efficiently within these markets. This structure is detailed in Fig. 2-7. Based on this structure, a two-stage scheduling method is proposed in [72] for the management of dispatchable generators, PV field, wind plants, and OLTC-equipped transformers. In the first stage, a day-ahead scheduler is proposed to reach the minimum generation cost while meeting a set of

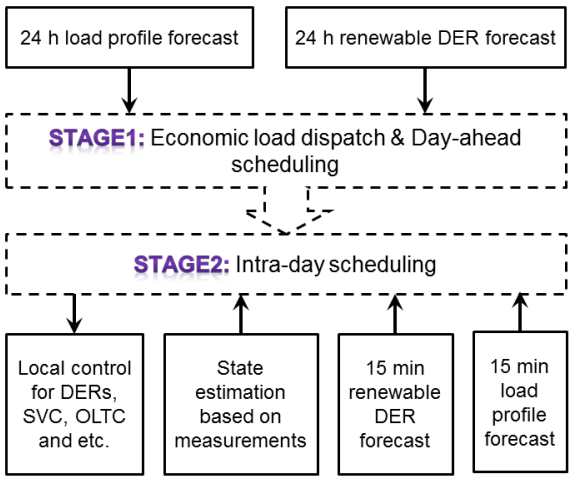

Fig. 2-7. Two-stage participation of DN operators in day-ahead and intraday energy markets

electrical and thermal loads based on forecasted data. At the second step, an intra-day scheduler is implemented for every 15-min interval to prevent the violations in distribution system constraints. Similarly, a dual-scheduling technique is presented in [73] where a day-ahead energy import/export is determined at the first step, while corrective set-point scheduling of DGs, ESs, OLTC-equipped transformers, and SVCs to compensate active/reactive and Volt/VAR deviations from the day-ahead commitment are obtained in the second step.

2.2.2 DISCOs in the wholesale market

Based on the structure of the electricity market in different countries, there is an option for DISCOs to trade with separate energy retail companies or directly participate in real-time markets to provide the necessary hybrid energy for the secure operation of their own grid [74-78]. In this regard, a bi-level programming model for the optimal participation of retailers and customers in an ADS is investigated in [79]. In the first level of the proposed methodology in [79], the retailer tries to maximize its profit by determining a set of flexible selling prices over

a day while the customers define their load levels corresponding to offering prices of the retailer in order to minimize the cost of purchasing power. Considering different load patterns of the customers, the objective function for each of the customers is defined separately. The utilization and operation scheduling of transportable energy storage systems with the aim of maximizing the profit of DISCO by participating in the day-ahead market is formulated in [80], which minimizes the total cost comprising the power imported from the upstream grid, renewable DERs purchasing cost, and DG running cost. This approach is applicable to the simultaneous control of active/reactive power.

Utilization of PEVs is one of the most prominent methods which is employed by DSOs during recent years to cope with the fluctuations of the energy market prices as well as uncertainties of DNs. In [81], the DISCO is responsible for PEVs' charging/discharging scheduling to minimize the total operational costs and emissions of the DN. These objectives have been accomplished in single and multi-objective optimization approaches. In [82], a local power company aims to maximize its economic benefits by proposing a flexible operation technique for PEVs in the form of an optimal management methodology of ADS. The presented methodology is jointly applied with an active mechanism of curtailment for the DERs besides the PEVs management. Moreover, two smart strategies of PEVs control are proposed in addition to evaluating the effect of the initial state-of-charge of PEVs.

2.2.3 Aggregated management of ADS

The utilization of the concept of physical and virtual microgrids is also an effective tool for the economic management of ADS [56]. High penetration of DGs in LV (secondary) DNs as one of the fundamental challenges of DSOs has been investigated in [41]. It focuses on

daily operation analysis of radial LV DNs, including microgrids, while studying the impacts of bidirectional power flow and renewable generation intermittency, which cause serious concerns in terms of high energy losses, line overloads, and over/under voltages. Ref. [65] covers the vital necessity to develop an organized method for the optimal construction of microgrids. In fact, it develops some optimized and efficient approaches to cluster DNs into a set of virtual microgrids that have the capability of self-adequacy [83]. Then, the potential benefits of installing both distributed reactive sources and energy storages are investigated to increase the self-adequacy of the designed microgrids [84, 85]. A similar study on microgrid formation for the daily operation of ADSs considering reliability indices and self-adequacy is accomplished in [66]. With the aim of the formation of microgrids, as can be seen in Fig. 2-8, the DN is clustered to several microgrids in which one or a limited number of microgrids are managed by DSO, and the rest of the microgrids are assets of other DISCOs.

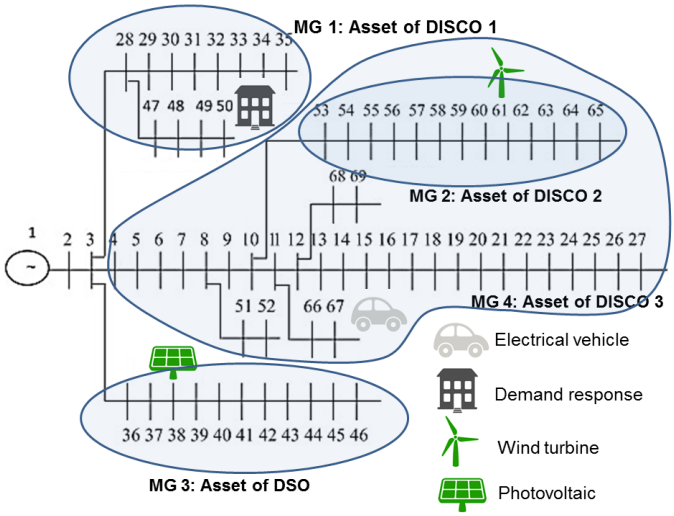

Fig. 2-8. Clustering of the network to several microgrids as DSO or DISCO assets

In such a situation, each of the DISCOs besides DSO can independently participate in energy markets; however, the DSO is still in charge of maintaining security of the grid. Based on this framework, a technique of employing several microgrids connected to others in an

ADS is presented in [49] with the aim of maximizing the benefit of each independent system. It proposes a methodology based on the model of "system of systems" in which the DISCO and microgrids are considered as individual agents with their own assets while having information exchange with each other based on a hierarchical optimization procedure. In a similar framework, [42] presents a dynamic EMS for ADSs based on microgrids management, considering both the influence of large-scale DERs integration and the interaction of energy in a DN. Moreover, an extended energy storage system is proposed in it using the remaining capacity of controllable DGs and energy storage units. In order to optimize the interactions among the group of microgrids and DSO and, subsequently, to maximize the profit of each individual, an interactive energy game matrix is defined. In [57], a simultaneous operation of generation and distribution systems with the cooperation of ISO and DSOs is proposed in which the optimal security-constrained scheduling of several thermal generating units from ISO's perspective besides the units existing in two microgrids from DISCO's prospective is accomplished. A decentralized plan based on the concept of "system of systems" is established to minimize the operational cost of individuals while satisfying the constraints related to secure operation of ISO and DISCOs.

2.3 Energy storage system management

Dynamic day-ahead scheduling of energy storage systems can benefit the ADSs in several technical operation aspects. The energy storage units can offer reliable local backup power for end-consumers while their tight proximity to consumers ensures the availability of supply in the event of an outage. In addition to improving the operating indices like power loss and voltage profile, other eye-catching potential supports can be provided by energy storage

systems, especially in large scale, like load leveling, peak shaving, frequency support, and islanding operation of microgrids. In [86], a single objective power loss minimization is considered to determine the charging/discharging schedules of an energy storage device in different sizes in the presence of PV units for a residential feeder. Economic, technical, and efficiency assessments of DN transformers, energy storage devices, and the DC/AC converters are investigated to achieve more valid and precise results. A dynamic programing instead of using other novel optimization algorithms is employed, and the results confirm the applicability and effectiveness of the presented methodology in both solution quality and convergence speed.

In addition to voltage and loss improvement, the scheduling of energy storage systems has also been investigated for other objectives as well. In [87], a review on potential applications of bulk storage systems, specifically on 1 MW battery energy storage in the Zurich grid, is provided. Three applications of this storage system in cases of peak shaving, frequency reserves, and islanded operation of a microgrid are extensively discussed. In [88], simulation and experimental results of the application of a novel procedure for charging/discharging scheduling of a battery energy storage system are reported. They utilize actual grid data to control an energy storage system with the objectives of power curve smoothing, peak load shaving, and voltage regulation of a distribution transformer. Peak shaving is considered as two different objectives for optimization (i.e. including cost of load and cost of state of charge) based on load forecasting methods. The optimization method reaches the optimal active power flow of the energy storage unit at each time interval. Results show that with the application of existing bulk energy storage at the substation end feeder, the energy storage unit cannot have a considerable impact on the voltage profile of the feeder; however, it can

serve the VAR load of the line and reduce the VAR load of the network. From another point of view, [89] discusses the application of a grid-scale energy storage system for load leveling in distribution systems besides the loss reduction. It explains the relation between the amount of current in DN lines and power loss reduction to demonstrate the potential value of peak-leveling for long-term loss reduction. Moreover, a quantitative survey is developed to investigate the possibility of loss reduction for situations in which the load of DN is shifted during time horizon, but not reduced in quantity. In addition to load leveling using an energy storage system, different factors affecting loss reduction are studied. Additionally, some specifications of energy storage including charge/discharge ramp rate and Ampere-hour capacity for the case of load leveling are analyzed. Increasing the DN capacity is one of the indices which is improved as the result of load leveling.

2.3.1 Compressed air energy storage

Over the past decades, a variety of diverse methods to realize CAESs have been undertaken. CAES units are demonstrated to be a practical solution to store power produced by solar, wind, or other renewable energy units. The capability of storing a large amount of energy in the form of compressed air is one of the most beneficial features of these CAESs [90-92]. Fast response, low maintenance costs, longer life cycle, no need to dispose of chemical wastes are among other advantages of CAESs. These factors have attracted significant attention of researchers for the employment of this technology.

CAESs have been utilized for different proposes in power systems. In the case of large-scale CAESs, authors in [93] propose a coordinated bidding strategy for a hybrid power plant (including a commercial CAES and a wind aggregator) to participate in day-ahead, balancing

intraday electricity markets. A similar study considering conditional value-at-risk to manage the financial risk in different scenarios of financial risk levels is presented in [77] while a gas turbine in the form of a simple cycle operation mode is added to the CAES. In [94], the operation strategy of a merchant CAES is formulated to reach optimal offering and bidding strategies for selling and purchasing the electricity, so that the risks related to errors of the price forecast can be controlled using information gap theory. Moreover, the proposed methodology is utilized to make separate hourly curves for bidding and offering. Ref. [95] presents a robust adaptive technique for a wind power producer jointed with a CAES system to optimally schedule the participation of coupled aggregators in the day-ahead electricity market. The uncertainties associated with wind power and price forecasts are modeled using robust optimization. Large-scale CAES systems have also been employed for participation in the spinning reserve and reactive power markets [96], as an energy storage technology for energy hubs [97], transmission capacity increment and transmission cost reduction [98], day-ahead energy markets [99], to increase the dispatchability, capacity factor, and total generation of wind power [35, 100], supply-demand energy balancing and demand responses [101], and for price arbitrage [102].

SCAES applications in DNs are growing significantly because of their lower investment costs and longer life-cycle compared to other storage technologies. For the stationary form of CAESs, authors in [7] employ a distribution size CAES for participating in the day-ahead electricity market. In [103], CAES technology is incorporated in the optimal scheduling of a small energy hub, which includes photovoltaic (PV) and demand response, to minimize risk from uncertainties associated with energy price, load demand, and solar irradiations. In [104], the reactive power capability of CAES is employed in the optimal operation of a DN, in which

a bi-objective dynamic optimal power flow problem is formulated and solved by Nash bargaining and second-order cone program. In [105], the authors propose a new configuration of a dispatchable compressed-air-assisted wind turbine for DNs, which is capable of improving the mechanical performances of the wind turbine and subsequently increasing its generation and dispatchability. A bi-level planning approach, considering the operation and spinning-reserve requirements of DNs, is offered in [106] for an islanded CAES equipped microgrid.

2.3.2 Plug-in electric vehicle

Without any doubt, the economic charging of PEV devices is one of the most noteworthy challenges for modern microgrids and DNs [107]. Network managers tend to reach higher penetration of PEV charging structures; on the other hand, the charging load of these units can significantly influence the economic and technical parameters of the network. Considering the fact that it is difficult to build or upgrade networks, novel charging control, and energy management strategies should be adopted in order to reach the proper integration of these units. As a result, several studies have been accomplished to control the PEVs charging load in ADSs. In [108], a detailed technique of coordinating PEV aggregators with a three-phase DN is studied. The presented hierarchical framework (i.e., including PEV level and DN level) can benefit both PEV and DSOs by minimizing the active power loss and the cost related to the PEV charging. In [109], the fuzzy logic is applied to provide an autonomous control for the charging load of PEVs with economic objectives as well as targets to maintain system voltage profiles. In [110], from the viewpoint of day-ahead scheduling, a day-ahead tariff of the DN is proposed to avoid grid congestions due to PEVs charging. The DLMP and minimal marginal congestion costs are considered as the basis of the day-ahead tariff.

Utilizing the predictions of hourly energy prices as well as the day-ahead tariff, the PEV fleet operator sets a schedule for vehicles to avoid congestions while decreasing the cost of the PEVs charging.

As a part of the parallelization of different sections of the electricity market and network operations, new concepts of decentralized control and management of systems have emerged recently. Agents and agent-based control of the system are among these novel concepts which have been proposed in several types of research for both planning and operation phases. Definition and tasks related to the modeling of them in ADSs are detailed in Table 2-3. Authors in [111] propose an agent-based approach for controlling the charging of EVs. Three different levels of EV management systems, including EV agents, local area agents, and coordinator agents, are considered besides the normal operation of ADS, emergency and demand reduction conditions are also studied in it. Ref. [112] focuses on the prediction of day-ahead hourly charging demand of EVs from the viewpoint of DSO. The copula method is employed for forming a nonlinear reliance among multivariate characteristics of a considerable number of EVs. Moreover, a stochastic model is presented for the generation of scenarios and estimating hourly non-controllable load demands. Furthermore, it presents two semi-automatic demand response policies that focus on charging schedule of the PEVs. The results would benefit aggregators by reducing both their electricity payments and peak demands.

2.4 Technical factors for ADS operation

The technical management of ADS with the aim of reaching optimal operation indices and power quality improvement is a key objective that is valuable to both the power supply side

Table 2-3. Possible agent-based outline for modeling of ADS

Agent	Responsibility
Grid	1. Energy trading 2. State estimation 3. Power routing 4. Voltage regulation 5. DG control signal 6. Ancillary service 7. Power matching
DG	1. Executing control commands 2. Sharing storage limits 3. Sharing generating forecasts
Feeder	1. Summing up loads connected to feeder 2. Sharing next hour capacity 3. Checking operating constraints violation
Storage	1. Sharing storage capacity 2. Responding to charge/discharge controlling commands
Consumer	1. Load forecasting 2. Sharing estimated required power for substation 3. Sharing demand response potential 4. Sharing PEV potential 5. Forecasting power of DGs connected to low voltage grid 6. Making price negotiation
Primary substation	1. Initiating route token 2. Initiating alarm token 3. Coordinating state estimation 4. Embedding control actions from GRID AGENT in token
Secondary substation	1. Summing up loads connected to it 2. Sharing next hour capacity 3. Checking operating constraints violation 4. Local state estimation

and the demand side. In fact, challenges related to this objective have been among the major concerns of power system managers during recent years, specifically for DSOs and DISCOs in distribution sections, which utilize a high number of different types of DGs and power electronic devices. Volt/VAR optimization, power loss improvement, harmonic suppression, and enhancement of reliability indices are noted as the main concerns in ADSs [113]. Research in these respects can be generally categorized into static and dynamic (hourly scheduling) types; however, some researchers have also paid attention to transient periods (several seconds to less than one hour) [114]. In this regard, we present static operating factors for day-ahead market participation.

2.4.1 Power loss/voltage profile management

The power loss and voltage profile improvements can be considered as the most vital technical indices for the management of ADSs because of their direct influences on the operation cost and satisfactory level of end customers. Regarding the dynamic operation of DNs, [115] implements a multi-objective optimization algorithm to minimize power loss, voltage deviation, and peak-valley difference. It schedules the power generation of two DGs as well as the interaction power of three microgrids at the common power coupling point in a distribution system. It separately provides results for the optimization of each objective as well as obtaining a Pareto-front of non-dominated solutions. Moreover, it is demonstrated that the proposed method can guarantee the desired profile for the voltage of buses. A hybrid optimization algorithm as the combination of particle swarm optimization and bacterial foraging algorithms is adopted to obtain the optimal solutions.

Reference [116] takes into account the coordinated application of OLTC, SVCs, and DG

reactive power as efficient reactive power control tools for a day-ahead operation scheduling of an ADS. Besides the minimization of active power losses, the voltage violation from a specified threshold is considered as the second objective function by defining a penalty function. Dynamic thermal rating is presented to achieve the desired level of network losses and voltage profile while the real-time line thermal limit is considered in the constraints. The Q/V droop controller technique with dead-band is utilized to regulate the reactive power intake or provision of DGs. In addition, operations of OLTC, SVC, and curtailment of DG units are investigated within the case studies for different values of DG penetration and objectives. Moreover, it proposes a voltage connection point based on local and central regulating strategies for the specific voltage controllers.

A study with a similar power loss and voltage objectives is implemented in [117] in the case of integration of PV units into ADSs. A method of preventing DN overvoltage based on dynamic active/reactive power droop control of a PV generation system is proposed in the study. By utilization of the presented technique, the obtained reactive power capacity of available PV units is fully operated to prevent overvoltage before any violation of the feeder voltage from standard limits. Moreover, a novel active power curtailment approach is formulated in addition to reactive power curtailment for PV units to ensure the prevention of overvoltage at the buses of DN. Results show that the proposed methodology has the ability to increase the installed capacity of PV units. Single objective voltage control in a DN is studied in [118] in which a novel approach for dividing the grid into a number of areas is firstly developed. Then validation of the proposed technique is assessed by using an illustrative example. Afterward, a multi-agent management system is formulated in the framework of two proposed decentralized voltage control methods, Thévenin equivalents, and

top-down sweep control method. It is assumed that each zone should be regulated by means of a controller located inside each distributed energy storage system. Therefore, impact of the DG units on the network is indirectly measured by the controllers of energy storage systems. The decrease of communication costs and computation burden is considered by assuming the operating information isolation of each zone.

2.4.2 Volt/VAR management methods

As one of the ancillary services in the power market, day-ahead optimization of reactive power has always been one of the main focuses for the secure operation of DNs. More specifically, static bi/multi-objective approaches of reactive power optimization for the ADS management mainly focus on the provision of a reliable reactive power margin and minimum voltage sag-swell after generation-load fluctuations[119]. From another point of view, as can be seen from Table 2-4, these methods can also be categorized into centralized and decentralized methods. The tendency for higher integration of renewable DERs is another reason which makes DN managers pay more attention to static reactive power optimization of the grid. These objectives are simultaneously considered in [120, 121] by utilizing a bifurcation theory-based voltage stability methodology. A scheme for optimal dispatch of the reactive power provided by wind farms to obtain the desired voltage limit at buses of a DN with the high penetration of wind power is presented in [122]. The proposed automatic voltage control is applied after the implementation of an adaptive clustering of the network to several zones. The presented clustering method has the ability to efficiently determine the accurate voltage control ranges for each of the wind farms. An optimal management method for reactive power of renewable-based DERs is proposed in [123] in which DERs deliver

Table 2-4. Comparison of different types of system control in ADS

Volt/VAR management method	**Advantages**	**Limitations**
Local control	1. Scalable 2. Low cost 3. Low needs for communication	1. Negative interaction of some devices 2. Necessitates complex safety restrictions 3. Problem in DGs integration
Centralized control	1. More efficient during most conditions 2. Less protection limitations to access the remote measurements	1. Necessitates more communication 2. No adaption to changes in feeder configuration 3. No adaption to changes in operation state 4. No coordination between different kinds of regulation devices 5. Problems for DGs integration
Model-based control	1. High coordination, optimal solution 2.Robust to change in system configuration and operation using real-time update of system state 3. Acceptable integration of DGs	1. Not highly scalable – control system for whole DN 2. High costs of implementation and then operation due to technical challenges of system robustness and efficiency

spinning reserve to transmission grids based on two different models of information gap decision theory; while the control of their corresponding active power is accomplished by the ISO, and the DN operator attempts to manage the uncertainty of the reserve power. It can considerably enhance the interactions between transmission networks and DERs. In [124], a two-stage daily Volt/Var management approach in DNs is presented by using feeder capacitors, and substation capacitors joined with OLTCs. In the first stage of Volt/Var management, a dispatch schedule for the feeder capacitors is specified based on reactive power heuristics. In the second stage, an optimization method is utilized to define the dispatch schedule of the substation devices considering the control actions of the feeder's capacitors.

Then, the reference voltage at the point of the secondary substation bus, as well as the transformer tap limits are improved by which the model adjusts to fluctuating load conditions. Interactions and information exchange are shown in Fig. 2-9 and Fig. 2-10, accordingly [125].

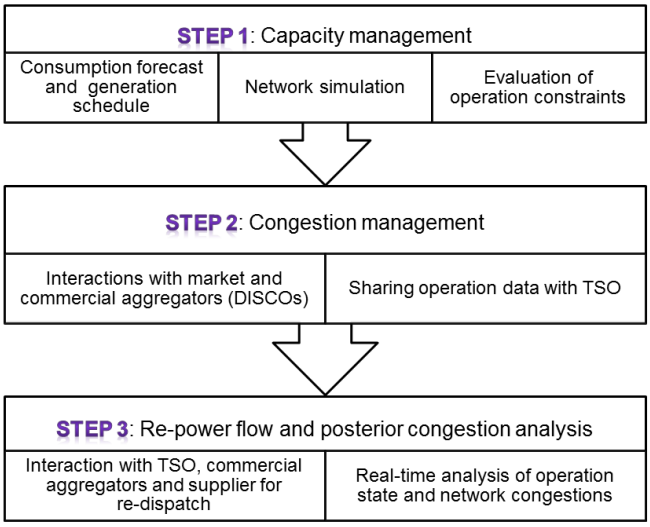

Fig. 2-9. Interactions of DSO with TSO and markets

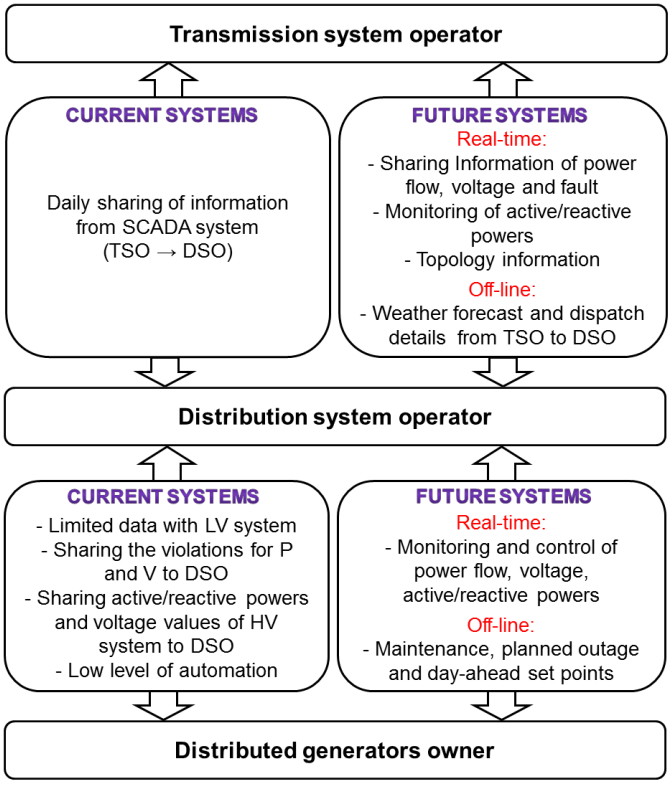

Fig. 2-10. Current and future data exchange of DSO with TSO and markets in ADS

2.4.3 Multi-objective operation of the grid

In this subsection, multi-objective approaches of ADS operation are studied. Obviously, operation methods with a pure focus on reactive power control are not efficient for implementation in practice from the operational viewpoint. However, some of these objectives have emerged as the result of significant changes in grid operation during recent years, along with the involvement of renewable resources, energy storage systems, and electricity market changes. One of these objectives is investigated in [126], where a static approach for minimizing the power curtailment of dispatchable DGs is considered as the main objective to remove voltage limit violations. Centralized control of active/reactive power, OLTCs, shunt capacitors, and remote switches is employed as the main tool to reach this goal. Reducing the number of switching operations of OLTC tap and shunt capacitors, as well as maintenance costs, are considered as other weighted factors in the objective function. In [127], the Volt/VAR and power loss management using DG units and VAR compensators are investigated using a decentralized approach. The proposed methodology firstly divides the DN into several areas with the individual Volt/VAR schemes. It is presumed that each zone is operated by a different DISCO. Then the optimal reactive power setpoint for controlling units existing in each of the areas is determined to obtain the best DN operating point with the minimum power loss.

In [128], uncertainties of PV units and loads are modeled as the main objects of voltage control in ADS while minimizing the active power loss. To this end, a robust voltage control based on the scenario generation and reduction for the forecasted power of renewable units and loads is proposed, which controls the reactive power of DG, continuous compensator, and switching capacitors. The proposed method is validated for the worst scenarios of maximum

generation and minimum load in the over-voltage situation and minimum generation with maximum load in the under-voltage scenario. Monte-Carlo simulation is applied to verify the robustness of proposed approaches. The voltage regulation for ADS based on the Nash equilibrium in game theory with the participation of power suppliers, active customers, and the DSO (i.e., the owner of the DN and the passive DGs and loads) is formulated in [129]. The DSO determines the voltage of buses, the reactive power of DGs, and the energy price for each player while maintaining the secure operation of DN. In addition to the main objective of voltage profile control, the problem is modeled as a min-max optimization problem in which suppliers tend to maximize the pay-off, active loads want to minimize the purchasing payment, and the DSO objective is to reach an optimal ADS operating point with the minimum power loss. Recently, application of power electronic devices for improvement of power quality in ADSs has gained more attention. However, this research topic needs more investigation, and [46] provides a study on the employment of power electronic transformers to reach more flexibility for power quality improvement. Compared to the traditional DN transformers, the power electronic-based transformers provide additional characteristics as a power quality controller. Simulations considering unbalanced three-phase loads, DN with the high number of harmonics, frequency flicker, and voltage dropping, are carried out to verify the effectiveness and applicability of the proposed control strategy using the proposed transformers.

In addition to static methods of technical operation and power quality improvement in ADSs, a considerable number of studies have been done by dynamic approaches. These dynamic methods can be carried out by the hourly scheduling of grid topology and devices existing in the DN or transient evaluation and control of DN performance.

2.5 Modeling of ADSs

In this section, a review of novel ideas for modeling of ADSs and developed methodologies of management and communication for the sake of automation of DNs is presented. In this regard, it illustrates recent studies on evaluation and analysis of ADS operation indices, mathematical modeling and analysis of DN software tools, and finally, the development of approaches for optimal control and automation in ADSs.

2.5.1 Operation indices

Electrical DN operating indices can be considered as a set of values that can manifest the current/future operating situations of the grid from different aspects [2, 130-136]. One of the most important indices in the distribution section is the reliability capability of the grid for secure power supply; however, there are a number of indices that have been formulated for the safe operation of the network from the DSO's viewpoint. It should be mentioned that some operating indices of the grid change continuously, which is partly because of the integration of new DERs in DNs or new regulations of power markets. The reliability evaluation of ADS is presented in [137] considering energy storage units and real-time electricity pricing. It models a DN, including microgrids and ES, at the first stage in which the output power of DGs is calculated based on the method of generalized capacity outage tables. Then, the Monte-Carlo simulation is applied to perform reliability evaluation. Different sizes of energy storage are analyzed for this task. In other words, the influences of DGs, ESs, and real-time pricing-based management strategy of energy storages on the DN reliability are investigated. System average interruption frequency index (SAIFI), system average interruption duration index (SAIDI), and expected ENS are calculated as reliability indices of the ADS to depict

the current condition of the grid. Three scenarios are considered based on the presence and number of energy storage units. In the first one, some of the load points of the microgrid are shed due to the failure of components without the presence of energy storage units; in the second scenario, the energy stored in the energy storage units can fully meet the shed load points; while, in the third scenario, energy storage can only partially meet the load demand of the microgrid.

Ref. [138] presents the experimental experiences of Unión Fenosa Distribución in PRICE-GDI for evaluation of loss, voltage, Volt/VAR indices in a pilot project after the integration of DG units in ADSs. It also describes key outcomes regarding the control of voltage profile in low/medium voltage grids with DERs (i.e., DG units, demand responses, and ESs). The offered solution is based on EMS, where power and voltage values are monitored in real-time and the control room center is able to send set-points to power electronic devices and generators which participate in centralized voltage control. Optimal set-points are calculated by a voltage control procedure, established by the Comillas Pontifical University. This methodology is applied to three cases. The first one is a real medium-voltage DN, including DGs, with the capability of connecting to medium/low voltage networks and a STATCOM device. The second case is an LV network located in a laboratory, where a DG and STATCOM are coupled to investigate the Volt/VAR functionality in LV grids. The last scenario is the study of DN by the University of Seville, which is capable of investigating the performance of a medium voltage grid with several types of generators and loads to overcome the technical and regulatory barriers of these scenarios.

Ref. [139] investigates problems caused by power electronic devices used in renewable-based DERs and formulates a probabilistic index to quantify the controllability of voltage of

buses and current in the lines of DNs, including single/multi-microgrids. A new index is formulated to optimally cluster the ADSs into a multi-microgrid network with optimized degrees of controllability, reliability, and supply-security indices. In order to evaluate the robustness of the offered design and the influences of interconnected various distributed DGs and reactive sources, several sensitivity analyses are carried out. SAIDI, SAIFI, and momentary average interruption frequency index (MAIFI) using annual outage duration, annual failure rate, and momentary failure rate are calculated and considered as reliability indices of multi-microgrid systems, while the supply-security factor ensures the adequacy of active/reactive power for microgrids.

In [71], a risk assessment task for transmission systems is implemented considering the influences of ADSs. As opposed to the previous studies, which completely ignore the characteristics of DNs in the modeling of transmission buses, this study considers the ADSs as a potential active system in the presence of DGs. Therefore, ADSs are modeled as a power supply in some time periods that can send power back to the upstream transmission network in addition to meeting local load demands. Based on the proposed hierarchical evaluation of the DN on risk assessment of transmission network, DGs are modeled as a supply for critical loads through re-dispatching during contingency (i.e., the islanded mode in [71]). In order to ensure the required high-reliability level for DN customers, the factor of available supply capacity is utilized. Moreover, an iterative evaluation procedure between DN and transmission system is implemented to develop the risk indices considering detailed structures of the ADS. Furthermore, the influence of some indices on system risk evaluation, such as location, outage probability, dispersion, and capacities of DGs, is studied. EENS, the probability of load curtailment, expected frequency of load curtailment, and a new severity

factor are considered as reliability indices for transmission systems. In [140], the Monte Carlo simulation is used to assess the reliability index of ADS for low/high levels of DG penetration. Two-case programming is formulated in which the load shedding strategy is modeled when there is an imbalanced generation-load situation. As opposed to the traditional failure-effect based approaches for DNs reliability evaluation, which study the effect of component failure and its consequences on loads and then calculate the reliability indices such as SAIFI and SAIDI, it analyzes the condition of DG high penetration with normal operation of all components, taking consideration of the possible power shortage caused by chaotic output of renewable-based DGs.

Another reliability assessment method based on the concept of capacity credit of DERs is provided in [141]. In EPS terminology, the term "capacity credit" is considered as a quantifying metric for the involvement of a unit to the adequacy of the generating system. In addition, a general probabilistic-based model of demand response is presented so that the end-user behaviors are discriminated by two coupling procedures: inter-temporal impact and instant response. The sequential Monte-Carlo simulation is also adopted to improve the computation efficiency. The uncertainties related to the behaviors of end customers are modeled by a hybrid possibility-probabilistic formulation that characterizes both specific characteristics and generic regularity of demand response. Besides, a novel index for evaluating the role of ADSs in bulk ancillary services markets is proposed in [142] considering different regulatory structures for transmission and DN market interactions. This procedure estimates the DN capabilities to support network stability by employing a hybrid representation of high/medium voltage substations and their relevant DNs with a geographic information system (GIS) based clustering method. Big data technology as another potential

tool is employed in [143] to evaluate an operational reliability index in ADSs, and predict the future reliability value of the grid from the current state of the system. To this end, this paper firstly analyzes the substantial influencing factors of reliability indices by the parallel association-rule mining algorithm. Then, these factors are used as input variables of an evaluation model based on the artificial neural network. Finally, forecasted operational reliability values are obtained using the developed model and real-time data. Input data for training and test of the neural network include the historical operational status and current states of DN devices and equipment, outage condition and time of units, geographic and weather information as well as image and field environment data.

2.5.2 Power flow

Obviously, several algorithms are needed for the numerical analysis of ADS performance. Load flow and economic load dispatch are among these tools which have been the subject of a large number of research publications in DNs along with the formulation and development of ADSs. These algorithms are essential for future planning/expansion of DNs as well as the determination of the best operating point of existing grids. In this respect, [144] presents an efficient algorithm to handle P-V nodes (i.e., DG connected nodes with the constant voltage control) based on loop analysis combined with the forward/backward sweep power flow. Because the main part of the proposed hybrid power flow has remained the same as forward/backward sweep power flow, this algorithm is suitable for weakly meshed DNs, and also is appropriate to deal with networks containing a large number of P-V nodes with varying branch R/X.

Another attempt to adopt the traditional power flow to the new structure of ADSs is

accomplished in [145], where a multi-temporal power flow algorithm is proposed to assess DER hosting ability of an ADS. In order to compensate for the inaccuracy of some convex relaxation-based power flow methods during periods of intensive DERs production, a number of linear constraints are added in the power flow formulation to guarantee an exact relaxation. Based on a comparison of the literature, the formulation of power flow in multiple time-scales can better evaluate functions of storage systems due to the temporal dependency of storage decision variables within an ADS in terms of charging and discharging procedures. To this end, a three-day period of simulation is implemented in [145] to reach at least one full charging/discharging cycle of the storage units. Utilization of PV units for different capacities and also conditions with/without storages are investigated to confirm the effectiveness of the proposed methodology in the case of reaching the maximum line current limits. In [146], the problem of unbalances in the operation of ADSs is analyzed using a three-phase DN load flow based on the symmetrical components. Besides modeling the fluctuating natures of wind turbines and PV units, the load model of center-tapped transformers, as one of the main novelties of the paper, is involved in the proposed formulation. In order to validate the effectiveness and applicability of the presented algorithm, it is simulated on the IEEE 8500-node test feeder as the largest IEEE PES distribution test system with 1177 distribution transformers connected to 1177 loads.

In [147], the problem of approximate solutions is studied for the nonlinear equations of the active/reactive power, which refer to the generation-demand balance in DNs. It presents the required conditions for the existence of a practical solution for power flow equations. Then a linear formulation to obtain the approximate active/reactive power value for demands of the P-Q buses is proposed. Instead of aiming at reaching a very close approximation of loss

value, solutions with tolerable error bounds are obtained, which are trustable for generic DN topology and branch impedances. It is proved that the proposed approximations and their corresponding analytical error bounds are linear in reference to active/reactive power at the buses. Moreover, results show that it is possible to consider the presented method for P-V buses by adding some manipulations. A novel methodology for backward/forward sweep based power flow in DNs is proposed in [148], where a direct process of Z_{bus} matrix and parameters of lines is modeled. To fix voltage magnitude at the specific buses of a network with multiple P-V buses, an approximate iterative solution is utilized. In fact, the modification of bus voltages is established based on the grid data and reactive power injection of units; and it is applicable to both the radial/weakly meshed DNs, and transmission grids.

Ref. [149] presents an optimal power flow to assist the DSO for economic dispatch of DER units. Its main contribution includes the utilization of voltage control to satisfy network security requirements and economic objectives, incorporation of unbalanced DN, and consideration of the structure and economics of the energy market for the ADSs. Previous methods of the voltage management in traditional DNs reduce load demand of the feeders and reach energy savings, while the approach in [149] can meet physical considerations of the ADS operation so that the voltage-dependent customers can optimally attain the economic objectives of the market. In other words, operational constraints and economic requirements of the optimal power flow are simultaneously incorporated. Another method for optimal power flow of ADSs is proposed in [150] using cutting-plane-relaxation. Considering significant attention in the branch flow models based on second-order cone programming, an investigation on different necessary assumptions and conditions for ensuring the relaxation exactness of the method is provided at the first stage. Then, the cutting-plane technique is

applied to overcome the exactness challenges of this model for ADSs, especially for networks with high penetration of renewable DERs. Afterwards, in order to adapt these conditions to the research objectives, a total power-loss-cut is introduced to ensure the conic relaxation exactness. Furthermore, [150] proposes a leaf branch current-cut method that can support the algorithm to avoid the relaxation inexactness of second-order cone programming in some leaf branches. Finally, some demonstrations of cutting-planes are presented to guarantee that the proposed model of relaxed optimal power flow reaches an acceptable degree of relaxation exactness and optimality, regardless of considering the power loss as one of the objectives.

2.6 Background, scope, and motivations of thesis

2.6.1 Stationary small-scale compressed air energy storage

The integration of DERs into the distribution level and utilization of various types of energy storage technologies and responsive loads has led to the emergence of new distribution grids, which are known as ADSs [135]. The development of ADSs has provided a platform for the high involvement of energy storages like CAES and EVCS as two potential energy storage technologies.

Based on the current technology, the investment cost for the CAES system is much lower than other technologies like battery bank energy storage at the same capacities [5, 151], while its lifetime is longer than battery banks. The utilization of CAES in ADSs can bring major benefits for the grid, and hence it is investigated in this chapter.

In terms of cost, the capital cost for each kWh of a 2 MWh, 500 kW battery bank (Sodium Sulphur) is estimated at 1000–1400$/kWh (total cost of $2–2.8 million [152]), while this cost for SCAES is only around 360-650$/kWh (total cost of $0.72–1.3 million).

In terms of controllability, SCAES can provide high ramp rates in several minutes. For the dynamic applications in microgrids, which require very fast responses within a minute, battery banks have some superiority over SCAES. At the same time, for day-ahead scheduling, which is operated hourly, capabilities of air turbines can assist SCAES to provide suitable responses for power systems.

In terms of storage efficiency, the current efficiency of SCAESs is not comparable with large battery banks. Roundtrip efficiency of battery banks exceeds 80%, while this parameter is about 70% for SCAES with current technology. However, it should be mentioned that the technology of SCAESs is not mature enough. As studied in [153], the technology progress of the thermal storage unit and utilization of phase change materials can increase this efficiency to 85% in a short period of time.

The last points should be considered in terms of the life cycle and operating costs. In both of these terms, SCAESs have superiorities over the battery banks. Since no chemical reactions are involved, the life span of SCAEs can reach up to 25 years and also, they only incur limited operating and maintenance costs compared to battery banks. Moreover, the number of charge/discharge operating cycles of SCAES is bigger than battery banks, which shows the highly robust feature of SCAES. The benefits of incorporating SCAES in ADSs are recommended in [154] to enhance the engineering feasibility of the microgrids participation in the day-ahead market.

Large-scale CAES systems (more than 3 MW and electric-to-electric efficiency of around 80%) have been studied for price arbitrage [102], supply-demand energy balancing, and demand responses [101, 155, 156], to increase dispatchability, capacity factor, and total generation of wind power [157, 158]. Besides, large-scale CAESs are employed for

participation in day-ahead energy markets [99], transmission capacity increase and transmission cost reduction [98], as an energy storage technology for energy hubs [97], and participation in the spinning reserve and reactive power markets [96]. The operation of large-scale CAES is also modeled; for example, Ref. [96] investigates the effects of thermodynamic models at the operating stages. In this regard, the thermodynamic effects of cavern state of charge (SOC) changes on the charging process, generation level on SOC, as well as discharging rate on heat rate, are analyzed. This study also linearizes and adds some constraints obtained from the thermodynamics of each operation stage into electrical modeling of the CAES.

Besides the wide range of applications of large-scale CAES, this technology has a great potential to be used in smaller scales at the distribution level (0.3-3 MW) or micro-scales at residential communities (less than 0.3 MW). Recent literature has studied the thermal modeling of micro- and SCAESs [152, 159-161]. Ref. [159] provides an experimental evaluation of a micro-CAES coupled with a wind turbine. The necessity for a resilient thermal storage unit is neglected in the thermal cycle modeling of [159], as the size of CAES is relatively small. In [160], the thermodynamic response of the charging and discharging cycles in the storage tank is numerically analyzed for micro-CAES coupled with a solar system. Some predictions of the system parameters from the thermodynamic analysis are used as essential data for designing the tank, compressor, and expander. Authors in [161] present the experimental result of a pilot SCAES plant with a water tank as thermal storage. A detailed analysis of SCAES with packed beds as the thermal storage is investigated in [152], where a high efficiency packed bed heat-exchanger (PBHE) is proposed to reduce the waste of energy and the required volume of the tank.

Other studies have investigated the electrical utilization of SCAESs. Considering the small capacity of SCAESs, the most potential applications of SCAEs are in the case of microgrids and DNs. In this regard, an expansion planning is accomplished in [162] employing advantages of SCAEs coupled with wind power. The results demonstrate that the energy cost of the community and capacity of transmission lines are significantly reduced using the proposed configuration. Another joint operation of wind and SCAES for microgrid applications is studied in [163]. A max-min operation approach has been considered to manage the uncertainty of wind power and minimize loss of the load and wind power curtailment. Similar objectives are considered in [164] to operate a microgrid, including SCAES, wind, and micro dispatchable DGs, to minimize operation cost of DG units as well as the penalty cost due to ENS. Ref. [106] takes advantage of the high ramp rate and quick start-up time features of SCAES to mitigate fluctuations of renewable-energy in the mixed planning-operation programming of an islanded microgrid. Authors in [165] use SCAES for frequency control of a microgrid, where an airflow controller is designed for SCAES to control the power generation/consumption of the CAES system to maintain the frequency stable. An investigation on different configurations of joint SCAES and wind power for remote microgrids, as well as an overview of air and thermal storage for small/medium-scale CAESs, are provided in [166]. Besides, it presents a detailed operation investigation on the distributed hybrid application of diesel, wind, and SCAES for a specified microgrid. Authors in [46] implement a conceptual cost-benefit analysis for the presence of a SCAES at distribution level with a high penetration of DERs, based on load and renewable energy generation time-series of Saxony-Anhalt. In [167], the maximum feeding time of diesel engines with CAES, the optimum volume of the tank, and the minimum mass of the tank is

investigated when a CAES is integrated with wind power. The application of SCAES at the DN using the same formulation of large-scale CAESs is presented in [168], where an expansion planning of microgrids is proposed to increase the capacity of existing networks using the joint operation of SCAES and wind power. The objective of [168] is to minimize the total electricity payment to the grid as well as the costs of equipment over the planning horizon.

Moreover, some other papers have studied the application of micro-CAESs in electrical systems. In this regard, a new modeling approach of micro-CAES as a demand response device in metropolitan areas is presented in [169]. Ref. [170] utilizes a micro-CAES as ES in a small-scale stand-alone PV power plant for a radio telecommunications base station. Optimal tank sizing of a micro-CAES combined with a PV system for residential buildings is studied in [171]. In [172], a model of non-supplementary fired CAES is presented in a hub of power and heat system. However, the electric-to-electric efficiency of energy storage units in [27] is only around 50% due to the lack of an efficient heat exchanger and also several simplifications to reach a linear model.

Another potential energy storage technology is to use the storage capacity of PEVs, which has attracted significant attention of grid operators along with the fast involvement of PEVs in transportation systems. However, charging/discharging procedures of PEVs have considerable impacts on DNs. The effects of large-scale PEVs in terms of environmental, economy, reliability, power losses, and voltage profile are discussed in [173-175]. In addition to distributed residential charging/discharging methodologies, finding a coordination method for EVCS as an integrated storage unit is a vital issue. Ref. [176] investigates this problem while considering power exchange limitations of the grid, and [177] considers further

congestion management in a grid with renewable DERs. In [178], an optimization methodology for the operation modeling of an EVCS with the ability of battery swapping is presented. The developed day-ahead scheduling considers the uncertainty of batteries and electricity prices using robust optimization. In [179], a convex model of EVCS scheduling is proposed to minimize the EV battery degrading cost and energy purchase cost from the upstream grid. Ref [180] proposes multiple charging options for EVCS to find the charging station with minimum charging cost, charging time, and traveling time. In [181], a new charging scheme for EVCS in a dynamic electricity pricing environment is developed, which allows PEVs to share their stored energy with other vehicles under an aggregated framework.

- **Motivation, approach, and contributions**

From the above literature review, there are a number of existing studies on the CAES applications in DNs. However, the thermal modeling of SCAES is different to the large-scale CAES in the sense of efficiency, thermal modeling of the heat exchanger unit, and loss destruction during compression and expansion procedures. Such differences have not been extensively noted in the literature, and most of the existing studies still use the conversion rates of large-scale CAESs for small-scale ones, which will cause non-negligible inaccuracies. Indeed, the scale of an energy storage based on mechanical procedures has a significant impact on the total efficiency of the unit. Therefore, we develop a detailed SCAES model to cover both the thermal and electrical processes rather than the simple electrical only formulations in the literature. To simplify the thermal models, we also show that complex thermal formulations can be replaced by two new approximate thermal-to-electric and electric-to-thermal rates (i.e., different from the large-scale CAESs) to make the models more

convenient and less complicated for future applications. The modeling sections of SCAES in this study are based on practical results of implementing pilot SCAES. Additionally, the presence of thermal modeling of PBHE in the obtained models can make the energy storage unit more efficient. In order to validate the model, the SCAES has been studied in a day-ahead scheduling case study.

Besides, there are also existing studies investigating the integration of EVCS in power grid operation, where the key issue, in this case, is the modeling technique of PEVs' charging/ discharging in relation to EVCS [4, 182]. Several techniques, as detailed in the literature, are adopted in this respect to model electric loads of the DN as the result of PEV charging. Note that it is important to reach an appropriate and realistic estimation for several key parameters like arrival time, departure time, and SOC of PEVs when entering EVCS. This study models all these parameters based on realistic data of a charging station, and Gaussian copula distribution function (CDF) is also applied to determine the availability of PEVs' stored energy. Moreover, the effects and potential benefits from the joint operation of SCAES and EVCS at the distribution level are also studied in the first technical chapter.

Conseqently, in this study, a framework for the participation of a DSO equipped with a SCAES in the day-ahead market is proposed. Then a coordinated strategy for the joint operation of SCAES and EVCS is offered. DSO, as the owner of ADS, is responsible for the scheduling of PEVs and SCAES, and sells/buys energy from/to the market after getting power forecasts from solar units to meet load demand and operating constraints. The proposed formulation considers the detailed electrical and thermodynamic models of SCAES, which can assist DSOs and distribution companies more accurately schedule grid operations.

Hence, the contributions of the first technical chapter are as follows:

- Developing a model of SCAES for DSO to participate in a day-ahead market, where SCAES is equipped with a PBHE to increase efficiency and reduce the size of on-land reservoir tank;
- Evaluating the actual thermal-electrical conversion rate for SCAES at distribution levels based on thermal formulations and practical results;
- Modeling highly uncertain behaviors of PEVs in the form of EVCS using Gaussian CDF, where EVCS is optimally coordinated with SCAES as an alternative ES;

2.6.2 Energy storage aggregator for electric distribution grids

Future power systems are anticipated to contain plugin electrical vehicles, wind, solar, and other interconnected micro energy grids [4, 12]. This growing integration of distributed renewable sources has caused considerable uncertainties to DNs. The role of energy storage units can mitigate the uncertainties in such situations. Energy storage systems, as an essential part of power systems, help grid operators to maintain the continuous power supply and improve the system reliability. Energy storage can also be used to meet electricity demand during peak times [6].

There exist a variety of energy storage units with different levels of maturity. Currently, the most-used form of energy storage is pumped-storage hydropower (PSH). PSHs can be constructed cheaper, especially for the storage of very large capacity in comparison to other types of energy storage [183]. However, establishing a PSH storage takes typically 3-5 years, which is not acceptable considering the current fast growth of EPSs. Besides, large-scale battery storage units are another promising technology for the operation of EPSs [184]. The battery storage units are utilized mainly for ancillary services or to support the large-scale

wind and solar integration in the current power system, by the provision of frequency regulation, grid stabilization as well as solar and wind power smoothing. It is noteworthy that the high investment cost is one of the most highlighted issues related to the employment of battery storage technology. Shorter life cycle compared to other storage technologies is another noticeable deficiency of battery storage.

However, along with the decentralization of EPSs as well as restructuring energy markets during recent decades, the involvement of small-scale RESs and storage units has been growing significantly. Therefore, the integration of SCAESs has found considerable attention for the applications in ADSs and microgrids. In this regard, some papers have used CAES to manage the uncertainties of renewable energies. To this end, an energy conversion system including compressed air and wind power is presented in [162], which can provide both distributed storage and energy provision for microgrids. Employing mixed-integer linear programming, the optimal wind power capacity, storage capacity, and transmission line capacity to the microgrid are calculated. In other words, the capabilities of CAES are included to configure an expansion planning for a microgrid. In [163], a novel model of a low-emission microgrid is proposed in which CAES units are utilized due to their high overall efficiency and flexibility. The uncertainty of wind power also is considered and modeled in the paper. A similar study is accomplished in [185] so that the system operator tends to minimize costs of carbon emission and grid operation through the utilization of an energy hub model of CAESs integrated with a multi-energy distribution grid. The authors construct a hub of energy, which includes a 13-node district heating network and a 13-bus power distribution grid. In fact, low-carbon economic dispatch is modeled to reach some optimal operating points for an energy hub at the distribution level. Authors in [164] use CAES units to tackle

uncertainties of wind power. Besides, the CAES is introduced as an alternative to manage the commitment of expensive diesel generators in the distribution system. A mixed-integer programming model and GAMS software are used to minimize the operation cost and wind curtailment of the grid. Ref. [186] deploys CASE to manage the power imbalance of a microgrid, including micro-turbines and RESs. The proposed methodology minimizes the total power loss, voltage deviation, emission, and operation costs during the operating period. A multi-objective grey wolf algorithm is applied for the optimization task. Another multi-objective optimization approach (using non-dominated sorting genetic algorithm-II) is adopted in [100] to reach the optimum exergy efficiency and investment cost for a combined system including solar energy, CAES, and a combined cooling, heating, and power unit. During the off-peak period, the presented configuration stores the electric power surplus of the gas turbine while it is released during on-peak time. In [106], quick start-up time and high ramp rate abilities of the SCAES are employed to mitigate fluctuations of renewable energy in the mixed planning-operation programming of an islanded microgrid. Authors in [165] use SCAES for frequency control of a microgrid while an airflow controller is designed for SCAES to control the power generation/consumption of the CAES system to maintain the frequency stable. An investigation on different configurations of joint SCAES and wind power for remote microgrids, as well as an overview of air and thermal storage for small/medium-scale CAESs, is provided in [166]. In addition, it presents a detailed operation investigation on the distributed hybrid application of diesel, wind, and SCAES for microgrids.

- **Motivation and contributions**

As it can be inferred from the literature, CAES storage units in the distribution level are

conventionally operated as an asset of the DSO. However, this consideration is not valid anymore, along with restructuring distribution markets in which the private sector tends to invest and operate renewable sources and energy storage units based on financial factors. In such a situation, owners of these units aim to maximize their profit separate from the security of the grid operation. To this end, in the second technical chapter, we propose an aggregator for privately owned CAES units. Based on the energy price received from the DSO, the CAES aggregator schedules storage units to reach maximum profit for CAES owners. Then, DSO, as the second agent, needs to maintain the security of the grid by coordinating CAES aggregator schedules and the power provision from grid assets (i.e., power generation of renewable sources, diesel units, and power needed to be purchased from the day-ahead market).

Hence, the contributions of this research are as follows:

- Proposing a two-agent methodology for the operation of distribution systems applicable for restructured distribution power markets which consider private owners of storage units;
- Linearizing formulated profit maximization problem for the CAES aggregator and solving it using a linear optimization toolbox;
- Optimal operation of the grid considering the scheduling of CAES aggregator aiming at simultaneous minimization power loss and emission.

2.6.3 Mobile energy storage systems

Recently, the concept of transportable storage systems is getting more attention in electric power research. For example, an energy management system is developed in [187], which

schedules transportable energy storage systems (TESSs) in the form of battery units in a DN to minimize the cost of the power imported from the grid. In [188], a planning-operation methodology is presented to allocate a single mobile energy storage system (MESS) in a DN for power losses minimization, voltage regulation, and energy arbitrage considering life cycles (i.e., 3000) and dynamic capacity of the battery. For the microgrid applications, the allocation of multiple TESSs to various microgrids is accomplished in [189] using a path-based greedy algorithm to minimize the operating cost of DN. A preference-incentive co-evolution technique for optimal power scheduling and reconfiguration of isolated microgrids equipped with shift-able loads is proposed, which exploits maximum transport capabilities of TESSs [190]. For resiliency/reliability applications, authors in [191] propose models for planning and operation of the TESSs to improve the resiliency/reliability of the grid after a disaster. Other research with the objective of resilience improvement for microgrids is provided in [192-194] to optimizes investments of TESSs in the first stage and determine their new locations after a disaster in the second stage. A reliability oriented study is accomplished in [195] based on Markov models and Monte Carlo simulation to evaluate the impacts of TESSs in islanding mode operation of DN. For service restoration applications: a Monte Carlo simulation-based two-stage stochastic restoration is developed in [196] to improve grid resilience while minimizing total cost. Another service restoration methodology is developed in [197] by the involvement of four agents (i.e., including load, DG, switch, and battery) while the impact of utilization of both stationary and mobile storage is developed. Finally, authors in [198] and [199] focus on the optimal determination of transportation routes. In [198], the time-location movement modeling of TESSs to minimize the daily operation cost of DN is studied; while a similarly detailed analysis is done in [199] to model transit periods and moving distances of TESSs, for power loss

minimization, based on a set of linear equations considering traffic congestion of roads.

- **Motivation and contributions**

As can be seen in the literature, battery banks and electrical vehicles are used to form mobile storage units; however, there is no research to employ CAES technology in this respect. To this end, novelties and contributions of this thesis are as follows:

- High investment costs and limited life cycles of mobile battery-based storage are considerable challenges for the widespread development of these systems. Hence, a novel concept of mobile CAES (MCAES) is proposed that is superior to the battery technology in terms of capital costs and lifespan. Additionally, a new formulation suited to the proposed framework is presented in which the number of mobile air tanks with a low construction cost is much higher than the number of motor-generators. Thus, MCAESs offer a larger size of storage with a higher level of dispatchability compared to TESSs at the same investment cost, as well as a lower level of uncertainty compared to the fleet of electric vehicles. Therefore, as can be deduced from case studies and results, besides the profit improvement for the distribution system operator (DSO), MCAESs deliver substantial improvements for key operating factors of the grid, including active power loss, ENS, and voltage stability index.
- In terms of solution approach, a new heuristic-based technique is proposed that overcomes deficiencies of traditional constraint handling methods by converting constraints related MCAESs into feasible ranges. This scheme, which is based on a forward-backward sweep, determines an appropriate range for charging/dicharging

of each motor-generator by which solutions are mapped of their feasible ranges and, subsequently, significantly increase the convergence quality and speed of the algorithm. Additionally, a new solution coding is proposed in which a single matrix will represent both commitment and dispatch matrices. Therefore, a notable size reduction in the dimension of the solution space is offered, which results in a further convergence speed enhancement. The proposed mathematical formulation and constraint handling models are valid and applicable for both mobile and stationary forms of CAES, which makes switching between two states possible.

- Determining traveling time for transportable storage units considering routes delays is one of the highlighted challenges for mobile storage technology. Several methods have been presented in the literature to calculate distances and offer a list of priorities involving delays due to road congestion. However, in Chapter 5, we firstly map the studied IEEE grid on the map of Sydney. Then, the most optimal routes are accurately determined based on hourly historical data of transportations using Google Maps API, which simply solves complications related to routing modeling.

2.7 Summary

With the emergence of ADSs, as the result of the incorporation of active elements in DNs, significant changes happened in both the planning and operation aspects of DNs. In this chapter, an in-depth survey of recent literature regarding the operation of ADSs is presented. To highlight the most important features, the operation of the DNs from economic and technical aspects is explored. The incorporation of different participants is characterized by economic factors, while different time horizons have been investigated in the technical

management of ADS. Finally, some features necessary for the active operation of DNs regarding modeling requirements have also been presented. The obtained categories provided in this study can assist grid operators in achieving the most efficient approaches for ADS operation. In all of these areas of applications, there is always a necessity for DN companies to explore existing facilities and management approaches and, subsequently, to put forward some novel practical solutions. From the literature, it is obvious that DSO and DISCO participation in the day-ahead energy market using maximum exploitation of renewable and storage systems are the most highlighted operation approaches in ADSs. In addition to economical factors, technical factors affecting the operation of ADS have also been investigated in this chapter.

Based on the review, storage systems have high impacts on technical factors (power loss, voltage profile, and stability, and energy not supplied) by tackling the stochastic nature of renewable energies. Considering a large number of works employing battery storage for DN, the number of research using SCAESs for ADS is limited. Moreover, there still exists a lack of research related to the aggregation of storage systems at the distribution level. Besides, mobile storage systems are shown to have considerable potential, specifically for grid operation, while there are very limited papers in this regard. Hence, this study will investigate these issues in the next chapters.

Chapter 3 Day-Ahead Market Participation of an Active Distribution Network Equipped with Small-Scale Compressed Air Energy Storage Systems

Large-scale CAES is conventionally used in power systems. However, the application of CAESs at the distribution level is limited because of differences in design and efficiency. On the other hand, the application of electrical batteries suited for DNs also faces challenges from high investment cost and significant degradation. In this regard, this chapter presents the participation of ADS equipped with a SCAES in the day-ahead wholesale market. To make CAES applicable to DNs, the thermal-electrical setting design of the SCAES coupled with a packed-bed heat exchanger is adopted in the operation of the grid, where SCAES performs as an energy storage for DNs to surpass existing deficiencies of battery banks. The electrical/thermal conversion rate has been modeled for the SCAES operation. Moreover, the operation strategy of the SCAES is optimally coordinated with an electric vehicle charging station (EVCS) as an alternative energy storage technology in deregulated DNs. To make EVCS simulation more realistic, the Gaussian Copula probability distribution function is used to model the behavior of the EVCS. The results obtained from different case studies confirm the value of SCAES as a reliable energy storage technology for DNs.

3.1 System configuration and Mathematical modeling

Fig. 3-1 shows the framework of the proposed configuration. As can be seen, all the elements are individually controlled by DSO using a supervisory data-exchange system, while

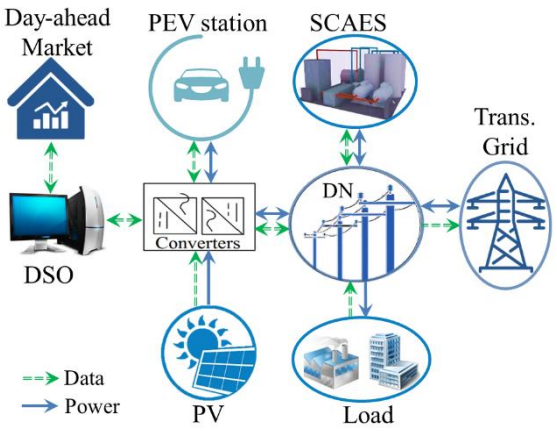

Fig. 3-1. Diagram illustration of proposed configurations

DSO is in contact with the TSO to get data of the day-ahead energy market. PV units as non-dispatchable DGs provide power for DN through electrical converters. EVCS and SCAES are two different types of energy storage in the system, with the ability to exchange power in both directions. While the power exchange of EVCS is accomplished using a bipolar converter, SCAES is directly connected to the grid. For an EVCS, electric chargers are used to exchange power between the grid and EVs. Because EVCS is scheduled to receive power from EVs' DC battery during some hours and refill them during other hours, it necessitates employing a bipolar converter as the chargers. However, because of using the air turbine and an AC generator during the discharging periods of the SCAES unit, it can be directly connected to the grid using a booster transformer. This configuration is designed to exploit spikes of energy price by charging and discharging of storage units during the scheduling horizon.

3.1.1 Formulation of small compressed air energy storage

Fig. 3-2 shows the schematic of SCAES. To avoid exergy loss during the charging mode, as it can be seen in this figure, a direct PBHE is located after the last compression stage (i.e., before the air enters into the tank), which reduces the required volume of storage [152, 161].

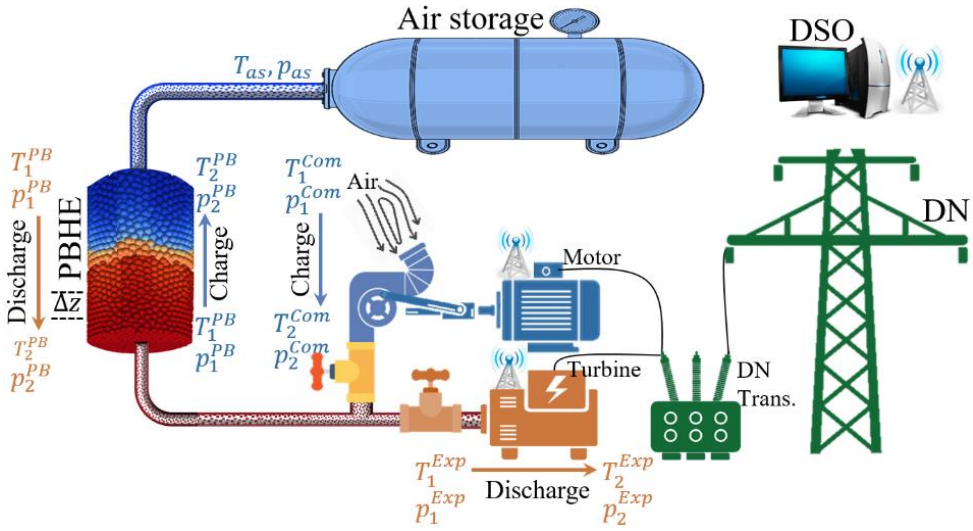

Fig. 3-2. A schematic of SCAES with packed bed heat exchanger

PBHEs are composed of solid particles with a high tolerance of temperature and pressure, which can provide high amounts of heat exchange while having relatively low-cost construction. The value of different energy loss parameters during thermal operation of CAES is calculated through thermal modeling based on the air stored in the tank (i.e., obtained from the previous hour) and the required input/ output power during charge/discharge. As an illustration, consider hour *n* is scheduled for compression based on the solution provided by the optimization algorithm. Then, considering the amount of air stored in the tank (i.e., a function of the status of CAES in previous hours) as well as the amount of power required to be stored for hour *n*, the value of thermal resistance and fluid pressure are different, which results in a specified fluid flow rate.

a) Thermodynamic modeling of SCAES

In this section, a numerical model for an adiabatic SCAES with a direct PBHE is developed. Thermal formulations of the chapter are mainly based on [152], while the value of CAES parameters in [46] as a practical implementation of SCAES are involved in

proposing valid design parameters for the presented SCAES. Compared with large-scale CAESs, the results of thermal simulations in this chapter demonstrate new thermal-electrical rates in both phases of compression and expansion, which are valid based on the experiment results offered by [46]. As such, an average actual value is obtained for the thermal-electrical efficiency of SCAES (i.e., suitable for DNs operation). As opposed to studies that have inappropriately used the SCAES with the same design setting of the large-scale CAES, implementation of thermal formulations in this chapter provides a key reference value for electrical modeling that omits the necessity for running a thermal model in future studies.

- **Compression and expansion**

Thermal modeling for compression and expansion modes of SCAES can be mathematically represented as follows. In this regard, the work and energy destruction in each mode are formulated. Then, actual electric-to-thermal and thermal-to-electric rates are calculated for applying to electrical modeling.

All works are estimated by the energy conservation law in volume control mode while neglecting variations in potential and kinetic energies from inlet to outlet [200].

$$\frac{\dot{W}^{\psi}}{\dot{m}^{\psi}} = c_p\left(T_2^{\psi} - T_1^{\psi}\right) \qquad \psi{=}Com, Exp \tag{3-1}$$

$$T_2^{\psi} = T_1^{\psi}\left(p_2^{\psi}/p_1^{\psi}\right)^{\varpi} \qquad \varpi = \begin{cases} (\gamma-1)/\gamma\,\eta_p & \psi{=}Com \\ \eta_p\,(\gamma-1)/\gamma, & \psi{=}Exp \end{cases} \tag{3-2}$$

$$W_{\Delta m}^{Com}{=}\Delta m\; c_p T_1^{Com}\left(\left(\frac{p_{as}(m{+}\Delta m){+}p_{lo}}{p_1^{Com}}\right)^{\frac{\gamma-1}{\gamma\,\eta_{p,ch}}} {-}1\right) \tag{3-3}$$

$$W_{\Delta m}^{Exp}=\Delta m\, c_p T_1^{Exp}\left(\left(\frac{p_2^{Exp}}{p_{as}(m-\Delta m)-p_{lo}}\right)^{\frac{\eta_{p,di}(\gamma-1)}{\gamma}}-1\right) \tag{3-4}$$

$$\frac{\dot{B}_d^{\psi}}{\dot{m}^{\psi}}=T_0\left(c_p\ln\frac{T_2^{\psi}}{T_1^{\psi}}-R\ln\frac{p_2^{\psi}}{p_1^{\psi}}\right) \qquad \psi=Com,Exp \tag{3-5}$$

The work per unit of mass in compressor/expander can be simply defined by (3-1); where W is work, m is the mass of air, c_p is the specific heat of the air in a constant pressure, and indices 1 and 2 refer to the inlet and outlet of SCAES compressor, PBHE, and expander in different stages. Additionally, Com is the index of compressor and Exp is the index of expander. In the aforementioned formulations, (T_1 and T_2) are considered as the (input and output) temperature of the fluid when passing a procedure. For example, in the case of compression mode, T_1 is the temperature of ambient air and T_2 is the temperature of the air flowing out of the compression stage. The output temperature T_2 of the gas fluid in the charging/ discharging modes is calculated in (3-2) as a function of compression/expansion ratio p_2/p_1; where γ is the ratio of specific heats defined as c_p/c_v (i.e., specific heat of the air in constant pressure/ specific heat capacity of the solid mass), and η_p is the polytropic efficiency. It should be noted, the pressure p_2 increases in the charging mode, as the storage pressure increases to approach p_{as}^{max}. There are the same symmetric variations for the pressure p_1 in the expansion mode. Then, based on (3-1) and (3-2), the required work for the compression of Δm is defined in (3-3) by adding the work needed to compress Δm to the required work to overcome tank pressure (i.e., as the result of previous compressions); where Δm refers to each increment of air, ch is the index for charging mode of SCAES, di is the index for discharging mode of SCAES, as is the index for air reservoir tank, and p_{lo} is any

pressure loss introduced before the air reaches the high-pressure air store (e.g., by the after-cooling heat exchanger). A similar work formulation is defined in (3-4) for the discharge mode, which depends on the current required expansion and storage pressure at the previous state. Besides, the exergy destruction in compressor and expander is calculated by (3-5); where B_d indicates the parameter of exergy destruction, T_0 is the ambient temperature, and R is the specific molar gas constant.

- **Packed-beds heat exchanger**

In the PBHE, there are two components, including fluid and solid gravel particles (solid phase). This section formulates changes of temperature in each of them in an incremental slice of PBHE over time as follows:

$$m_f c_f \frac{dT_f}{dt} = -v_f A \rho_f c_f \frac{dT_f}{dz} \Delta z - \hat{h}_{vlm} A \Delta z \left(T_f - T_s\right) \tag{3-6}$$

$$m_f = \rho_f \varepsilon A \Delta z \tag{3-7}$$

$$\frac{d\rho_f}{dt} = \frac{d\left(\rho_f v_f\right)}{dz} \tag{3-8}$$

$$(1-\varepsilon)\rho_s c_s \frac{dT_s}{dt} = -A \frac{d}{dz}\left(\lambda_s \frac{dT_s}{dz}\right) - \hat{h}_{vlm}\left(T_s - T_f\right) \tag{3-9}$$

$$m_s = \rho_s (1-\varepsilon) A \Delta z \tag{3-10}$$

Based on the law of energy conservation, the energy rate balance of PBHE is given in (3-6) for the fluid in a slice at height Δz and an area A of heat exchanger; where f is the index for fluid, c_f is the specific heat capacity of the fluid mass, v is the velocity of the fluid, ρ is the density of the mass, $\hat{h}$ is the heat transfer coefficient, vlm is the index for volumetric heat transfer coefficient, η is the energy efficiency of SCAES, and s is the index for solid elements.

In fact, from net heat input as the result of fluid flow in PBHE ($-v_f A\rho_f c_f \frac{dT_f}{dz}\Delta z$), a part will be exchanged with the solid phase ($-\hat{h}_{vlm}A\Delta z\left(T_f - T_s\right)$) and the rest ($m_f c_f \frac{dT_f}{dt}$) will be consumed to change fluid temperature. The mass of fluid in the slice Δz is calculated by (3-7); where, ε is the void fraction. Due to changes in fluid temperature and pressure over the operation time, fluid density ρ_f will change as modeled by (3-8). Noteworthy, only temperature change rate in the Z direction is considered, and change rate in X and Y directions are neglected to simplify equations.

Similarly, the energy rate balance for the solid phase is defined by (3-9), where λ is the thermal conductivity. The temperature change rate of the solid phase of the PBHE ($(1-\varepsilon)\rho_s c_s \frac{dT_s}{dt}$) is equal to the summation of the heat conduction through the solid phase in the Z-direction $\left(-A\frac{d}{dz}\left(\lambda_s \frac{dT_s}{dz}\right)\right)$ and heat exchange with the fluid ($-\hat{h}_{vlm}\left(T_s - T_f\right)$). The mass solid in the slice Δz is calculated by (3-10).

In this chapter, all formulations related to heat conduction between particles of PBHE are neglected. In other words, the temperature of particles is considered to be the same. This assumption is correct when the Biot number Bi (i.e., is calculated in (3-12) as a measure of the ratio of resistance to heat transfer via conduction to the resistance of heat transfer via convection) is much lower than 1. Based on the empirical formula (3-11) presented in [200], the volumetric heat transfer coefficient $\hat{h}_{vlm}$ between the gravel and air is given.

$$\hat{h}_{vlm} = 700\left(G/d_{par}\right)^{0.76} \tag{3-11}$$

$$Bi = \frac{\hat{h}\, L_c}{\lambda_s} = \frac{\hat{h}_{vlm} d_{par}}{2\lambda_{par} a_{par}} \tag{3-12}$$

where G is the core mass velocity, d_{par} is the particle diameter, Bi is the Biot number, L_c is the characteristic length scale for heat transfer, and par is the index for the particle of the heat exchanger.

Then, considering gravel particle diameter of 10 mm leads to a Biot number around 0.01. Because Bi$\ll$ 1, it can be assumed that it is seldom necessary to solve the conduction equation [200]. The dynamic model of CAES in the form of equations incorporated into the optimization model is solved by CFD discrete computational method [200] for each iteration of optimization based on charging-discharging values during scheduling horizon.

- **Input/output formulation of SCAES**

With the aim of thermal modeling of SCAES, this subsection formulates the input/output powers and efficiency of storage based on the exergy destruction approach as follows [152, 201]:

$$W^{Com} = W^{Exp} + B_d^{Com} + B_d^{Exp} + B_l^{ga} + B_l^{PB} + B_d^{PB} \tag{3-13}$$

$$Bl^{PB} = mc^{PB} T_0 \left(\frac{T_{t1}^{PB}}{T_0} - \frac{T_{t2}^{PB}}{T_0} - ln \frac{T_{t1}^{PB}}{T_{t2}^{PB}} \right) \tag{3-14}$$

$$\eta^{AE} = W^{di} / W^{ch} \tag{3-15}$$

Exergy dispatch in the SCAES is formulated in (3-13) in which W^{Com} and W^{Exp} in charging/discharging cycles are determined by (3-3) and (3-4); where ga is the index for exhausted gas, PB is the index for PBHE. Exergy destructions in PBHE are calculated by (3-5) for both charging/discharging modes; while B_l^{ga} is exergy loss in the exhaust gas exiting the final expansion stage, the Bl^{PB} refers to exergy loss in PBHE. Assuming a constant specific heat capacity c^{PB} for PBHE, the exergy loss B_l^{PB} when the temperature in PBHE

decreases from temperature T_{t1}^{PB} in the time $t1$ to T_{t2}^{PB} in the time $t2$ is determined by (3-14). Pressure drop in the PBHE is formulated based on the Ergun equation [201]. B_d^{PB} is the exergy destroyed in the PBHE from pressure losses and lengthwise conduction of heat along the bed and accounts for the remainder of the charge work. The value of this parameter is approximately equal to B_l^{ga}+B_l^{PB} based on [161]. Finally, (3-15) can be used to evaluate the electric-to-electric efficiency of SCAES. Then, the values of charging conversion rate $a^{ch} = 1 - \left(B_d^{Com} + B_l^{PB,ch} + B_d^{PB,ch}\right)/W^{ch}$ and discharging conversation rate $a^{di} = 1 - \left(B_d^{Exp} + B_l^{ga} + B_l^{PB,di} + B_d^{PB,di}\right)/W^{di}$ are calculated to be used in electrical modeling of SCAES. In fact, instead of considering a constant value for the thermal-electrical conversion rates ($a^{ch/di}$) of SCAES, the value of these parameters during each charging/discharging cycle is evaluated based on the thermal formulations within each iteration of the algorithm. Then, the obtained results are substituted in (3-17) and (3-18). Besides, considering the fact that SCAES hourly charging/discharging the energy of the unit is limited to its nominal range of operation, thermal constraints related to parameters like pressure and temperature for the piping system, compression/expansion stages, and thermal storage are satisfied within the operation horizon. However, in the case of the storage component, the volume of compressed air into it needs to be controlled to prevent high pressure and temperature inside the tank. This amount is constrained to the maximum capacity of the storage unit by (3-22) and (3-23). In fact, the thermal limitations and constraints related to thermodynamics of SCAES are transformed and presented in electrical formulations.

b) Electrical modeling of SCAES

$$OC^{AE}=\sum_{t=1}^{N_T} P_t^{AE,ch} VOM^{ch}+P_t^{AE,di}\left(HR^{di}NG+VOM^{di}\right) \quad (3\text{-}16)$$

where, OC is the operating cost of SCAES, and AE is the index for SCAES, P is the active electric power, VOM is the variable operating cost of SCAES, HR^{di} is the fuel heat rate for the discharging phase of SCAES, NG is the cost of natural gas, t is the index of time, and N_T is the number of hours in scheduling.

In the case of SCAESs, the operating cost is a small value compared with the other daily operating costs of the DN. Besides, as opposed to large-scale CAES, which needs a reheat procedure during discharge phases, there is no need for burning fuel for SCAES since the loss of energy in the PBHE is negligible [152]. Therefore, the total operating cost of SCAES can be regarded as a negligible amount and neglected in this research.

$$V_t^{AE,ch} = a^{ch} P_t^{AE,ch} \quad \forall t \quad (3\text{-}17)$$

$$P_t^{AE,di} = a^{di} V_t^{AE,di} \quad \forall t \quad (3\text{-}18)$$

$$V_{min}^{AE,ch} U_t^{AE,ch} \le V_t^{AE,ch} \le V_{max}^{AE,ch} U_t^{AE,ch} \quad \forall t \quad (3\text{-}19)$$

$$V_{min}^{AE,di} U_t^{AE,di} \le V_t^{AE,di} \le V_{max}^{AE,di} U_t^{AE,di} \quad \forall t \quad (3\text{-}20)$$

$$U_t^{AE,ch} + U_t^{AE,di} \le 1 \quad \forall t \quad (3\text{-}21)$$

$$S_{t+1}^{AE} = S_t^{AE} + V_t^{AE,ch} - V_t^{AE,di} \quad \forall t \quad (3\text{-}22)$$

$$S_{min}^{AE} \le S_t^{AE} \le S_{max}^{AE} \quad \forall t \quad (3\text{-}23)$$

$$S_{ini}^{AE} = S_{N_T}^{AE} \quad (3\text{-}24)$$

where V is the energy equal with compressed/expanded air, a is the energy conversion rate of SCAES, P is electrical power, V_{min}^{AE} is the minimum energy equal to compressed/expanded

air, V_{max}^{AE} is the maximum energy equal to compressed/expanded air, U is the binary variable indicating ON/OFF or active/deactivate, S is the level of stored energy in the air tank, $S_{min\ (max)}^{AE}$ is the minimum (maximum) capacity of the air tank of SCAES, $S_{ini(Nt)}^{AE}$ is the air stored in the SCAES tank in the first hour (last hour).

It is considered the system operator can exploit all the available air stored in the reservoir tank during the scheduling period. In the operation procedure of the SCAES, ambient air is compressed into the tank during the injection cycle by consuming $P_t^{AE,ch}$ and using electrical-thermal efficiency factor a^{ch} based on (3-17). A similar procedure for discharge mode is defined in (3-18); while charging/discharging energies of SCAES are limited by (3-19) and (3-20), SOC for the storage unit is formulated by (3-21). As indicated in (3-22), SCAES has a specified capacity which limits the total charging/discharging energy amounts. Obviously, the SCAES can operate in one of the charging or discharging modes during each hour as formulated in (3-23), where the initial amount of energy S_{ini} should be equal to the amount of stored energy at the last hour of scheduling $S_{N_T}^{AE}$ based on (3-24).

3.1.2 Formulation of DSO participation in day-ahead market

$$max\,[Profit] = Rev^{GR} - PC^{al} - OC^{AE} \tag{3-25}$$

$$Rev^{GR} = \sum_{t=1}^{N_T} P_t^{GR,ex}\pi_t^{DA,sal} - P_t^{GR,im}\pi_t^{DA,buy} \tag{3-26}$$

$$PC^{al} = \sum_{t=1}^{N_T} P_t^{al}.\pi_t^{DA,buy} = \sum_{t=1}^{N_T}\sum_{l=1}^{N_L} r^l\left(i_t^l\right)^2 \pi_t^{DA,buy} \tag{3-27}$$

$$P_t^{PV} + P_t^{GR,im} + P_t^{AE,di} + P_t^{CS,gm} = P_t^{GR,ex} + P_t^{AE,ch} + P_t^{CS,cm} + P_t^{D} + P_t^{al} \qquad \forall t \tag{3-28}$$

where, Rev is the revenue harvested from transactions with the market, PC is the operating cost of the grid due to power loss, *GR* is the index for the grid, ex is the index for exported power to the upstream grid, day-ahead is the index for the day-ahead market, PV is the index for solar units, im is the index for imported power from the upstream grid, sal is the index for selling power to the day-ahead market, *buy* is the index for buying power from the day-ahead market, π is the price of electricity in the day-ahead market, al is the Index for the active power loss of the grid, l is the index for branch number of the grid, N_L is the number of grid branches, r is the electrical resistance of the branch, i is the electrical current of the branch, CS is the index for EVCS, gm is the index for power generation mode of EVCS, cm is the index for power consumption mode EVCS, and D is the index for load demand.

DSO aims to maximize its day-ahead profit by (3-25), which is defined as the difference between DSO's revenue of transaction with the market (selling/buying based on (3-26)) and the total operating costs (i.e., power losses and SCAES operation cost). The cost of active power losses of the network is formulated by (3-27). Balance of supply and demand is formulated in (3-28); while the uncertainty of solar units is neglected in this study.

3.1.3 Formulation of EVCS

The EVCS is considered as an energy storage unit in this research and formulated as follows.

$$0 \le P_t^{CS,\Lambda} \le P_t^{CS,tc} U_t^{CS,\Lambda} \qquad \forall t, \Lambda = gm, cm \qquad (3\text{-}29)$$

$$U_t^{CS,gm} + U_t^{CS,cm} \le 1 \qquad \forall t \qquad (3\text{-}30)$$

$$P_t^{CS,tc} = \gamma^{CS} n_t^{CS} \qquad \forall t \qquad (3\text{-}31)$$

$$n_t^{CS} = \min\left(N^{CS}, N_t^{EV,cdf}\right) \qquad \forall t \qquad (3\text{-}32)$$

$$E_t^{CS}=E_{t-1}^{CS}+P_t^{CS,cm}\eta^{CS,cm} - P_t^{CS,gm}/\eta^{CS,gm} + E_t^{CS,ar} - E_t^{CS,dp} \qquad \forall t \qquad (3\text{-}33)$$

$$E_t^{CS,\Re} = \sum_{k=1}^{n_t^{CS}} E_{t,k}^{EV,\Re} \qquad \forall t, \Re=Arr, Dep \qquad (3\text{-}34)$$

$$E_t^{CS} \le Ca^{CS} \qquad \forall t \qquad (3\text{-}35)$$

$$SOC_{min}^{EV} \le SOC_t^{EV} \le SOC_{max}^{EV} \qquad \forall t, \forall PEV \qquad (3\text{-}36)$$

$$TC^{EV} = \frac{Cap^{EV}(1 - SOC_t^{EV})DoD^{EV}}{\eta^{CS,cm}\, P^{EV}} \qquad \forall t, \forall PEV \qquad (3\text{-}37)$$

where, tc is the index for the total hourly capacity of EVCS, EV is the index for PEV, dp is the index for the departure of PEVs, ar is the index for the arrival of PEVs, N^{CS} is the number of available chargers in EVCS, cdf is the index for CDF based data generation, $\gamma^{CS}$is the charging/discharging capacity of chargers in EVCS, $n_t^{CS}$is the hourly number of potential serving-charger in EVCS, k is the index of PEV, η^{CS} is the efficiency of chargers in EVCS, E is the level of electrical stored energy in EVCS, Ca is the electrical capacity of EV or EVCS, SOC is the EVCS's state of charge, and $SOC_{\min\,(max)}^{EV}$ is the minimum (maximum) SOC of PEVs when entering EVCS.

Power generation/consumption of EVCS is limited to the total capacity of EVCS by (3-29) and (3-30) in each hour, while this hourly capacity is calculated by (3-31) using the chargers' capacity and the number of available PEVs (n_t^{CS}). Parameter n_t^{CS} in (3-32) is constrained by the number of chargers and the number of PEVs entering to the station, generated by CDF which will be detailed in Section 3.1.3. The power level of EVCS as calculated by (3-33) is changing continuously as the result of power exchange with the grid as well as the

arrival/departure of PEVs (3-34), while the positive variable of E_t^{CS} should be limited within its nominal capacity of charging (3-35). From the other side, the EVCS operator sets a minimum SOC level for PEVs entering the station by (3-36) to reach a higher amount of available reserve energy during peak hours. SOC_t^{EV} for each PEV can be obtained from $((AER - d_t^{EV})/AER) \times 100\%$ using the travelled distance (d^{EV}) and all-electric range (AER) [202]. Besides, the required time for recharging of PEVs (TC^{EV}) is formulated by (3-37) based on their SOC and electrical specifications of battery and charger.

3.1.4 Formulation of distribution grid operational constraints

Management of the grid is subjected to operating constraints, as illustrated by (3-38)-(3-41).

$$0 \leq P_t^{GR,im} \leq \left(\bar{P}_{NET} + P_{max}^{AE,Exp} + Ca^{CS}\right) U_t^{GR,im} \qquad \forall t \qquad (3\text{-}38)$$

$$0 \leq P_t^{GR,ex} \leq \left(P_{max}^{AE,Com} + Ca^{CS} + P_t^{PV}\right) U_t^{GR,ex} \qquad \forall t \qquad (3\text{-}39)$$

$$0 \leq U_t^{GR,im} + U_t^{GR,ex} \leq 1 \qquad \forall t \qquad (3\text{-}40)$$

$$0.95 \leq Vol_t^B \leq 1.05 \qquad \forall t \qquad (3\text{-}41)$$

where, Vol is the per-unit of voltage at load points, and B is the index for buses of the grid. The importing power of grid considering the marginal situation of $P_t^{PV}=0$ is constrained by the aggregation of load demand and the power required for charging energy storage units (3-38); while considering the marginal state $P_t^D=0$, the exporting power to the upstream grid is constrained by the power provided by DERs and storage units (3-39). In (3-38) and (3-39), $P_{max}^{AE,Exp}$ and $P_{max}^{AE,Com}$ refer to maximum power of SCAES expander and compressor, respectively. Given the small amount of power loss, it is not included in these two marginal

situations. To maintain the voltage power quality, the acceptable range for the voltage of buses is limited to [0.95, 1.05] by (3-41). In order to consider the network constraints for day-ahead operation while determining hourly voltage profile Vol_t^B of the buses and branch current i_t^l for power loss calculation, a direct iterative distribution AC power flow based on Bus-Injection to Branch-Current (BIBC) matrix **BIBC** and Branch-Current to Bus-Voltage (BCBV) matrix **BCBV** (3-42)-(3-44) [203] is run for each hour of scheduling (i.e., for each candidate solution of the optimization algorithm). All DG and storage units are modeled as PQ sources.

$$I_i^k = I_i^r\left(V_i^k\right) + jI_i^i\left(V_i^k\right) = \left(\frac{P_i + jQ_i}{V_i^k}\right)^* \tag{3-42}$$

$$[\Delta V^{k+1}] = \mathbf{BCBV}\ \mathbf{BIBC}\ [I^k] \tag{3-43}$$

$$[V^{k+1}] = [V^0] + [\Delta V^{k+1}] \tag{3-44}$$

where V_i^k and I_i^k are the bus voltage and equivalent current injection of bus i at the k-th iteration, respectively. I_i^r and I_i^i are the real and imaginary parts of the equivalent current injection of bus i at the k-th iteration, respectively. The **BCBV** and **BIBC** matrix are calculated as in [203].

3.1.5 Copula modeling

It is a challenging issue to generate random inputs while maintaining their inherent dependence when they are not distributed based on standard multivariate probability functions. Besides, limited types of dependence can be modeled by some of the currently available standard multivariate distributions. Moreover, using these distributions cannot guarantee to reach sensible and real results. In this chapter, the CDF is employed to model

the behaviors of the PEVs. Compared to other estimation methods, CDF can interpolate multivariate-data nonlinearly. A Gaussian copula is a modeling option to present the dependence between variables. For a d-dimensional copula, the Gaussian copula is a distribution over the unit cube $[0,1]^d$. The copula of $(X_1, X_2, \dots X_d)$ is defined as the joint cumulative distribution function of $(U_1, U_2, \dots U_d)$:

$$C(u_1, u_2, \dots c_d) = \Pr[U_1 \leq u_1, U_2 \leq u_2, \dots U_d \leq u_d] \tag{3-45}$$

In fact, all dependence information between components of $(X_1, X_2, \dots X_d)$ are modeled in copula C. For a given correlation matrix $\mathcal{R}\epsilon[-1,1]^{d\times d}$, the Gaussian copula with parameter matrix $\mathcal{R}$ can be written as:

$$c_{\mathcal{R}}^{G} = \frac{1}{\sqrt{\det \mathcal{R}}} exp\left(-\frac{1}{2} \begin{pmatrix} \Phi^{-1}(u_1) \\ \vdots \\ \Phi^{-1}(u_d) \end{pmatrix}^{T} .(\mathcal{R}^{-1}\text{-}I) \begin{pmatrix} \Phi^{-1}(u_1) \\ \vdots \\ \Phi^{-1}(u_d) \end{pmatrix} \right) \tag{3-46}$$

where Φ^{-1} is the inverse cumulative distribution function of a standard normal distribution, and I is the identity matrix. Noteworthy, there exists the reverse procedure for this modeling process, which can be used to generate pseudo-random samples from general classes of multivariate probability distributions, and it is possible to generate a sample $(U_1, U_2, \dots U_d)$ from the copula distribution. Therefore, the required sample can be constructed by:

$$(X_1, X_2, \dots X_d) = \left(F_1^{-1}(U_1), F_2^{-1}(U_2), \dots, F_d^{-1}(U_d) \right) \tag{3-47}$$

Since PEV variables (including traveled distance and entry time to EVCS) are statistically dependent, a dual CDF is generated based on the actual data of PEVs [204]. A Gaussian CDF with correlation factor [1, 0.77665; 0.7766, 1] is used to generate the data. To this end, data from 50 PEVs are based for the generation of 2000 units (i.e., the number of vehicles in the

fleet of PEVs under contract with EVCS).

3.2 Solution algorithms

The presented problem is divided into two sections. The first part is the thermal formulation of the problem, which is solved using a finite step method (FDM). FDM is a numerical method for solving differential equations by approximating them with difference equations (i.e., using finite differences to approximate the derivatives). In our study, FDM becomes an excellent approximation for the work required when using mass increments equal to or less than 10^{-2} kg. Hence a mass increment of 10^{-2} kg is used for the numerical model to guarantee the convergence of the solution.

The second part of the problem (electrical part) is solved by swarm robotics search & rescue (SRSR) optimization algorithm. This algorithm was proposed by one of the authors in 2017 based on the artificial intelligence of a swarm of robots that are utilized for a search & rescue mission [131], and it has been compared with a number of previously presented algorithms in terms of convergence quality and convergence speed. Reasonable superiority of the SRSR algorithm compared to previous optimization algorithms had been demonstrated in [131]. For benchmark functions, the SRSR was applied on several standard benchmark functions and a practical EPS problem in several real-size case studies (i.e., unit commitment for thermal units with up to 100 generating units, which includes more than 4800 mixed-integer and continuous variables) in medium and large scales [205, 206]. It is noted that the dimension of the current problem is much lower than those previously solved by SRSR. Besides, while the evolutionary algorithms may not be reliable for real-time cases due to their stochastic natures, for day-ahead problems which the operator has enough time to run the

algorithm with a larger number of initial solutions and iterations, it is expected the algorithm will reach very close to optimal solutions which can be suitably utilized in real applications.

In this research, the number of initial solutions and the number of function evaluations (as the stop criterion) are considered to be 100, 15000, respectively. There exist four control parameters in the optimization algorithm, including movement factor, Sigma factor, Sigma limit, and Mu factor, while the first three factors are automatically tuned, and the last factor is set to 0.7. The program has been run 20 times, and the best result has been presented in the chapter. The execution time of the program (joint thermal-electrical modeling) is about 7 minutes for each run. Since an evolutionary algorithm is employed for the optimization task, a constraint handling method based on penalty factors [207] is used to remove infeasible solutions that guarantee operational constraints are always met.

3.3 Case study and results

In this study, simultaneous cooperation of a SCAES and an EVCS as energy storage units is investigated for the participation of an ADS in the day-ahead energy market. IEEE 33-bus DN with the load-demands of 3.7MW and 2.3MVAR is used as the test system [208]. This research focuses on the daily operation of the ADS; therefore, previous studies are the basis to select the proper locations for the installation of PVs and energy storage units. The aim is to determine a daily operation of the DN to maximize the total profit of DSO (i.e., owner of the network's components) from participating in the market.

The production patterns of solar units shown in Fig. 3-3, located on buses 12, 17, 22, 31, and 33 are used for simulation [9]. The power factor of all PV units is considered 0.9 due to the presence of electronic converters.

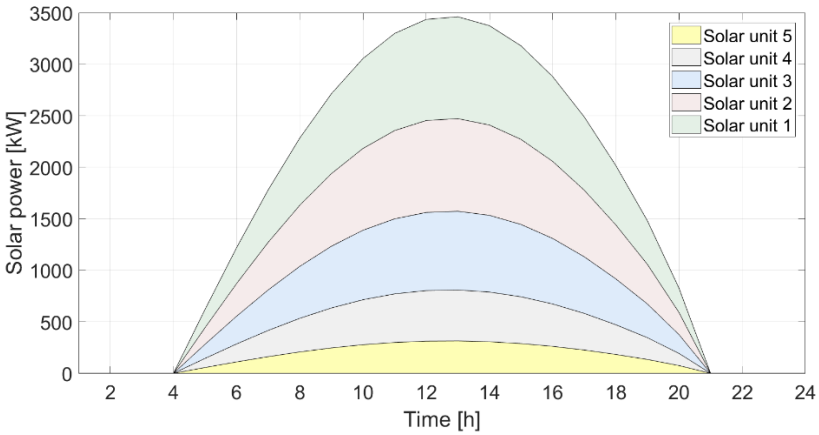

Fig. 3-3. Accumulative generation profile of PVs

The detailed specification of adiabatic SCAES is provided in Table 3-1. The minimum capacity of SCAES corresponds to the pressure in which SCAES cannot provide a constant amount of power. Prices for sale/purchase of energy in the market are shown in Table 3-2.

Table 3-1. Data for SCAES [152]

Max & Min capacity [kWh]	Motor capacity [kWh]	Generator capacity [kWh]	Location bus	Initial state [kWh]	Reservoir capacity [m^3]
2000 & 350	500	500	28	1000	182

Table 3-2. Selling/Purchasing Energy Prices in Market [Cent]

Hour	1	2	3	4	5	6	7	8	9	10	11	12
Selling	63	53	51	50	51	52	63	67	73	80	80	80
Buying	106	106	106	106	106	106	106	125	135	135	135	135
Hour	13	14	15	16	17	18	19	20	21	22	23	24
Selling	70	69	73	79	80	71	66	67	72	77	67	63
Buying	135	135	135	135	135	135	135	125	125	125	125	106

Noticeably, the selling price is lower than the cost of electricity purchased from the grid due to transmission costs. There are several types of PEVs (e.g., PEV-20, PEV-30, PEV-40, and PEV-60) based on the all electrical range (AER) factor in which the numeric index indicates the vehicle AER in terms of miles [202].

We use the PEV-20 in this chapter which has proven its market potential over time. All cars in the fleet of PEVs have been considered to be manufactured by Nissan with an energy capacity of 100 kWh and also have similar contracts with EVCS [209]. Based on a bilateral contract, the EVCS operator uses PEVs with SOC not less than 50% when entering a parking station, and the minimum duration of staying in the EVCS is 6 hours. In exchange for that, there is no parking cost for these vehicles. If a vehicle leaves the car park before this period, the car owner should pay a very low price of energy for the remaining hours. Transactions of other vehicles with EVCS are not modeled in this study. In the following, the conditions and assumptions for five scenarios are presented to validate the effectiveness of the proposed methodology. Then, the detailed investigation and comparison of the obtained results of different scenarios are provided in the last subsection.

3.3.1 Scenario 1: Base case

In this scenario, solar and energy storage units (EVCS and SCAES) are not considered in the model. This scenario provides base values for normal operation of the standard IEEE 33-bus DN.

3.3.2 Scenario 2: Without energy storage units

This scenario considers the presence of PVs while EVCS and SCAES are not involved in the grid operation. The voltage limit [0.95, 1.05] p.u. for buses is not applied in this case. Hourly loads of buses are generated using the normal distribution function that ranges within ±20% of the nominal load for all the scenarios. Active and reactive loads for network buses are shown in Fig. 3-4.

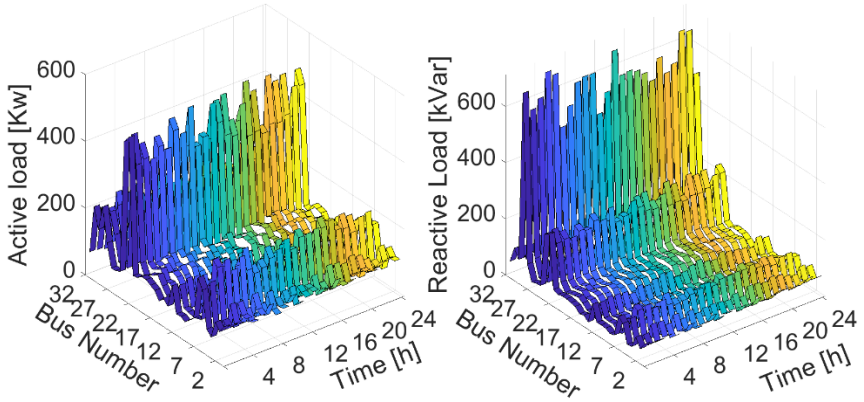

Fig. 3-4. Hourly active and reactive loads (24 hours) for 33-bus Network

3.3.3 Scenario 3: Solar units and EVCS

This scenario investigates the simultaneous cooperation of PV units as generation sources and EVCS as an energy storage unit. EVCS considers DOD as 0.4 to extend the life cycle of batteries. If the SOC of a PEV at the leaving time is less than its initial charge level when entering the charging station, EVCS must pay the cost of the used energy at the price of the wholesale market. The EVCS uses level 3 chargers with a maximum capacity of 96 kW. The SOC and entrance time of PEVs using CDF are depicted in Fig. 3-5.

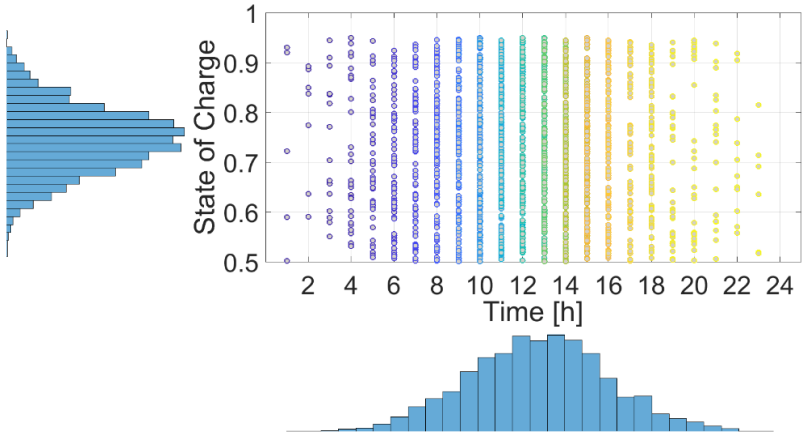

Fig. 3-5. PEVs' SOC and arrival time (EVCS located on bus 18)

It can be seen that the middle hours of the day have the highest power availability for

EVCS.

3.3.4 Scenario 4: Solar units and SCAES

In Scenario 4, the EVCS unit in Scenario 3 is replaced by a SCAES system. Besides the electrical specifications detailed in Table 3-1, the constant thermal factors of SCAES and PBHE are simulated based on the experiment results of [161] as well as the simulations of [152]. Two compression stages ($p_2 = 8.106\ Mpa$) are considered for SCAES while a pressure drop of 5 kpa is assumed for each packed bed which results in the pressure ratio of $r = 8.97$). The minimum and maximum storage pressure are 2.027 and 8.106 MPa, respectively.

3.3.5 Scenario 5: Solar units, EVCS and SCAES

This scenario explores the benefit of simultaneously utilizing EVCS and SCAES. The potential advantages and weaknesses of each type of storage units are investigated in this scenario. The specifications of both energy storages are considered as the same as previous scenarios.

3.3.6 Comparison of results and discussions

In the case of Scenario 1, the simulation result indicates that the active hourly loss of the grid is 210.98 kW, while the voltage profile at bus 18 has the lowest value, which is not within the acceptable voltage range 0.95~1.05 p.u. for the normal network operation. Since there is no generation unit, all the power needed to meet the demand should be purchased from the upstream grid. However, as it can be deduced from Fig. 3-6, adding PV units in Scenario 2 cannot prevent bus voltage violations during certain hours of the day, as the sunlight is only

available in the day time.

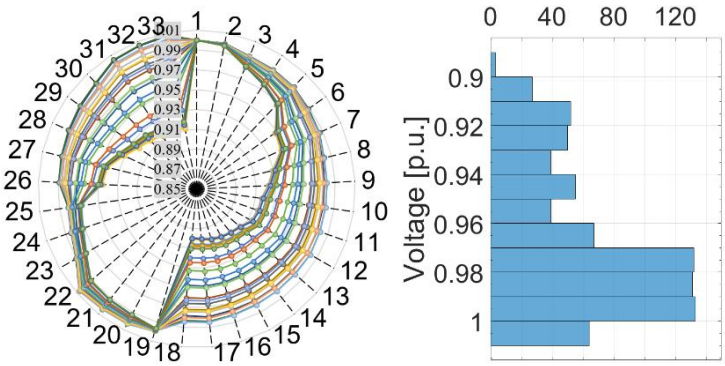

Fig. 3-6. 24-hour voltage profile of buses and relevant histogram; Scenario 2

Maximizing the net profit of the daily operation of the grid is the ultimate aim of the DSO in a restructured power market. However, the operation conditions of the network play key roles in maintaining the security of operation as well as satisfying the quality of service. In this regard, changes in hourly active power losses and voltage profiles of buses, as two major operation factors, are illustrated in Fig. 3-7 and Fig. 3-8 for all the scenarios. Compared to the base case in which the changes of power loss solely follow the hourly variations of load demand, the power provision of solar DERs significantly reduces the power loss of the system. However, the amount of power loss in Scenario 2 is still not controllable since the solar units are not dispatchable. Surprisingly, the total/hourly power loss in most of the hours is increased by using only EVCS and SCAES in Scenarios 3 and 4, respectively, which is due

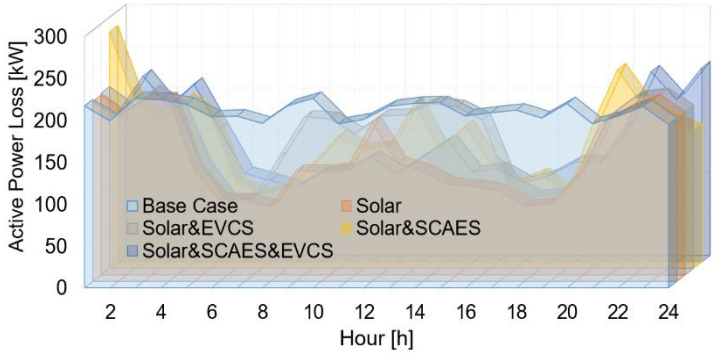

Fig. 3-7. Daily active power loss comparison of the grid, all scenarios

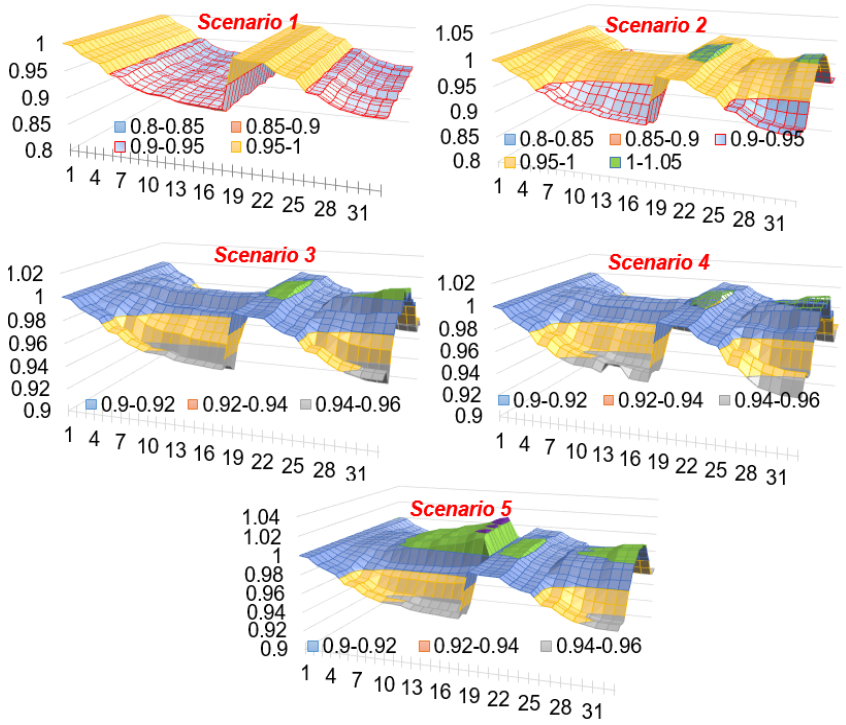

Fig. 3-8. Voltage profile of grid buses for 24h scheduling, all scenarios

to the profit maximization objective.

The availability of EVs in Scenario 3 and the charging pattern of SCAES in Scenario 4 are other reasons for such degradation. It can be seen that the simultaneous use of these two devices provides a significant power loss reduction in Scenario 5. The energy provided during high accessibility of EVCS is exchanged with SCAES to control the power loss, which has a negative impact on the revenue of DSO. Noteworthy, certain availability of SCAES is a reason for the superiority of SCAES over EVCS.

In the case of the voltage profile of the network in Scenarios 1 and 2, the lack of generation causes the voltage violations at some buses of the grid in some hours. The other scenarios can sufficiently improve the voltage of buses to reach the defined range (0.95-1.05 p.u.). Despite similar voltage profiles in Scenarios 3 and 4, the indicator of voltage profile over all buses

$\left(\sum_t^{N_T}\sum_B^{N_{Bus}}(Vol_t^B-1)^2/N_T.N_{Bus}\right)^{0.5}$ or these scenarios are 0.0224 and 0.0227 p.u., respectively, which shows a slight superiority of SCAES in terms of voltage improvement. This value for Scenario 5 is 0.0207 p.u. It is evident from Fig. 3-8 that employing both the EVCS and SCAES at the same time can considerably enhance the voltage profile to about 1.04 p.u. at some hours. Evidently, the voltage values at deep voltage points of the grid are set to near the lower margin of 0.95 p.u. for several hours, which means the algorithm does intend to sacrifice the profit for voltage profile enhancement. Based on Fig. 3-9, the comparison of power provision and demand of EVCS in Scenarios 3 and 5 illustrates that the share of charging station generation is decreased after SCAES participation in Scenario 5.

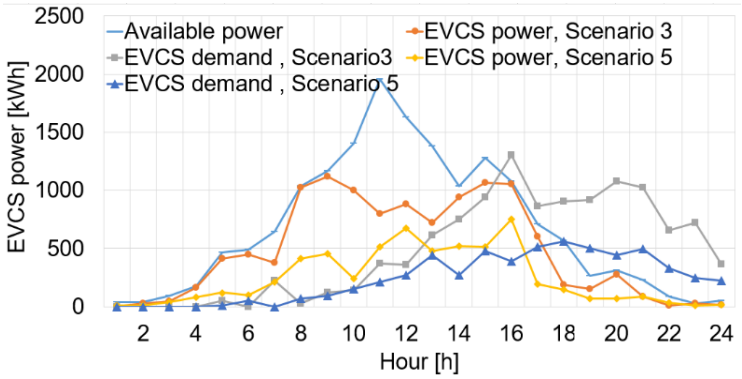

Fig. 3-9. Power provision and power shift of EVCS for 3rd and 5th scenarios

It can be inferred that no more generation is needed to reach the maximum profit despite having available capacity. The reason for not exploiting the full capacity of EVCS is that a large number of PEVs do not have SOC more than 50%. Moreover, scheduling should be accomplished in such a way that energy received from PEVs returns to vehicles during the next hours. EVCS should adopt a demand management approach to control the usage of available batteries. In addition, a load shifting can be observed in both scenarios from peak demand hours of the main grid to the last hours of the day; this is due to the departure pattern

of PEVs as well as the optimization preference of the algorithm. The charging/discharging pattern of SCAES for Scenarios 4 and 5 is shown in Fig. 3-10.

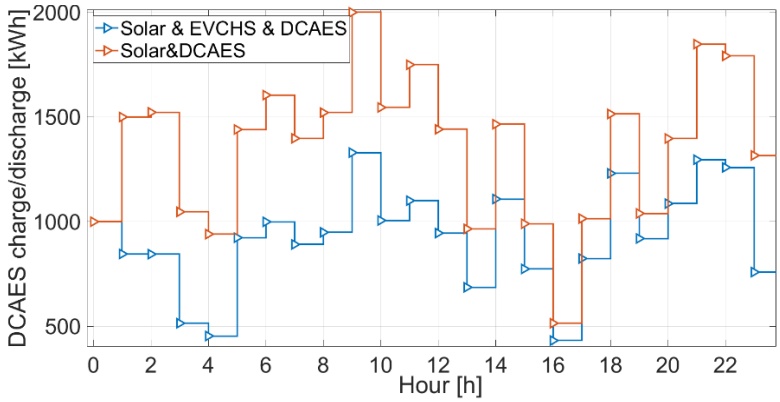

Fig. 3-10. Charge/discharge pattern of SCAES

Similar to the EVCSs, the share of energy provision of SCAES is decreased in the joint operation, which means the coupled SCAES and EVCS can handle larger grids. Considering the load shifting of EVCS during the last hours of the day, which plays the role of extra demand, the SCAES can provide energy during these hours to maintain the security of the grid. Compared with the sole operations of energy storage systems in Scenarios 3 and 4, SCAES exploits nearly the full available capacity on hours 11 and 23 and provides $519 more profit in Scenario 4 considering the lower thermal-electrical conversion rate. Although EVCS is a dispatchable ES, some involving factors like availability of PEVs, maximum DOD, and minimum period of staying in EVCSs are critical factors, which downgrade the ultimate quality of EVCS services. Besides, SCAES can provide a uniform amount of at least 500 kW during the scheduling horizon; however, EVCS available capacity changes to much more/fewer amounts in some hours. A comparison of the daily power loss and DSO profit for five given scenarios is detailed in Table 3-3.

Table 3-3. Final comparison of different scenarios

	Scenario 1	Scenario 2	Scenario 3	Scenario 4	Scenario 5
24h power loss [kW]	5055.9	3504.3	4037.3	3774.2	3434.7
Operation profit [$]	-11598.3	-6248.4	-5859.3	-5340.9	-4587.1

The hourly transactions of DSO with the market are illustrated Fig. 3-11. It can be seen that energy storage units aim to gain their profits from those hours, while PV units generate at their maximum power. This is because a large share of the total hourly load demand is met by the local generation, in particular for the hours when the energy price is high. Obviously, SCAES can reach a better performance compared to EVCS in terms of voltage profile, power loss, and profit maximization. This is mainly because of the uncertainties in PEVs' arrival and departure times and their SOC when arriving at EVCS.

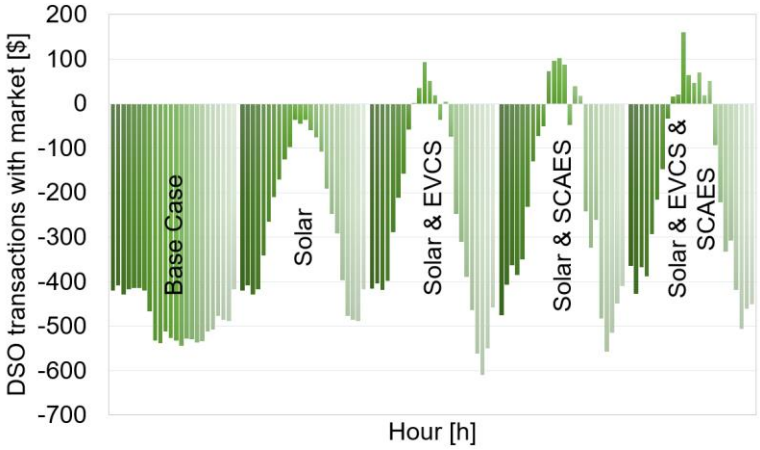

Fig. 3-11. 24h financial transactions of DSO with market

It should be noted that, this chapter models the SCAES using practical thermal-electrical conversion rates $a^{ch/di}$, which are lower than bulk-size CAESs. However, these rates are variable during the scheduling horizon, and the average efficiency of 71.16 % is harvested for SCAES, which means a^{ch} and a^{di} can be calculated as 0.8435 if the approximate assumption of $a^{ch} = a^{di}$ is considered. Hence, as opposed to large-scale CAES which have $a^{ch} = a^{di} =$

0.9, this value can be regarded as a reference for future research in DNs. In this regard, it is hopeful that SCAESs can reach an efficiency close to the large-scale CAESs with the advancement of phase change materials in thermal storages.

3.3.7 Performance analysis over the life cycle

This subsection investigates and compares the performance of SCAES with other alternative energy storage technologies (such as the Li-ion battery and EVCS technologies) for the whole life cycle. Their performance is simulated over a one-year cycle and will be normalized and expanded to their life cycle, considering the energy storage capital cost. In this regard, the yearly load demand of the grid is generated with the same approach adopted for daily operation. Profile of solar power generation and price of energy are based on the data provided by the Australian Energy Market Operator for the year 2019 [9]. Thermal parameters of SCAES are considered to be as the same as Scenario 4 for all days. The required data of battery storage units are provided in [12]. A comparison of DSO profit employing SCAES, battery bank, and EVCS for one year is depicted in Fig. 3-12 (daily in *subplot a* and cumulative in *subplot b*). Obviously, it can be seen that the daily profit of using battery banks is higher than other technologies due to their higher electric-to-electric efficiency. However, considering different capital costs and the number of life cycles for energy storage technologies, a fair comparison can be accomplished by considering these parameters. Based on [152], the total capital cost for a 2 MWh, 500 kW battery bank is estimated at $2–2.8 million, while this cost is estimated to be $0.72–1.3 million for SCAES. For a similar capacity of EVCS with the given number of chargers in this chapter, a capital cost of $1.1–1.6 million is estimated [180]. The highest capital costs are selected for the comparison task in the next

step. The numbers of charging cycles over lifetime for the battery bank, SCAES, and EVCS in the distribution grid are approximately 20000, 10000, 5000, respectively. Considering one full charge-discharge cycle per day, Fig. 3-12 (c) shows the life span profit considering the total capital expenditure of the energy storage unit.

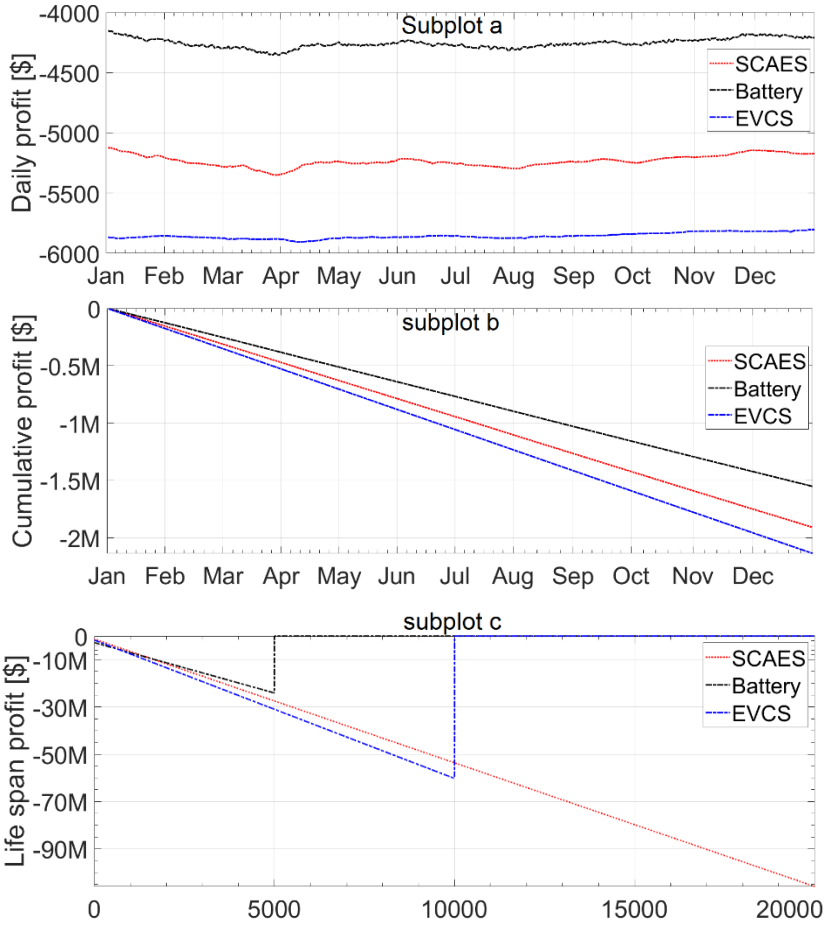

Fig. 3-12. Comparison of SCAES, Battery, and EVCS (a) daily DSO profit for a one-year period, (b) cumulative DSO profit for a one-year period, (c) cumulative DSO profit for the life span

The cost of operation and maintenance (O&M) is neglected in this case study for all the technologies; however, CAES has the lowest O&M cost followed by EVCS and battery bank. It can be seen that the battery bank can provide the highest saving during the first 5000 cycles while having the highest capital cost. Obviously, SCAES can provide much more profit

in the long term due to its longest life cycle.

3.4 Summary

In this chapter, the application of a utility-size SCAES as a potential energy storage technology for the participation of ADS in the wholesale power market is proposed. The thermal modeling of SCAES brings a new thermal-electrical conversation rate, which is suitable for SCAES utilization at the distribution level. The effectiveness of SCAES is evaluated by comparing EVCS performance in different scenarios of the sole and joint operation. Based on five operation scenarios presented in this study, the following results are obtained:

- Compared with EVCS, SCAES can assist the DSO to reach higher profits in the sole operation scenario. In addition, considering the benefits of SCAES over EVCS in the sense of power loss reduction and voltage profile improvement, SCAES can be employed as a reliant storage unit for other objectives in DN operation as well.
- Utilization of SCAES besides the EVCS can be an appropriate option for DSO to suitably tackle the uncertainty of EVCS, or other similar storages, in the joint operation mode.
- Although the SCAES thermal/electrical conversion rate 0.85 is currently lower than the corresponding rate 0.95 of bulk-size CAESs, the result of this study demonstrates that it is still an applicable energy storage technology for ADSs operation.
- Generation insufficiency, as well as uncertainties of the solar units and EVCS during the starting and ending hours of the day, are mitigated using SCAES.

The proposed SCAES can be operated as an asset of a DSO or be employed as a part of an aggregator. In this chapter, the first option of market participation was implemented. In the next chapter, an aggregated model will be developed for SCAES units, which can participate in the wholesale electricity market in cooperation with DSO.

Chapter 4 Joint Operation of a Compressed Air Energy Storage Aggregator and a Distribution System Operator for Participation in Day-Ahead Market

While large-scale CAESs have many applications in generation and transmission power systems based on the state-of-the-art, this chapter proposes the application of SCAESs as a new potential storage system in the daily operation of an ADS, joining the DSO for the participation in a day-ahead wholesale market. A two-agent modeling approach is formulated. The first agent is responsible for aggregating SCAES units and profit maximization of the aggregator based on the DLMP. The DSO, as the second agent, receives day-ahead scheduling from the independent SCAES aggregator and is responsible for the secure operation of the ADS utilizing solar and dispatchable DGs as well as purchasing power from the wholesale market. Linear programming is used for the formulation and optimization of the SCAES aggregator, while a bi-objective optimization algorithm (with the objectives of minimum operating cost as well as minimum power loss and emissions in different scenarios) is employed for DSO scheduling.

4.1 System configuration

The aggregated configuration and power/data exchange of the units for the proposed methodology is shown in Fig. 4-1. As can be seen, SCAES units are not under the operation of the DSO anymore and have been aggregated. The reason behind such aggregation is that the small-scale DG and energy storage units in most of the countries are not allowed to

Fig. 4-1. A structure of the proposed ADS configuration

participate in the electricity markets based on regulations and policy of markets [210]. Hence, the aggregation of storage units is an obligatory decision. In such a situation, two different structures can be considered for the participation of the CAES aggregator. First, the aggregator can participate in the day-ahead market individually and separate from DSO to enjoy the profit earned from price arbitrage in the market.

However, there always exists some risks for the aggregator due to fluctuations and uncertainties of the energy price. Consequently, CAES owners may take part in the faced risks. Second, the DSO participates in the market, and certain values of DLMP for different buses in different hours are sent to the CAES aggregator. This hourly DLMP (i.e., received from DSO) is normally lower than the market price. In the second framework, the benefit of the aggregator will be a share of CAES owners' profit (i.e., determined with a bilateral contract with the owner). This chapter follows the second structure in which no risk is considered for aggregators and CAES owners. In both structures, the scheduling of CAESs is needed to be sent to the DSO. After receiving the schedule from the aggregator, DSO needs to optimally schedule the power generation of diesel units and power purchase from the day-

ahead market to satisfy its own objectives considering the grid load demand and power forecast of solar units. Besides, the secure operation of the distribution system is a non-compromising issue for DSO, which is subject to grid constraints. In this chapter, it is assumed that solar units are non-dispatchable. It should be noted, the distributed model of ADS is used for the power flow simulation.

4.2 Problem formulations

In this section, the mathematical formulations for DSO objectives, CAES aggregator modeling, and operational constraints are provided.

4.2.1 Objective functions

$$Opt\{Objective\} = [\min f_1 \ , \min f_2 \ , \min f_3 \ ] \tag{4-1}$$

$$f_1 = Em = F^e \sum_{i=1}^{N_{DG}} \sum_{t=1}^{N_T} \left(a_i^{DG} P_{i,No}^{DG} + b_i^{DG} P_{i,t}^{DG}\right) U_{i,t} \tag{4-2}$$

$$f_2 = P^{Loss} = \sum_{t=1}^{N_T} \sum_{l=1}^{N_{Bus}} \sum_{m>l}^{N_{Bus}} G_{l,m} \begin{bmatrix} V_{l,t}^2 + V_{m,t}^2 - \\ 2V_{l,t}V_{m,t}cos\left(\delta_{l,t} - \delta_{m,t}\right) \end{bmatrix} \tag{4-3}$$

$$f_3 = OC^G = \sum_{t=1}^{N_T} P_t^{GRI} \pi_t^{Mar} + \pi^f \sum_{i=1}^{N_{DG}} \sum_{t=1}^{N_T} \left(a_i^{DG} P_{i,No}^{DG} + b_i^{DG} P_{i,t}^{DG}\right) U_{i,t} \tag{4-4}$$

In this chapter, three objectives are considered for DSO as follows:

The first one is to minimize the emissions produced by diesel generators in (4-2) [211]. a_i^{DG} and b_i^{DG} are the fuel consumption coefficients of diesel unit i, $P_{i,No}^{DG}$ is the nominal capacity of diesel unit i, $P_{i,t}^{DG}$ is power generation of diesel unit i at time t, F^e is the fuel-to-emission conversion rate, and $U_{i,t}$ refers to the ON/OFF status of diesel units.

The second objective is to minimize the total active power loss of the DN in (4-3) [11]. $G_{l,m}$ is the branch conductance between l^{th} and m^{th} buses, $V_{l,t}$ and $\delta_{l,t}$ refer to the magnitude and phase angle of the voltage of l^{th} node at time t, respectively.

The third objective is to minimize operating cost of the grid OC^G which includes the cost of buying power P_t^{GRI} from the day-ahead energy market and the fuel cost of running diesel units (4-4). Parameters π_t^{Mar} and π^f are the energy price in the day-ahead market and the fuel price, respectively. The operating and maintenance cost of diesel units are not considered in this chapter.

4.2.2 CAES aggregator formulations

$$V_{j,t}^{CAE,Inj} = a_j^{Inj} P_{j,t}^{CAE,Inj} \qquad \forall t, \forall j \qquad (4\text{-}5)$$

$$V_{j,min}^{CAE,Inj} U_{j,t}^{CAE,Inj} \le V_{j,t}^{CAE,Inj} \le V_{j,max}^{CAE,Inj} U_{j,t}^{CAE,Inj} \qquad \forall t, \forall j \qquad (4\text{-}6)$$

$$P_{j,t}^{CAE,Dis} = a_j^{Dis} V_{j,t}^{CAE,Dis} \qquad \forall t, \forall j \qquad (4\text{-}7)$$

$$V_{j,min}^{CAE,Dis} U_{j,t}^{CAE,Dis} \le V_{j,t}^{CAE,Dis} \le V_{j.max}^{CAE,Dis} U_{j,t}^{CAE,Dis} \qquad \forall t, \forall j \qquad (4\text{-}8)$$

$$U_{j,t}^{CAE,Inj} + U_{j,t}^{CAE,Dis} \le 1 \qquad \forall t, \forall j \qquad (4\text{-}9)$$

$$S_{j,0}^{CAE} = S_{j,N_T}^{CAE} = S_{j,ini} \qquad \forall j \qquad (4\text{-}10)$$

$$S_{j,min}^{CAE} \le S_{j,t}^{CAE} \le S_{j,max}^{CAE} \qquad \forall t, \forall j \qquad (4\text{-}11)$$

$$S_{j,t+1}^{CAE} = S_{j,t}^{CAE} + V_{j,t}^{CAE,Inj} - V_{j,t}^{CAE,Dis} \qquad \forall t, \forall j \qquad (4\text{-}12)$$

$$P_t^{ACE} = \sum_{j=1}^{N_{CAE}} P_{j,t}^{CAE,Dis} - P_{j,t}^{CAE,Inj} \qquad \forall t \qquad (4\text{-}13)$$

$$OC_t^{CAE} = \sum_{j=1}^{N_{CAE}} P_{j,t}^{CAE,Inj} VOM_{j,t}^{CAE,Inj} \qquad \forall t, \forall j \quad (4\text{-}14)$$
$$+ P_{j,t}^{CAE,Dis}\left(HR_j^{CAE,Dis} H_{NG} + VOM_{j,t}^{CAE,Dis}\right)$$

$$\max Rev^{ACE} = \sum_{t=1}^{N_T} (P_t^{ACE} \pi_t^{DLP} - OC_t^{CAE}) \quad (4\text{-}15)$$

In the case of presented SCAES, two operation phases of air injection Inj and power discharge Dis are considered. To this end, the stored energy $V_{j,t}^{CAE,Inj}$ in the storage tank of CAES j at time t is formulated by (4-5), where a_j^{Inj} is the charging energy conversion rate and $P_{j,t}^{CAE,Inj}$ is the active power consumed to charge CAES. The amount of hourly energy storage as defined in (4-6) is limited to the minimum $V_{j,min}^{CAE,Inj}$ and maximum $V_{j,max}^{CAE,Inj}$ hourly storage capacities, where $U_{j,t}^{CAE,Inj}$ is a binary indicator of injection operation mode. The power produced during the discharging mode of the CAES $P_{j,t}^{CAE,Dis}$ as a function of discharging energy conversion rate a_j^{Dis} and required stored energy $V_{j,t}^{CAE,Dis}$ is calculated in (4-7). As indicated in (4-8), this required energy during discharge mode is limited to the minimum value $V_{j,min}^{CAE,Dis}$ and maximum value $V_{j.max}^{CAE,Dis}$ due to physical limitations of conversion systems, where $U_{j,t}^{CAE,Dis}$ is the binary indicator of discharging mode of the CAES. Obviously, a CAES unit can be operated in only one of the states of idle, charging, or discharging mode during each time step in (4-9). Besides, the energy stored in the storage tank of CAES at the first hour of scheduling $S_{j,ini}$ and at the last hour S_{j,N_T}^{CAE} should be equal; and they are set to the predefined value $S_{j,0}^{CAE}$ by (4-10). Eq. (4-11) defines the minimum $S_{j,min}^{CAE}$

and maximum $S_{j,max}^{CAE}$ air storage capacities of the jth CAES. The variation of stored energy level in the CAES tank as the result of charging/discharging is given in (4-12). While the formulations (4-2)-(4-12) model each of the SCAESs, the total power available P_t^{ACE} for CAES aggregator ACE as a sum of charging/discharging power of CAESs is calculated by (4-13). The operation cost of a CAES unit OC_t^{CAE} is given in (4-14) where $VOM_{j,t}^{CAE,Inj}$ and $VOM_{j,t}^{CAE,Dis}$ are the variable operating costs of a CAES during injection and discharge modes, respectively. Considering a gas turbine in discharging procedure as simple cycle mode of CAES, $HR_j^{CAE,Dis}$ refers to fuel heat rate for discharging phase of CAES and H_{NG} is the price of natural gas. However, considering the small scale and the lack of gas turbines in the presented CAES units, the operating cost of these units is neglected in this study. Therefore, maximizing the revenue of the aggregator Rev^{ACE} is formulated as the sum of hourly profits/costs, which is obtained from selling/purchasing power to/from DSO P_t^{ACE} at the local energy price π_t^{DLP}. It is assumed that the energy conversion rates for charge and discharge procedures are considered to be a fixed value and $a_j^{Inj} = a_j^{Dis} = 0.85$. Note, this value is lower than that for large-scale CAESs due to lower thermal efficiency of the heat exchanger in SCAESs.

4.2.3 Distribution power flow equations:

$$P_l = \sum_{m=1}^{N_{Bus}} V_l V_m Y_{l,m} \cos\left(\Theta_{l,m} - \delta_l + \delta_m\right) \tag{4-16}$$

$$Q_l = -\sum_{m=1}^{N_{Bus}} V_l V_m Y_{l,m}\, sin\left(\Theta_{l,m} - \delta_l + \delta_m\right) \tag{4-17}$$

Power flow equations for active and reactive powers are defined in (4-16) and (4-17); where P_l and Q_l are the injected active and reactive powers at the l^{th} node. V_l and δ_l are the amplitude and angle of voltage at l^{th} node. $Y_{l,m}$ and $\Theta_{l,m}$ are the amplitude and angle of the $(l,m)^{th}$ entry of bus admittance matrix.

4.2.4 Operating constraints

a) Bus voltage limit:

$$V_{min} \leq V_i \leq V_{max} \tag{4-18}$$

The voltage of buses should be limited within the operating range $[V_{min}, V_{max}]$, where V_{min} and V_{max} are the minimum and maximum acceptable voltage values of the i^{th} node, and V_i is the voltage magnitude of the i^{th} node.

b) Distribution line limits:

$$\left|P_{ij}^{line}\right| \leq P_{ij,Max}^{line} \tag{4-19}$$

Eq. (4-19) limits the power flow of transmission lines P_{ij}^{line} due to thermal capacity of branches, where $P_{ij,Max}^{line}$ is the maximum power transmitted between nodes i and j.

c) Power balance constraints:

$$\sum_{i=1}^{N_{DG}} P_{i,t}^{DG} + \sum_{i=1}^{N_{PV}} P_{i,t}^{PV} + P_t^{ACE} + P_t^{GRI} = P_t^{Dem} + P_t^{Loss} \qquad \forall t \tag{4-20}$$

The power generation-demand balance of the grid is given by (4-20), where $P_{i,t}^{DG}$ is the

power generation of diesel DGs, $P_{i,t}^{PV}$ is the power generation of solar units, and P_t^{Dem} is the hourly load demand of the grid.

d) DG resources modeling:

In general, DG units in the DN are modeled as PV and PQ nodes [212]. Considering DGs as a PV model, they can generate reactive power while keeping the voltage amplitudes within an acceptable range. In this study, the PQ model is adopted to formulate DGs in the distribution grid.

4.3 Solution approach

The flowchart for the solution methodology proposed in this chapter is depicted in Fig. 4-2.

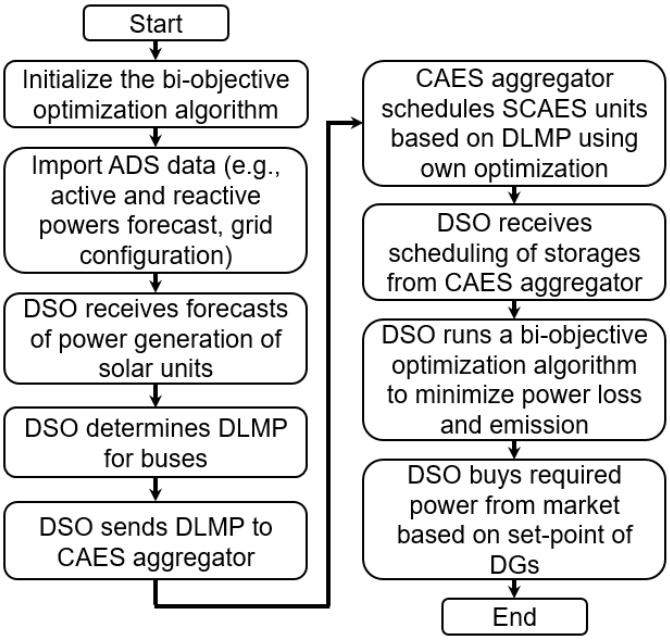

Fig. 4-2. The flowchart of the proposed methodology

As aforementioned, the presented problem is divided into two sub-problems. The first part should be solved by the CAES aggregator, which is an optimization problem to maximize the

profit of each CAES unit based on DLMP received by DSO. Because the formulations in this part have been linearized, it can be easily solved by an available linear programming toolbox. In this chapter, the *linprog* package of the MATLAB software is used to solve this sub-problem. After determination of the scheduling for CAES units, the power generation of diesel units, as well as the power needed to be purchased from the day-ahead market, should be scheduled by DSO in the second sub-problem. In this regard, the bi-objective SRSR optimization algorithm is used to optimize the financial or operational objective functions for DSO. Noteworthy, this optimization algorithm was proposed by one of the authors in 2017 based on the artificial intelligence of a swarm of robots that are utilized for a search & rescue mission [131]. The number of function evaluations (as the stopping criterion) and initial solutions are 10000 and 100, respectively. The number of solutions in the Pareto front is limited to 50. While the first three controlling parameters (i.e., movement factor, Sigma factor, and Sigma limit) of the algorithm are tuned automatically, and the last controlling parameter (i.e., Mu factor) is considered to be 0.7.

It should be noted that the DLMP is considered to be calculated and has been sent by DSO to the aggregator before scheduling. In fact, LMP is a way for wholesale electric energy prices to reflect the value of electric energy at different locations, accounting for the patterns of load, generation, and the physical limits of the transmission system. There are a large number of studies that have detailed calculation of DLMP for ADSs. At the distribution level, after estimating the wholesale energy price for the next 24 hours, the DSO calculates the DLMP based on its own objectives. For example, a DSO may increase the price for some end buses of a feeder during peak hours to encourage nearby DG units to increase their generation and compensate for voltage drop. In this chapter, the DLMP is negatively correlated with the

voltage of the buses.

4.4 Results and discussion

In this study, the simultaneous scheduling of a CAES aggregator, as well as generating

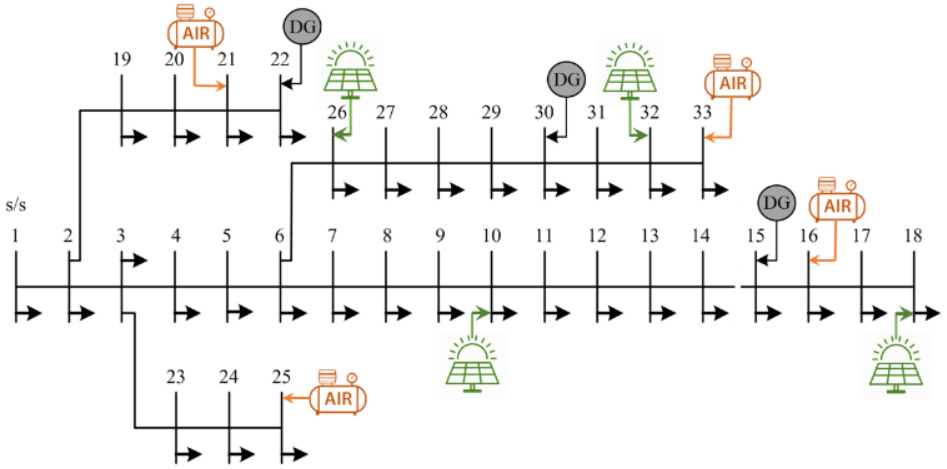

Fig. 4-3. Configuration of IEEE 33-bus test system

units of the DSO, is investigated for the participation in the day-ahead electric power market. IEEE 33-bus DN (Fig. 4-3) with a load of 3.7MW and 2.3MVAR is used as the test system [213]. It is assumed that the locations of storage and generating units are predefined as the current problem is operation scheduling. The power generation of solar units located at buses 10, 18, 26, 32 is detailed in Fig. 4-4.

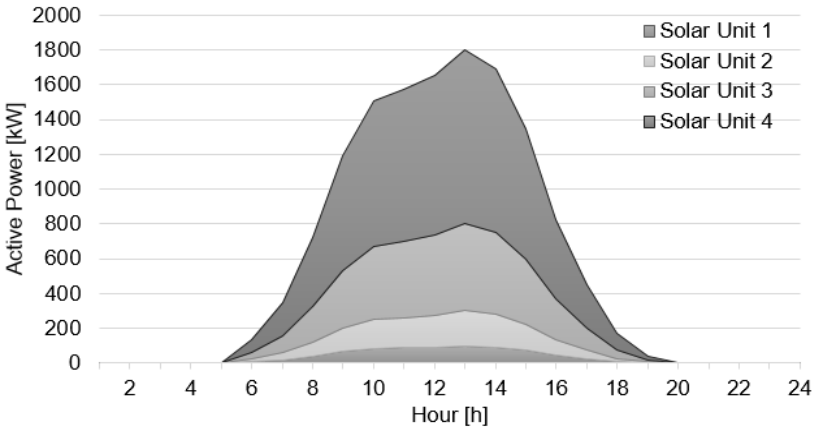

Fig. 4-4. Power generation of solar units

The hourly active and reactive power demands of the DN are depicted in Fig. 4-5 and Fig. 4-6, respectively.

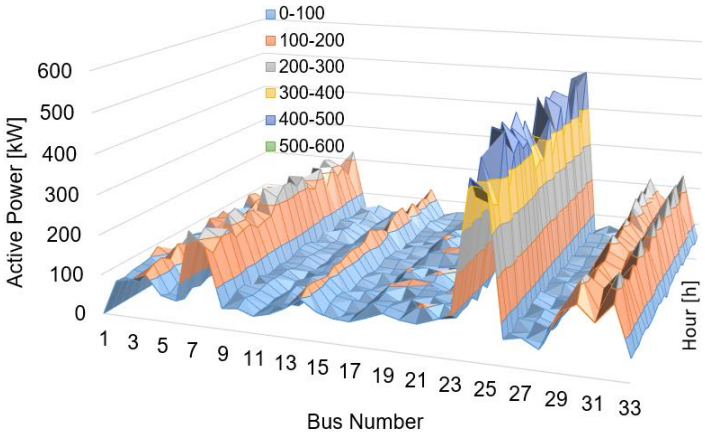

Fig. 4-5. Active load demand of the grid for a 24h scheduling

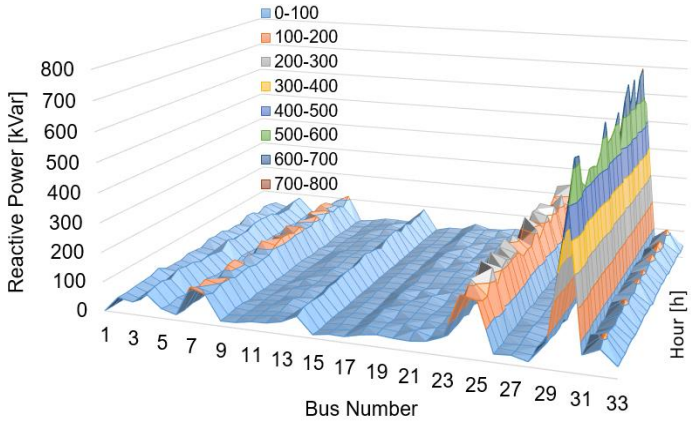

Fig. 4-6. Reactive load demand of the grid for a 24h scheduling

The specification of CAES and diesel units are detailed in Table 4-1 and Table 4-2, respectively.

Table 4-1. Specification data for CAES units

	Location [Bus]	Max & Min capacity [kWh]	Initial state [kWh]	Cha/Dis ramp rate [kWh]	Conversion rate
Unit 1	16	750 & 75	75	400	0.85
Unit 2	21	450 & 45	225	250	0.85
Unit 3	25	800 & 80	160	400	0.85
Unit 4	33	550 & 55	165	250	0.85

Table 4-2. Specification data for diesel units

	Location [Bus]	Max & Min capacity [kW]	Power factor	fuel a & b consumption factors [L/kWh]	CO2 emission factor [kg/L]
Unit 1	15	550 &100	0.9	0.116 & 0.08145	2.68
Unit 2	22	800 &150	0.9	0.111 & 0.07932	2.68
Unit 3	30	1000 & 200	0.9	0.107 & 0.07764	2.68

In the CAESs specification, the minimum capacity refers to the pressure at which the unit cannot provide constant power. In this chapter, four scenarios with different operating objectives are considered as follows.

4.4.1 Scenario 1: Base case

This scenario is to investigate the status of the grid without considering power generation (renewable and conventional) or storage units. In this scenario, the total 24h active power of the grid is 5055.9 kW. Contour and histogram diagrams for the voltage profile of the grid are depicted in Fig. 4-7.

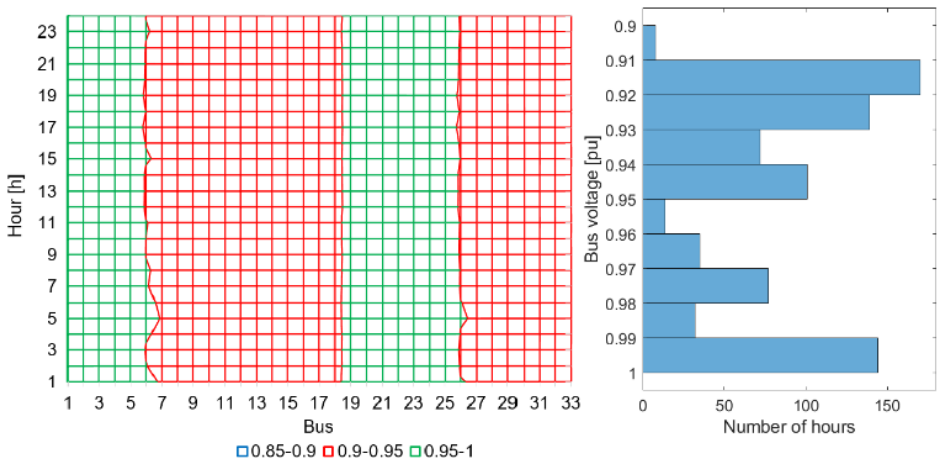

Fig. 4-7. 24h voltage profile of grid before allocation of DGs and storage units

As can be seen, some of the buses (e.g., 7-18 and 27-33) are located deep voltage points of the grid, where their voltage value violates the acceptable limit [0.95-1.05 p.u.].

Noteworthy, some markets consider 0.9 p.u. as the lower boundary of this acceptable limit, and increasing voltage profile regarded as a power quality factor is provided in the ancillary service market.

4.4.2 Scenario 2: Emission & power loss objectives

In the second scenario, two objectives of emission and power loss have been considered for DSO optimization. CO_2 emission per unit of diesel fuel consumption is 2.68 kg [211]. In order to evaluate the impact of CAES aggregator, two sub-scenarios with and without the presence of CAES aggregator are presented. The set of optimal solutions for both cases are shown in Fig. 4-8. As can be seen, an increment in the involvement level of diesel generators results in a reduction of total power loss of the grid; this is because a major part of local loads can be supplied locally, and there is no need to be supplied from the upstream grid.

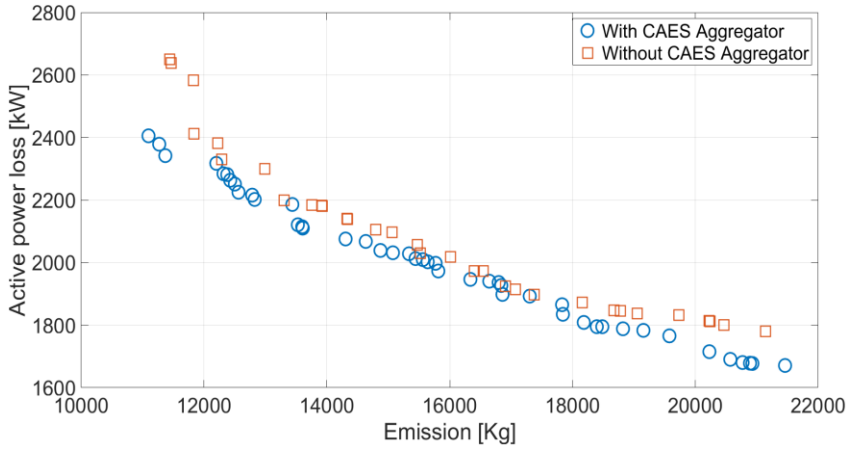

Fig. 4-8. Bi-objective optimum 24h operation of the grid considering emission and power loss as objective functions (Scenario 2)

Noteworthy, separate from the operating cost of diesel generators, diesel units should commit in the daily operation to increase the voltage profile of the buses during the hours in which solar units cannot supply power due to lack of sun irradiation. Besides, it is evident

that adding a CAES aggregator has a significant impact on decreasing power loss of the grid, especially when diesel generators are not involved in the operation of the system (i.e., where emission has very low values between 10000-12000 kg). The DLMP determined by DSO considering the CAES aggregator's participation in the grid operation is shown in Fig. 4-9.

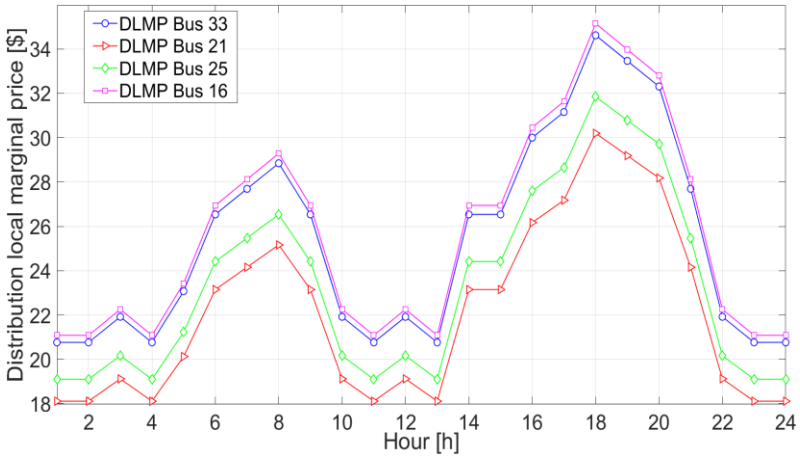

Fig. 4-9. Distribution locational marginal price of buses

It can be deduced that the buses located at the end side have higher DLMP values. Such an approach is adopted by DSO because generators and storage units located in the proximity to the substation have fewer effects on the voltage profile regulation and power loss reduction. Optimal scheduling of the storage units obtained by the CAES aggregator is depicted in Fig. 4-10. Evidently, the aggregator exploits peaks of the DLMP price to maximize the total profit of CAES owners; that is the reason charging/ discharging pattern of the CAES units follows that of DLMP.

4.4.3 Scenario 3: Emission & operating costs objectives

This scenario considers CO_2 emission and operating costs of the grid as the objective functions. Noteworthy, the simultaneous minimization of both objectives is a contradictive

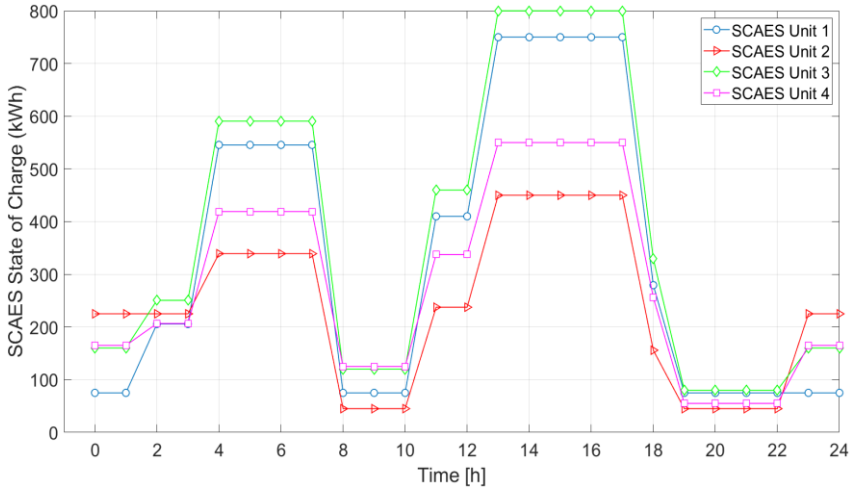

Fig. 4-10. Energy variations of SCAESs during 24h scheduling

issue. On the one hand, less usage of diesel units to minimize emissions leads the grid toward more drop on the voltage profile of the network due to more power supply from the upstream grid. On the other hand, the price of energy during the middle hours of the day is higher than the cost of running diesel units. Therefore, it necessitates a compromise to reach an optimal schedule of fuel-based units and power purchased from the upstream grid. In this study, the fuel price for diesel units is 0.999 $/L. Fig. 4-11 shows the set of solutions of the given bi-objective optimization problem with the same sub-scenarios of with/without CAES aggregator. It can be seen that the CAES aggregator could reduce the cost of operation in a wide range of operation, even though the CAES units are not under the control of the DSO anymore and also are scheduled to maximize their own profit. Moreover, it can be seen that considering the same configuration, operating points with lower emission values are available when involving the CAES aggregator. It demonstrates that even having the conflicting objectives of DSO (i.e., to minimize operating costs) and CAES aggregator (i.e., to maximize its own profit), DSO benefits from the private operation of CAES units.

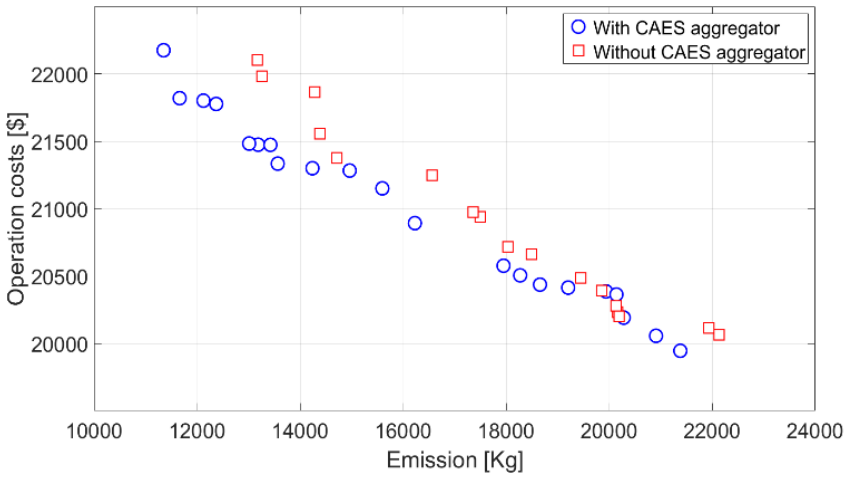

Fig. 4-11. Bi-objective optimum 24h operation of the grid considering emission and power loss as objective functions (Scenario 3)

Additionally, for the operating points with the least operational costs (e.g., around $20000), less CO_2 emission means fewer operating hours of diesel units and more utilization of CAESs units. Hence, the extended life cycle is expected for diesel units, while CAESs units are more resilient devices (because of having fewer combustion cycles and also the potential of using air turbines for the discharging mode).

4.4.4 Scenario 4: Power loss & operating costs objectives

The last scenario, as can be seen in Fig. 4-12, is to find the optimum operating points of the current configuration with the objective of total active power loss and operating cost. Minimizing the power loss results in an increase in the costs (either from diesel usage or purchasing power from the day-ahead market). Usually, importing power from the upstream grid cannot be efficient for power loss reduction, especially when there are large load demands at the ending buses. It may even make the situation worse in some cases.

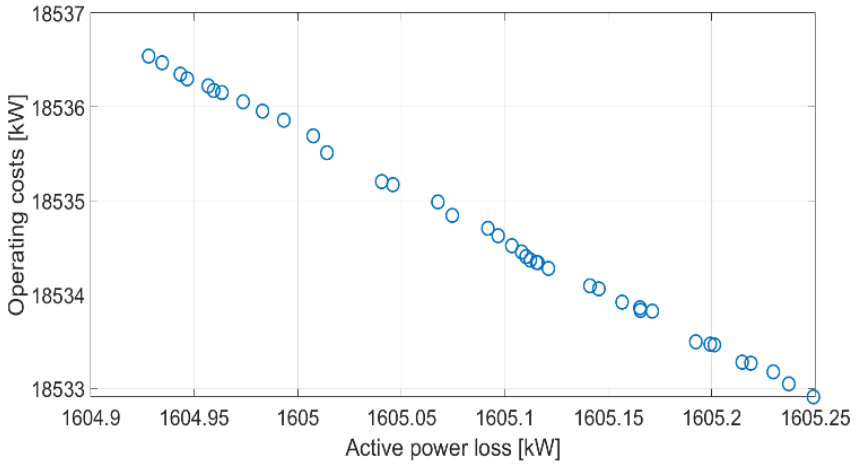

Fig. 4-12. Bi-objective optimum 24h operation of the grid considering operating cost and power loss as objective functions (Scenario 4)

Therefore, considering the fact that CAES units are individually controlled and cannot significantly increase the voltage profile during the whole scheduling period (because they take the role of loads in some hours), diesel units are the last option; the optimization algorithm prefers to use them as little as possible, to only meet voltage constraint, trying not to increase operating costs. Finally, all solutions are converged to near marginal points, and a Pareto-front solution limited to a narrow range is created.

4.5 Summary

This chapter has proposed the concept of CAES aggregator for ADSs. The aggregator scheduled the charging/discharging patterns of storage units using the proposed linear programming to maximize their own profit based on local prices. Considering the results obtained from three bi-objective scenarios, it can be deduced that independent operations of CAES units not only had no adverse effects on the financial and technical operation of the grid but also do assist DSO to exploit the potential of the current grid's assets more optimally. Noteworthy, this chapter developed a methodology for CAES units; however, this structure

of market participation is also extendable and applicable for other types of storage as well.

The utilization of stationary energy storage units as an inseparable part of ADS is experiencing significant changes recently. On the most highlighted changes that has metamorphosed the DN operation is the development of transportable ESs. These mobile energy storage units have the potential for stationary operation during regular operation of the grid and also for transporting energy during emergencies. In this regard, the next chapter will present and model a novel concept of mobile CAES units that are superior in several aspects compared to current mobile energy storage systems.

Chapter 5 Mobile Compressed Air Energy Storage for Active Distribution Systems

This chapter proposes a novel concept of mobile CAES in an electric DN to improve grid operating factors. The proposed configuration models transportable air storage tanks carrying stored energy among the locations of motor-generators placed on some distribution nodes/buses. Employing several storage tanks, higher dispatchability and storage capacities are obtained. To overcome routing challenges for trucks, using Google Maps API, the configuration of the grid is mapped on the urban region of the city of Sydney, Australia, to accurately model distances between current and targeted locations, unavailability of tanks during traveling, route congestions, and fuel consumptions. To solve the obtained CAES operation problem, a new heuristic mathematical method is proposed to convert constraints of the mobile CAES (MCAES) model into feasible search spaces, which significantly improves the convergence quality and speed. Additionally, this method offers a technique of solution coding to use the same solution vector for both commitment and dispatch of MCAES, which reduces the solution dimension and computational burden. Since the proposed solution method is applicable to both stationary and mobile CAESs, operating results for both are presented and compared. The methodology is applied to IEEE 136 bus DN in addition to IEEE 33-bus DN to demonstrate the competence of MCAES when dealing with larger-scale grids to efficiently assist the DN's operator in optimizing total operating profit, active power loss, ENS, and voltage stability index of the grid. The generation of fuel-based generators is also optimized to maintain the secure operation of the grid.

The rest of the chapter is organized as follows. Sections 5.1-5.4 provide detailed modeling of

proposed MCAES, distributed generations (DGs), and operational constraint of the grid. Case studies and results for three scenarios with different schemes of generation/storage participation are presented in Section 5.5. Finally, Section 5.6 draws a conclusion from the obtained results Problem formulation and mathematical modeling

5.1 Mobile compressed air energy storage

This study proposes a new concept of CAES units with transportable storage tanks and stationary motor-generator units. As can be seen in Fig. 5-1, the CAES system includes a certain number of mobile storage tanks $\mathcal{M}$ that can be charged or discharged at the location of motor-generators, where motor-generator units $\mathcal{G}$ are stationary and located at candidate power distribution buses.

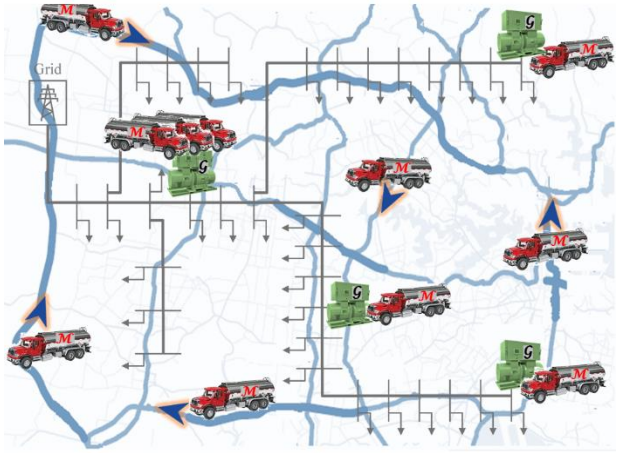

Fig. 5-1. The schematic of the proposed CAES system with several mobile storage units

In fact, a motor-generator unit can only operate when connecting to one of the mobile storage tanks. Three operating modes, including charging $\mathcal{C}$ (i.e., air compression into mobile tanks), discharging $\mathcal{D}$ (i.e., power generation from their stored energy), and idle are considered for a CAES unit (i.e., a motor-generator connected to a tank). Obviously, a mobile tank is unavailable when it is moving from one bus location to another. Additionally, each

operating hour from the scheduling horizon may be broken into several sub-periods. Although a motor-generator can be physically connected to several tanks simultaneously, it can only charge/discharge one of them during each sub-period, and other tanks remain idle. The number of mobile tanks in the proposed system may be much more than the number of motor-generators.

5.1.1 Mathematical modeling

The modeling of the proposed MCAES is detailed as follows:

$$V_{m,t,c}^{\mathcal{M},\mathcal{C}} = \alpha_c^{\mathcal{G},\mathcal{C}} P_{m,t,c}^{\mathcal{G},\mathcal{C}} \qquad \forall m, \forall t, \forall c \qquad (5\text{-}1)$$

$$\mho_{m,c}^{\mathcal{G},\mathcal{C}} U_{m,t,c}^{\mathcal{G},\mathcal{C}} \le V_{m,t,c}^{\mathcal{M},\mathcal{C}} \le \Omega_{m,c}^{\mathcal{G},\mathcal{C}} U_{m,t,c}^{\mathcal{G},\mathcal{C}} \qquad \forall m, \forall t, \forall c \qquad (5\text{-}2)$$

$$\Omega_{m,c}^{\mathcal{G},\mathcal{C}} = min\left(\rho_c^{\mathcal{G},\mathcal{C}}, q_m^{\mathcal{M}}\right) \qquad \forall m, \forall c \qquad (5\text{-}3)$$

$$\mho_{m,c}^{\mathcal{G},\mathcal{C}} = \sigma_c^{\mathcal{G},\mathcal{C}} \Omega_{m,c}^{\mathcal{G},\mathcal{C}} \qquad \forall m, \forall c \qquad (5\text{-}4)$$

$$P_{m,t,c}^{\mathcal{G},\mathcal{D}} = a_c^{\mathcal{G},\mathcal{D}} V_{m,t,c}^{\mathcal{M},\mathcal{D}} \qquad \forall m, \forall t, \forall c \qquad (5\text{-}5)$$

$$\mho_{m,c}^{\mathcal{G},\mathcal{D}} U_{m,t,c}^{\mathcal{G},\mathcal{D}} \le V_{m,t,c}^{\mathcal{M},\mathcal{D}} \le \Omega_{m,c}^{\mathcal{G},\mathcal{D}} U_{m,t,c}^{\mathcal{G},\mathcal{D}} \qquad \forall m, \forall t, \forall c \qquad (5\text{-}6)$$

$$\Omega_{m,c}^{\mathcal{G},\mathcal{D}} = min\left(\rho_c^{\mathcal{G},\mathcal{D}}, q_m^{\mathcal{M}}\right) \qquad \forall m, \forall c \qquad (5\text{-}7)$$

$$\mho_{m,c}^{\mathcal{G},\mathcal{D}} = \sigma_c^{\mathcal{G},\mathcal{D}} \Omega_{m,c}^{\mathcal{G},\mathcal{D}} \qquad \forall m, \forall c \qquad (5\text{-}8)$$

$$U_{m,t,c}^{\mathcal{G},\mathcal{C}} + U_{m,t,c}^{\mathcal{G},\mathcal{D}} \le 1 \qquad \forall m, \forall t, \forall c \qquad (5\text{-}9)$$

$$1 \ge \sum\nolimits_{m=1}^{N_M} \left(V_{m,t,c}^{\mathcal{M},\mathcal{C}} / \rho_c^{\mathcal{G},\mathcal{C}} + V_{m,t,c}^{\mathcal{M},\mathcal{D}} / \rho_c^{\mathcal{G},\mathcal{D}}\right) \qquad \forall t, \forall c \qquad (5\text{-}10)$$

$$P_{t,c}^{\mathcal{G}} = \sum\nolimits_{m=1}^{N_M} \left(P_{m,t,c}^{\mathcal{G},\mathcal{D}} - P_{m,t,c}^{\mathcal{G},\mathcal{C}}\right) \qquad \forall t, \forall c \qquad (5\text{-}11)$$

$$V_{t,c}^{\mathcal{G}} = \sum\nolimits_{m=1}^{N_M} \left(V_{m,t,c}^{\mathcal{M},arr} - V_{m,t,c}^{\mathcal{M},dep}\right) + \sum\nolimits_{m=1}^{N_M} \left(V_{m,t,c}^{\mathcal{M},\mathcal{C}} - V_{m,t,c}^{\mathcal{M},\mathcal{D}}\right) \qquad \forall t, \forall c \qquad (5\text{-}12)$$

$$S_{m,t+1}^{\mathcal{M}} = S_{m,t}^{\mathcal{M}} + \sum\nolimits_{c \in C_B} \left(V_{m,t,c}^{\mathcal{M},\mathcal{C}} - V_{m,t,c}^{\mathcal{M},\mathcal{D}}\right) \qquad \forall m, \forall t \qquad (5\text{-}13)$$

$$S_{m,min}^{\mathcal{M}} \le S_{m,t}^{\mathcal{M}} \le q_m^{\mathcal{M}} \qquad \forall m, \forall t \qquad (5\text{-}14)$$

$$S_{m,min}^{\mathcal{M}} = (1 - \mathfrak{h}_m^{\mathcal{M}}) q_m^{\mathcal{M}} \qquad \forall m \qquad (5\text{-}15)$$

$$S_0^{\mathcal{MG}} = S_{N_T}^{\mathcal{MG}} = \sum_{m=1}^{N_M} S_{m,ini} \qquad (5\text{-}16)$$

$$S_0^{\mathcal{MG}} = \sum_{m=1}^{N_M} S_{m,0}^{\mathcal{M}} \qquad (5\text{-}17)$$

$$S_{N_T}^{\mathcal{MG}} = \sum_{m=1}^{N_M} S_{m,N_T}^{\mathcal{M}} \qquad (5\text{-}18)$$

$$OC_t^{\mathcal{G}} = \sum_{m=1}^{N_M} \sum_{c \in C_B} \sum_{t=1}^{N_T} \left(P_{m,t,c}^{\mathcal{G},\mathcal{C}} \phi_{t,c}^{\mathcal{G},\mathcal{C}} + P_{m,t,c}^{\mathcal{G},\mathcal{D}} \phi_{t,c}^{\mathcal{G},\mathcal{D}} \right) \qquad \forall t \qquad (5\text{-}19)$$

$$P_{t,c}^{\mathcal{G},\psi} = \sum_{m=1}^{\bar{N}_{t,c}} P_{m,t,c}^{\mathcal{G},\mathcal{D}}, \psi = \mathcal{C}, \mathcal{D} \qquad \forall m, \forall t, \forall c \qquad (5\text{-}20)$$

$$FC_t^{\mathcal{M}} = \sum_{m=1}^{N_M - 1} d_{m,t}^{\mathcal{M}} F_m^{\mathcal{M}} \qquad \forall t \qquad (5\text{-}21)$$

$$R^{\mathcal{MG}} = \sum_{t=1}^{N_T} \sum_{c \in C_B} \left(P_{t,c}^{\mathcal{G},\mathcal{D}} \pi_t^{\mathcal{S},m} - P_{t,c}^{\mathcal{G},\mathcal{C}} \pi_t^{\mathcal{S},b} \right) - \sum_{t=1}^{N_T} \left(FC_t^{\mathcal{M}} + OC_t^{\mathcal{G}} \right) \qquad (5\text{-}22)$$

In (5-1), $V_{m,t,c}^{\mathcal{M},\mathcal{C}}$ is the amount of compressed energy during charging mode flowing into mobile tank m, with $m \in \{1, 2, \dots, N_M\}$, at candidate bus $c \in C_B = \{c_1, c_2, \dots, c_{N_C}\}$ and time step $t \in \{1, 2, \dots, N_T\}$, where one hour is chosen for the sampling time step. $P_{m,t,c}^{\mathcal{G},\mathcal{C}}$ is the amount of power to be received by CAES from the grid for compression and $\alpha_c^{\mathcal{G},\mathcal{C}}$ is the power-to-energy conversion rate. The hourly amount of energy stored in each storage unit is limited by (5-2), in which the upper bound $\Omega_{m,c}^{\mathcal{G},\mathcal{C}}$ and lower bound $\mho_{m,c}^{\mathcal{G},\mathcal{C}}$ are defined in (5-3) and (5-4), respectively; $U_{m,t,c}^{\mathcal{G},\mathcal{C}}$ is a binary variable indicating charging status of the CAES (i.e., $U_{m,t,c}^{\mathcal{G},\mathcal{C}} = 1$ means that tank m is being charged at time t by the motor-generator located at bus c, and $U_{m,t,c}^{\mathcal{G},\mathcal{C}} = 0$ means it is not charged). As opposed to stationary CAES units in which hourly charging/discharging rates are a share of total storage capacity, these rates are considerable, and the corresponding capacity in one hour maybe even higher than the storage

capacity of a tank in the case of MCAESs. Therefore, as indicated in (5-3), the maximum hourly compression capacity $\Omega_{m,c}^{\mathcal{G},\mathcal{C}}$ of a CAES is defined as the minimum between nominal energy compression rate $\rho_c^{\mathcal{G},\mathcal{C}}$ of the motor unit and energy storage capacity of m^{th} mobile tank $q_m^{\mathcal{M}}$. To maintain stability of the unit during charging and prevent frequent short-time operation of the motor-generator, a minimum charging rate $\mho_{m,c}^{\mathcal{G},\mathcal{C}}$ as a percentage $\sigma_c^{\mathcal{G},\mathcal{C}}$ of the maximum charging rate is defined in (5-4).

The electric power provided by the CAES unit located at candidate bus c during discharging mode $P_{m,t,c}^{\mathcal{G},\mathcal{D}}$ is calculated in (5-5), where $a_c^{\mathcal{G},\mathcal{D}}$ refers to the discharging conversion rate and $V_{m,t,c}^{\mathcal{M},\mathcal{D}}$ is the energy required for the generation of the scheduled power. The energy conversion rates for charge and discharge procedures are a fixed value $\alpha_c^{\mathcal{G},\psi} = 0.85;\ \psi = \mathcal{C},\mathcal{D};\ \forall c$ [7]. Similar to the charging mode, the amount of energy provision during discharging mode is bounded by a minimum and maximum value due to physical limitations as in (5-6). As the discharging rate of the generator $\rho_c^{\mathcal{G},\mathcal{C}}$ may be higher than the storage capacity of a mobile tank $q_m^{\mathcal{M}}$, the upper discharging limit of units $\Omega_{m,c}^{\mathcal{G},\mathcal{D}}$ is formulated by (5-7). Noteworthy, running the generator during the discharge period needs a minimum pressure. Therefore, a discharging stability rate $\sigma_c^{\mathcal{G},\mathcal{D}}$ is considered to determine the lower discharging bound $\mho_{m,c}^{\mathcal{G},\mathcal{D}}$ in (5-8). Considering $U_{m,t,c}^{\mathcal{G},\mathcal{C}}$ and $U_{m,t,c}^{\mathcal{G},\mathcal{D}}$ as binary variables referring to on/off status of the motor-generator during charging and discharging periods respectively, one of the states of charging, discharging, and idle can be considered for a CAES based on (5-9) in each operating period. If both $U_{m,t,c}^{\mathcal{G},\mathcal{C}}$ and $U_{m,t,c}^{\mathcal{G},\mathcal{D}}$ are zero, the motor-generator is in the idle state.

Since only some of the mobile tanks are available during hour *t* at bus *c*, the hour *t* of

scheduling horizon is divided into several timeslots, so that a certain amount of time is allocated to each storage tank committed to the charging/discharging procedures of a specific bus (i.e., simply calculated by $V_{m,t,c}^{\mathcal{M},\mathcal{C}}/\rho_c^{\mathcal{G},\mathcal{C}}$ and $V_{m,t,c}^{\mathcal{M},\mathcal{D}}/\rho_c^{\mathcal{G},\mathcal{D}}$). Obviously, the number of the mobile tanks is available at bus *c* may change from one hour to another, and the summation of these timeslots for each motor-generator should be less than one hour as in (5-10). It is assumed that the movement of a transportable tank and the start of its commitment at a new bus happens only at the beginning of a scheduling hour. Moreover, changing the pipe connection between the motor-generator unit and mobile tanks at a bus is accomplished by utilizing automatic shifting valves, and the time required for these actions is negligible and not considered in this study. Considering the positive sign for power generating of storage units and the negative sign for power purchasing from the grid, the N_T-hour power profile $P_{t,c}^{\mathcal{G}}$ of CAES units is determined in (5-11). The hourly energy available at the place of each CAES unit, $V_{t,c}^{\mathcal{G}}$, presented in (5-12) includes two core terms, first from arrival $V_{m,t,c}^{\mathcal{M},arr}$ and departure $V_{m,t,c}^{\mathcal{M},dep}$ of mobile tanks transferring energy among the candidate buses, second from charging/discharging energy as the result of power exchange with the grid that increases/decreases the energy level at the relevant bus. Finally, the energy level of the mobile tanks $S_{m,t+1}^{\mathcal{M}}$ in the next hour is calculated in (5-13) by having the current level of energy $S_{m,t}^{\mathcal{M}}$ and scheduled hourly amount of charging energy $V_{m,t,c}^{\mathcal{M},\mathcal{C}}$ calculated in (5-1) and discharging energy $V_{m,t,c}^{\mathcal{M},\mathcal{D}}$ calculated in (5-5). In this formula, $V_{m,t,c}^{\mathcal{M},\mathcal{C}}$ and $V_{m,t,c}^{\mathcal{M},\mathcal{D}}$ are non-zero only when a tank is conected at a particular bus c, and are zero for all other buses. The energy level in mobile banks, due to physical constraints, is bounded in (5-14) by a maximum value $q_m^{\mathcal{M}}$ and a minimum value $S_{m,min}^{\mathcal{M}}$ (i.e., defined as a share $(1-\mathfrak{h}_m^{\mathcal{M}})$ of

the maximum value in (5-15) where $\mathfrak{h}_m^{\mathcal{M}}$ is the depth of discharge and is assumed 0.95 in this study). As indicated in (5-16), the amount of energy stored in the MCAES system in the first hour $S_0^{\mathcal{MG}}$in (5-17) and the last hour $S_{N_T}^{\mathcal{MG}}$in (5-18) of scheduling need to be the same. Noteworthy, this value is lower than that for large-scale CAESs due to the lower thermal efficiency of the heat exchanger in SCAESs. The total hourly operation cost of a CAES system $OC_t^{\mathcal{G}}$ is given in (5-19) where $\phi_{t,c}^{\mathcal{G},\mathcal{C}}$ and $\phi_{t,c}^{\mathcal{G},\mathcal{D}}$ are the variable operating costs of a CAES unit during charging/discharge modes, respectively. No simple cycle mode is considered for the CAES units. As defined in (5-20), the total power generation $P_{m,t,c_i}^{\mathcal{G},\psi}$ of a motor-generator at a timestep t is calculated as the summation of its charge/discharge powers during sub-timestep $\bar{t}$. Besides, an hourly fuel cost $FC_t^{\mathcal{M}}$ is considered for moving tanks as formulated in (5-21) where $d_{m,t}^{\mathcal{M}}$ refers to *km* traveling distance between bus location of a tank at time t and its bus location at the next hour, and $F_m^{\mathcal{M}}$is per/*km* fuel consumption of tank m (constant during one operation day). Finally, profit from the commitment of an MCAES system $R^{\mathcal{MG}}$ is determined in (5-22) where electric power provided/demanded by storage is exchanged with the grid at the selling $\pi_t^{\mathcal{S},m}$/ purchasing $\pi_t^{\mathcal{S},b}$ price. This chapter assumes that $\rho_c^{\mathcal{G},\psi} > q_m^{\mathcal{M}};\ \psi = \mathcal{C},\mathcal{D}\ \forall m, \forall c$ which means the charge/discharge capacity of the motor-generator is bigger than the capacity of each mobile tank.

5.1.2 *Location matrix* formation of mobile CAESs

In order to make the problem as realistic as possible, as can be seen in Fig. 5-2, the location of buses of an IEEE distribution grid is mapped on the urban area of the city of Sydney. The actual distances between buses are calculated using the Google Maps API.

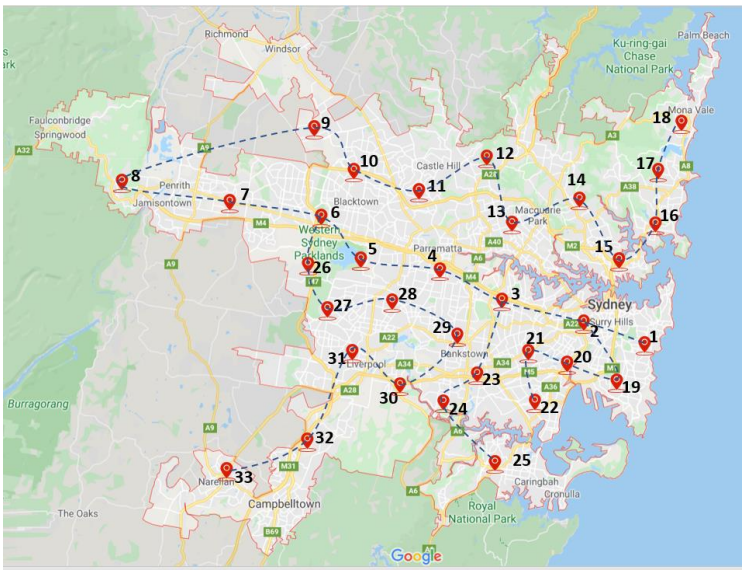

Fig. 5-2. The schematic IEEE 33-bus mapped on Sydney urban area

Considering a constant speed for trucks carrying storage tanks by neglecting delays due to the road traffic, the time-distance matrix for the given IEEE test system is determined. This matrix is considered to be the same for the length of the scheduling horizon. As Sydney is one of the largest modern cities in the world, it may take more than an hour for the truck to travel from one bus to another. Therefore, there is a need for the development of an approach to modify the matrix of traveling by considering the time-distance between a start point and destination location.

In this regard, the proposed following algorithm modifies the randomly generated matrix of tanks movements $\mathbf{M} = [C_{m,t}]_{N_M \times N_T}$, and $C_{m,t}$ is uniformly generated from integers in C_B, indicating the bus location of the m-th tank during the t-th scheduling period. The N_M dimensional matrix $\mathbf{M}$ indicates the bus location of each of the tanks during the N_T scheduling period. In other words, $C_{m,t}$ shows the mth tank is sitting at the location of the bus c_i at time t. The tank movement scheduling is formed as follows. For example, as can be seen, the first

tank moves from $C_{1,1}$ at the first hour to $C_{1,2}$ in the second hour. We use lowercase for scalars, lowercase bold for vectors, and capital bold for matrices.

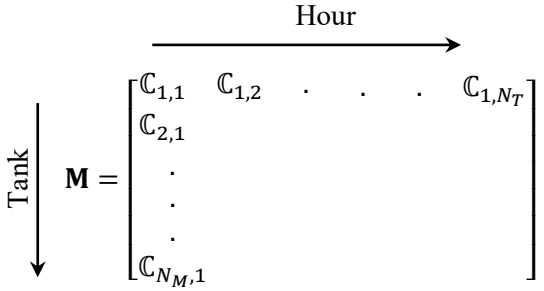

Initialization

1. Initialize the modified matrix of tank scheduling $\breve{\mathbf{M}}$ by:

$$\breve{\mathbf{M}} = \mathbf{M} \tag{5-23-a}$$

2. Initialize an on-the-way (unavailability matrix) of tanks $\boldsymbol{\mathcal{O}}=[0]_{N_M \times N_T}$. The indicator $\boldsymbol{\mathcal{O}}$ refers to hours in which tanks are moving between two buses and are not available for charge-discharge. This matrix is formed based on the time-distance among buses.

3. Initialize $\boldsymbol{\Delta}$ as the required time for a truck to move from bus *i* to bus *j*:

$$\boldsymbol{\Delta}_{i,j} = \left\lceil \mathfrak{D}_{i,j} / \mathfrak{s} \right\rceil \tag{5-23-b}$$

where $\lceil \xi \rceil$ is the ceiling function which finds the least integer greater than or equal to ξ, $\mathfrak{D}_{i,j}$ is the distance between two individual buses *i* and *j* (i.e., calculated by Google Maps) in the unit of *km* and; hence $\mathfrak{D}$ is the bus-distance matrix (with the dimension of $N_B \times N_B$ where N_B is the number of buses in the distribution grid), $\mathfrak{s}$ is the speed of trucks carrying tanks (i.e., similar and constant for all trucks). As speed for trucks carrying storage tanks is constant, by neglecting delays due to the road traffic, $\boldsymbol{\Delta_{i,j}}$ determines the time required for a truck to move from bus *i* to bus *j*.

4. Initialize the location of mobile tanks at the first hour:

$$C_{m,1} = \lambda_m \qquad \forall_m \qquad \text{(5-23-c)}$$

where the $\boldsymbol{\lambda}_m$ is mth row of the vector $\boldsymbol{\lambda}$. The mth element of the vector $\boldsymbol{\lambda}$ defines the location of tank m at the first hour of schedule (i.e., a pre-defined value.)

5. Initialize the number of idle hours for mobile tanks:

$$\boldsymbol{\tau} = [0]_{N_M} \qquad \text{(5-23-d)}$$

As stated in (5-23-d), it is assumed that there are no restrictions about the required number of operating hours from the previous scheduling day.

Loop calculation

For m from 1 to N_M, do the following:

Set variables $\vartheta = 1,\ t = 2,\ \varepsilon = \boldsymbol{\tau}_m$.

While $t<N_T + 1$, do the following:

1. Calculate scalar values of the current location $\ell^{\mathcal{C}}$, next location $\ell^{\mathcal{N}}$, and time distance θ as follows:

$$\ell^{\mathcal{C}} = \mathbf{M}_{m,\vartheta} \qquad \text{(5-24-a)}$$

$$\ell^{\mathcal{N}} = \mathbf{M}_{m,t} \qquad \text{(5-24-b)}$$

$$\theta = \boldsymbol{\Delta}_{\ell^{\mathcal{C}},\ell^{\mathcal{N}}} \qquad \text{(5-24-c)}$$

where $\mathbf{M}_{m,\vartheta}$ is (m,ϑ) element of $\mathbf{M}$, $\mathbf{M}_{m,t}$ is the (m,t) element of $\mathbf{M}$, and $\boldsymbol{\Delta}_{\ell^{\mathcal{C}},\ell^{\mathcal{N}}}$ is the $(\ell^{\mathcal{C}},\ell^{\mathcal{N}})$ element of $\boldsymbol{\Delta}$.

2. Calculate elements of $\breve{\mathbf{M}}$ and $\boldsymbol{\mathcal{O}}$ based on three possible situations, given locations and time distance between two buses:

$$\begin{cases} t{=}t{+}1, \quad \varepsilon{=}\varepsilon{+}1; & \text{if } \ell^{\mathcal{C}}{=}\ell^{\mathcal{N}} \\ \breve{\mathbf{M}}_{m,t}{=}\ell^{\mathcal{C}}, \quad t{=}t{+}1, \quad \varepsilon{=}\varepsilon{+}1; & \text{if } \theta{>}\varepsilon \\ \boldsymbol{\mathcal{O}}_{m,t-\theta:\,t-1}{=}\text{inf}, \quad \vartheta{=}t, \quad t{=}t{+}1, \varepsilon{=}0; & \text{if } \theta{<}\varepsilon \end{cases} \qquad \text{(5-24-d)}$$

If the location of a tank in the next hour is the same as the current location, the algorithm proceeds to the next hour without changing the scheduling matrix $\breve{\mathbf{M}}$. The second situation is when enough idle hours for moving from one bus to another is not met; therefore, the tank should stay in the current location. In the third situation, the relocation happens since the tank can reach the next location after traveling θ hours, and these hours are marked with inf as the sign for out of operation.

Final adjustment

1. Apply idle hours onto modified movement matrix $\breve{\mathbf{M}}$ to reach the final scheduling matrix $\widetilde{\mathbf{M}}$:

$$\widetilde{\mathbf{M}}_{m,t} = \max(\breve{\mathbf{M}}_{m,t}, \boldsymbol{\mathcal{O}}_{m,t}) \qquad \forall m, \forall t \qquad (5\text{-}25)$$

where $\widetilde{\mathbf{M}}_{m,t}$ is the (m, t) element of $\breve{\mathbf{M}}$.

5.1.3 Proposed CAES constraint handling formation

Traditionally, a large number of constraint handling techniques in the soft computing realm are employed; some superiorities and weaknesses can be considered for each one. In this study, a heuristic approach is proposed for the MCAES system in which the wide infeasible ranges of solution space are converted into limited ranges. Therefore, the algorithm will have an opportunity of reaching a smaller feasible range for each decision variable and, subsequently, a much higher chance of achieving a globally optimum solution. Then, no infeasible solution is generated in each iteration of the algorithm.

a) Forward approach

Initialization

1. Initialize an N_T hour energy scheduling matrix $\mathbf{S}^{\mathcal{M}}$ for moving tanks (5-26-a). The energy

of the first hour of scheduling is defined as the same as the initial amount $\boldsymbol{s}_{m,ini}$ in (5-26-b).

$$\mathbf{S}^{\mathcal{M}} = [0]_{N_M \times N_T} \tag{5-26-a}$$

$$\mathbf{S}^{\mathcal{M}}_{m,1} = \boldsymbol{s}_{m,ini} \qquad \forall m \tag{5-26-b}$$

where $\boldsymbol{s}_{m,ini}$ is the m-th row of $\boldsymbol{s}_{ini}$.

2. Initialize a decision matrix $\boldsymbol{\chi}^{\mathcal{M}}$ with random values $x_{m,t}$ from the interval [0,1] for tanks energy scheduling in (5-26-c) while $x_{m,t}$=0 if $\boldsymbol{\mathcal{O}}_{m,t}$=$inf$, as the value *inf* refers to the hours in which tanks are moving between two buses and not available for charging/discharging procedures.

$$\boldsymbol{\chi}^{\mathcal{M}} = \left[x_{m,t}\right]_{N_M \times N_T} \tag{5-26-c}$$

To scale down the dimension of the problem, as opposed to traditional methods which use two different matrixes (i.e., one binary for unit status and one for their dispatch), a new codification technique is proposed in which the matrix $\boldsymbol{\chi}^{\mathcal{M}}$ is used for defining both charging/idle/discharging status of units and their corresponding amount. In this regard, a value of -0.5 is added to the matrix $\boldsymbol{\chi}^{\mathcal{M}}$ to scale the middle axis down to zero. Then, as defined in (5-26-d), the sign function determines the charging/ discharging/ idle status of units $U^{\mathcal{G}}$ (i.e., +1, -1, 0) for values bigger, lower than and equal to zero; while $\mathbf{U}^{\mathcal{G}}_{m,t} = 0 \quad if \ \boldsymbol{\mathcal{O}}_{m,t} = inf$ which shows units are not available for charging/discharge when they are on-the-way.

$$\mathbf{U}^{\mathcal{G}}_{m,t} = \begin{cases} +1 & \text{if } \left(\boldsymbol{\chi}^{\mathcal{M}}_{m,t} - 0.5\right) > 0 \\ 0 & \text{if } \left(\boldsymbol{\chi}^{\mathcal{M}}_{m,t} - 0.5\right) = 0 \\ -1 & \text{if } \left(\boldsymbol{\chi}^{\mathcal{M}}_{m,t} - 0.5\right) < 0 \end{cases} \tag{5-26-d}$$

Then, the matrices charging state $\mathbf{U}^{\mathcal{G},\mathcal{C}}_{m,t} = \max\left(\mathbf{U}^{\mathcal{G}}_{m,t}, 0\right)$ and discharging state $\mathbf{U}^{\mathcal{G},\mathcal{D}}_{m,t} = -\min\left(\mathbf{U}^{\mathcal{G}}_{m,t}, 0\right)$ are determined (i.e., to be used in (5-2) and (5-6)), in which active/reactive state of motor-generator within each sub-time step is shown by 1/0.

3. Initialize the matrix $\boldsymbol{\chi}^{\mathcal{G},\varpi}$ in (5-26-e) as input for calculating energy charge/discharge of mobile tanks.

$$\boldsymbol{\chi}_{m,t}^{\mathcal{G},\varpi} = \left(2 \times \left(\boldsymbol{\chi}_{m,t}^{\mathcal{M}} - 0.5\right)\right) \mathbf{U}_{m,t}^{\mathcal{G},\varpi} \qquad \varpi = \mathcal{C}, \mathcal{D}; \quad \forall m, \forall \mathrm{t} \quad \text{(5-26-e)}$$

The term $\left(\boldsymbol{\chi}_{m,t}^{\mathcal{M}} - 0.5\right)$ scales all random values down within [-0.5, +0.5], in which positive values refer to charging and negative values for discharging. Then, the term "× 2" maps them again within [-1, +1]. Then, all values of matrices $\boldsymbol{\chi}^{\mathcal{G},\mathcal{C}}$ are within [0, 1] and $\boldsymbol{\chi}^{\mathcal{G},\mathcal{D}}$ are within [-1, 0]. Noteworthy, using the proposed approach, both commitment and dispatch states of units are detached from a single matrix

Loop calculation

For t from 1 to N_T, do the following.

Set single-hour vectors for the available capacity to reach the upper limit of tanks $\boldsymbol{\Delta}_m^{\mathcal{M}}$ (5-27-a), the available capacity to reach the lower limit of tanks $\boldsymbol{\Upsilon}_m^{\mathcal{M}}$ (5-27-b) where $\mathfrak{h}_m^{\mathcal{M}}$ refers to the depth of discharge of tanks as defined in (5-15), and movement scheduling of mobile tanks $\boldsymbol{\mu}_m$ (5-27-c).

$$\boldsymbol{\Delta}_m^{\mathcal{M}} = \boldsymbol{q}_m^{\mathcal{M}} - \mathbf{S}_{m,t}^{\mathcal{M}} \qquad \forall m \qquad \text{(5-27-a)}$$

$$\boldsymbol{\Upsilon}_m^{\mathcal{M}} = \mathbf{S}_{m,t}^{\mathcal{M}} - \left((1 - \mathfrak{h}_m^{\mathcal{M}})\, \boldsymbol{q}_m^{\mathcal{M}}\right) \qquad \forall m \qquad \text{(5-27-b)}$$

$$\boldsymbol{\mu}_m = \widetilde{\mathbf{M}}_{m,t} \qquad \forall m \qquad \text{(5-27-c)}$$

Given formulations (5-27-a)-(5-27-c) for every single hour, the second loop for calculating the energy of tanks is implemented. This loop calculates these energies, considering the limitations of both tanks and motor-generator units.

For c from the set $\{c_1, c_2, \ldots, c_{N_C}\}$, do the following.

Calculate a binary vector $\boldsymbol{k}$ in which the corresponding element is 1/0 if tanks are

available/unavailable at bus c_i (i.e., the place of selected motor-generator) (5-28-a). Given the maximum charging/discharging rates in (5-3) and (5-7), the amount of energy charging/discharging for all mobile tanks $\boldsymbol{v}_m^{\mathcal{M},\mathcal{CD}}$ is calculated in (5-28-b). As these values are not constrained to compression/expansion rates of motor-generator of bus c, Eq. (5-28-c) for applying the maximum rates and Eq. (5-28-d) for the minimum rates are used to reach constrained dispatch $\tilde{\boldsymbol{v}}_m^{\mathcal{M},\mathcal{CD}}$.

$$\boldsymbol{k}_m = \begin{cases} 1 & \text{if} \quad \boldsymbol{\mu}_m = c \\ 0 & \text{if} \quad \boldsymbol{\mu}_m \neq c \end{cases} \qquad \forall m \qquad (5\text{-}28\text{ -a})$$

$$\boldsymbol{v}_m^{\mathcal{M},\mathcal{CD}} = \left(\boldsymbol{\chi}_m^{\mathcal{G},\mathcal{C}}\, \boldsymbol{\Delta}_m^{\mathcal{M}} + \boldsymbol{\chi}_m^{\mathcal{G},\mathcal{D}}\, \boldsymbol{\Upsilon}_m^{\mathcal{M}}\right)\boldsymbol{k}_m \qquad \forall m \qquad (5\text{-}28\text{ -b})$$

$$\tilde{\boldsymbol{v}}_m^{\mathcal{M},\mathcal{CD}} = \max\left(\min\left(\boldsymbol{v}_m^{\mathcal{M},\mathcal{CD}}, \boldsymbol{\Omega}_{m,c}^{\mathcal{G},\mathcal{C}}\right), -\boldsymbol{\Omega}_{m,c}^{\mathcal{G},\mathcal{D}}\right) \qquad \forall m \qquad (5\text{-}28\text{ -c})$$

$$\tilde{\boldsymbol{v}}_m^{\mathcal{M},\mathcal{CD}} = \begin{cases} 0 & \text{if} \quad \tilde{\boldsymbol{v}}_m^{\mathcal{M},\mathcal{CD}} > 0 \;\&\; \tilde{\boldsymbol{v}}_m^{\mathcal{M},\mathcal{CD}} < \mho_{m,c}^{\mathcal{G},\mathcal{C}} \\ 0 & \text{if} \quad \tilde{\boldsymbol{v}}_m^{\mathcal{M},\mathcal{CD}} < 0 \;\&\; \tilde{\boldsymbol{v}}_m^{\mathcal{M},\mathcal{CD}} > -\mho_{m,c}^{\mathcal{G},\mathcal{D}} \end{cases} \qquad (5\text{-}28\text{ -d})$$

where $\boldsymbol{k}$ indicates tank availability at bus c (i.e., the place of selected motor-generator), and $\boldsymbol{v}_m^{\mathcal{M},\mathcal{CD}}$ is the amount of energy charging/discharging of the m-th tank, and $\boldsymbol{\chi}_m^{\mathcal{G},\varpi}$ is energy charging/discharging probability value of tanks (i.e., still within the interval [0,1]). As feasible ranges of operations are applied by (5-26-a)-(5-28-d), none of the generated solutions violate the constraints. Therefore, the only remaining constraint is (5-10), which should be met using the following *IF* condition within the second *For* loop. Considering the total operating hour of a motor-generator as $\hbar$ defined in (5-28-e):

$$\hbar = \sum\nolimits_{m=1}^{N_M} \left(\frac{\tilde{\boldsymbol{v}}_m^{\mathcal{M},\mathcal{CD}}\, \mathbf{i}_{\boldsymbol{m}}^{\mathcal{M},\mathcal{C}}}{\rho_c^{\mathcal{G},\mathcal{C}}} - \frac{\tilde{\boldsymbol{v}}_m^{\mathcal{M},\mathcal{CD}} \mathbf{i}_{\boldsymbol{m}}^{\mathcal{M},\mathcal{D}}}{\rho_c^{\mathcal{G},\mathcal{D}}} \right) \qquad \forall m \qquad (5\text{-}28\text{ -e})$$

where the charging binary index $\mathbf{i}_{\boldsymbol{m}}^{\mathcal{M},\mathcal{C}}$ and the discharging binary index $\mathbf{i}_{\boldsymbol{m}}^{\mathcal{M},\mathcal{D}}$ are defined as

$$\mathbf{i}_{\boldsymbol{m}}^{\mathcal{M},\mathcal{C}} = \begin{cases} 1 & \text{if } \widetilde{\boldsymbol{v}}_m^{\mathcal{M},\mathcal{CD}} > 0 \\ 0 & otherwise \end{cases} \qquad \forall m \qquad \text{(5-28-f)}$$

$$\mathbf{i}_{\boldsymbol{m}}^{\mathcal{M},\mathcal{D}} = \begin{cases} 1 & \text{if } \widetilde{\boldsymbol{v}}_m^{\mathcal{M},\mathcal{CD}} < 0 \\ 0 & otherwise \end{cases} \qquad \forall m \qquad \text{(5-28-g)}$$

If a generated solution has already met the constraint (5-10) (i.e., $\hbar < 1$), the hourly final energy charge/discharge pattern $\mathbf{V}_{m,t}^{\mathcal{M},\mathcal{CD}}$ for the time t is calculated by $\mathbf{V}_{m,t}^{\mathcal{M},\mathcal{CD}} = \widetilde{\boldsymbol{v}}_m^{\mathcal{M},\mathcal{CD}}\ \forall m$, otherwise:

If $\hbar > 1$, do the following:

The extra operating hour needs to be removed by decreasing the energy compression /expansion of the motor-generator. The required decrement dispatch probabili $\boldsymbol{r}_m^{\mathcal{G},\mathcal{CD}}$ is calculated in (5-29-a). Then, the new energy dispatch is calculated in (5-29-b) in which additional charging/discharging periods are removed.

$$\boldsymbol{r}_m^{\mathcal{G},\mathcal{CD}} = (\hbar - 1)\frac{\widetilde{\boldsymbol{v}}_m^{\mathcal{M},\mathcal{CD}}}{\sum_{i=1}^{N_M}\left|\widetilde{\boldsymbol{v}}_i^{\mathcal{M},\mathcal{CD}}\right|} \qquad \forall m \qquad \text{(5-29-a)}$$

$$\mathbf{V}_{m,t}^{\mathcal{M},\mathcal{CD}} = \widetilde{\boldsymbol{v}}_m^{\mathcal{M},\mathcal{CD}} - \left(\rho_c^{\mathcal{G},\mathcal{C}}\left(\boldsymbol{r}_m^{\mathcal{G},\mathcal{CD}}\mathbf{i}_{\boldsymbol{m}}^{\mathcal{M},\mathcal{C}}\right) - \rho_c^{\mathcal{G},\mathcal{D}}\left(\left|\boldsymbol{r}_m^{\mathcal{G},\mathcal{CD}}\right|\mathbf{i}_{\boldsymbol{m}}^{\mathcal{M},\mathcal{D}}\right)\right) \qquad \forall m \qquad \text{(5-29-b)}$$

Final adjustment

Finally, the existing energy of tanks $\mathbf{S}_{m,t}^{\mathcal{M}}$ is updated in (5-30) for the whole scheduling horizon within the second loop based on current energy exchange $\mathbf{V}_{m,t}^{\mathcal{M},\mathcal{CD}}$.

$$\mathbf{S}_{m,t+1}^{\mathcal{M}} = \mathbf{S}_{m,t}^{\mathcal{M}} + \mathbf{V}_{m,t}^{\mathcal{M},\mathcal{CD}} \qquad \forall m \qquad \text{(5-30)}$$

b) Backward approach

The backward approach is designed to modify the current energy charge/discharge pattern $\mathbf{V}_{m,t}^{\mathcal{M},\mathcal{CD}}$ of MCAESs to meet the fair operation condition (5-16). In this regard, the backward approach starts from the last hour of the scheduling horizon toward the first one to make sure the summation of the energy level in the whole MCAES system is the same at the first and last hour. After preparing some initial data, the backward approach may be similar to the forward approach in some parts and formulations.

Loop calculation

For decreasing counter t from N_T to 1, do the following.

Set the parameter $\boldsymbol{\eta} = [0]_{N_M}$, $\boldsymbol{\mu}_m$=$\widetilde{\mathbf{M}}_{m,t}$, and also set $\mathcal{g}$=inf and ʒ=0.

While ($|\mathcal{g}|$ is less than e^{g}) or (ʒ is greater than $e^{ʒ}$), do the following:

During each iteration of *While* loop, the commitment shares of some of the units are increasing/ decreasing to meet the mismatch of energy between the first and last stored energy. In this regard, some units may reach their high/low generation limits and therefore are needed to be removed from the commitment procedure. Hence, $\boldsymbol{\eta}$ is defined as a N_M dimensional vector with initial values of zero to indicate motor-generators which have reached their maximum charging/discharging capacity, $\mathcal{g}$ is the energy surplus/shortage defined in (5-31-b), e^{g} is a user-defined termination criterion for energy mismatch, ʒ is an iteration counter, and $e^{ʒ}$ is a user-defined termination criterion for the counter ʒ. In the backward approach, firstly, the $N_T$hour energy stored in the tanks is recalculated in (5-31-a) using cumulative-sum on the time horizon t. The variable $\mathbf{S}_{m,t}^{\mathcal{M}}$ has the same value as that calculated in (5-30) at the first iteration of the backward

approach.

$$\mathbf{S}_{m,t}^{\mathcal{M}} = \sum_{j=1}^{t} \boldsymbol{s}_{m,ini}\, \mathbf{V}_{m,j}^{\mathcal{M},\mathcal{CD}} \qquad \forall m, \forall t \qquad \text{(5-31-a)}$$

$$\mathcal{g} = \sum_{m=1}^{N_M} \boldsymbol{s}_{m,ini} - \sum_{m=1}^{N_M} \mathbf{S}_{m,N_T}^{\mathcal{M}} \qquad \text{(5-31 -b)}$$

The modified available capacity $\tilde{\boldsymbol{\Delta}}_m^{\mathcal{M}}$ and $\tilde{\boldsymbol{\Upsilon}}_m^{\mathcal{M}}$ are calculated as follows, while $\boldsymbol{\Delta}_m^{\mathcal{M}}$ and $\boldsymbol{\Upsilon}_m^{\mathcal{M}}$ are calculated using (5-27-a) and (5-27-b).

$$\tilde{\boldsymbol{\Delta}}_m^{\mathcal{M}} = \boldsymbol{\Delta}_m^{\mathcal{M}}(1\text{-}\boldsymbol{\eta}_m) \qquad \forall m \qquad \text{(5-31 -c)}$$

$$\tilde{\boldsymbol{\Upsilon}}_m^{\mathcal{M}} = \boldsymbol{\Upsilon}_m^{\mathcal{M}}(1\text{-}\boldsymbol{\eta}_m) \qquad \forall m \qquad \text{(5-31 -d)}$$

Then the index is reset to zero as $\boldsymbol{\eta}_m = 0 \ \ \forall m$. To calculate the dispatch share of each unit from surplus energy, after calculating $\boldsymbol{\mu}_m$ as defined (5-27-c), the index $\boldsymbol{\varphi}_m$ which indicates whether tanks are available at the location of a candidate bus in (5-31-e):

$$\boldsymbol{\varphi}_m = \begin{cases} 1 & \text{if} \quad \boldsymbol{\mu}_m = \text{inf} \\ 0 & \text{if} \quad \boldsymbol{\mu}_m \neq \text{inf} \end{cases} \qquad \forall m \qquad \text{(5-31 -e)}$$

In the next step, the charging/discharging energy of tanks at hour t is recorded in a temporary variable $\boldsymbol{v}_m = \mathbf{V}_{m,t}^{\mathcal{M},\mathcal{CD}} \quad \forall m$ and the value of energy at this hour firstly is set to zero $\mathbf{V}_{m,t}^{\mathcal{M},\mathcal{CD}} = 0 \ \ \forall m$ and then modified at the next steps. The share of each unit from surplus/shortage of energy $\boldsymbol{\emptyset}_m$ is defined as follows:

$$\boldsymbol{\emptyset}_m = \begin{cases} -\dfrac{\tilde{\boldsymbol{\Upsilon}}_m^{\mathcal{M}} \boldsymbol{\varphi}_m}{\sum_{m=1}^{\mathcal{N}_M} (\tilde{\boldsymbol{\Upsilon}}_m^{\mathcal{M}} \boldsymbol{\varphi}_m)} |\mathcal{g}| & \text{if} \quad \mathcal{g} > 0 \\ +\dfrac{\tilde{\boldsymbol{\Delta}}_m^{\mathcal{M}} \boldsymbol{\varphi}_m}{\sum_{m=1}^{\mathcal{N}_M} (\tilde{\boldsymbol{\Delta}}_m^{\mathcal{M}} \boldsymbol{\varphi}_m)} |\mathcal{g}| & \text{if} \quad \mathcal{g} \leq 0 \end{cases} \qquad \forall m \qquad \text{(5-31 -f)}$$

For c from the set $\{c_1, c_2, \dots, c_{N_C}\}$, do the following:

Within the second loop, firstly, the energy charging/ discharging for mobile tanks $\boldsymbol{v}_m^{\mathcal{M},\mathcal{CD}}$ at the given time t is calculated in (5-32) while $\boldsymbol{k}_m$ is determined as defined in (5-28-a).

As can be seen, the term $\boldsymbol{\emptyset}_m$ modifies the previous old dispatch $\boldsymbol{v}_m^{\mathcal{M},\mathcal{CD}}$.

$$\boldsymbol{v}_m^{\mathcal{M},\mathcal{CD}}=\left(\boldsymbol{v}_m^{\mathcal{M},\mathcal{CD}}+\boldsymbol{\emptyset}_m\right)\boldsymbol{k}_m \qquad \forall m \quad (5\text{-}32)$$

Similar to the forward approach, Eqs. (5-28-c) and (5-28-d) need to be applied to $\boldsymbol{v}_m^{\mathcal{M},\mathcal{CD}}$ to reach the constrained dispatch $\tilde{\boldsymbol{v}}_m^{\mathcal{M},\mathcal{CD}}$. Then, the last stage is to check if the operating period $\hbar$ of the motor-generator is within the regular one scheduling hour based on (5-28-e). If this constraint is not met, the following IF condition is applicable; otherwise, the current dispatch is considered as the final one $\mathbf{V}_{m,t}^{\mathcal{M},\mathcal{CD}}=\tilde{\boldsymbol{v}}_m^{\mathcal{M},\mathcal{CD}}\ \forall m$.

If $\hbar$ is greater than 1, do the following:

In the same way as the forward approach, Eqs. (5-29-a) and (5-29-b) are used to modify the current violated solution. Since some units may reach their maximum or minimum capacity within the While condition in the backward approach, the variable $\boldsymbol{\eta}_m$ is updated as in (5-33).

$$\boldsymbol{\eta}_m=\boldsymbol{\eta}_m+\mathbf{i}_{\boldsymbol{m}}^{\mathcal{M},\mathcal{C}}+\mathbf{i}_{\boldsymbol{m}}^{\mathcal{M},\mathcal{D}} \qquad \forall m \qquad (5\text{-}33)$$

At this stage, the final energy charge/discharge of selected tanks is updated as $\mathbf{V}_{m,t}^{\mathcal{M},\mathcal{CD}}=\tilde{\boldsymbol{v}}_m^{\mathcal{M},\mathcal{CD}}\ \forall m$.

Final adjustment

Then, $\mathfrak{z}=\mathfrak{z}+1$ and $\mathscr{g}$ is recalculated in (5-31-b); if one of the termination conditions is met, the while condition is terminated.

Up until here, the energy charging/discharging pattern for all mobile tanks is calculated

based on the proposed forward-backward approach. As can be seen, the constraints related to CAES units are converted to the feasible limits during the programming approach, which then, based on (5-1) and (5-5), the power transactions with the grid are determined.

5.2 Distributed generators

The distribution grid needs some DGs to participate in the operation of the grid to improve operational factors or to help the DSO to implement a secure operation. In this end, solar units and fuel-based dispatchable DGs are modeled in this study.

5.2.1 Solar units

For solar units, the generation of units is constant during each hour of scheduling and also non-dispatchable. The detailed specifications of these units (i.e., including generation pattern, location, and capacity) are presented in the case study section. Given the hourly power generation of the solar PV unit $P_{\mathcal{y},t}^{\mathcal{y}}$ where $\mathcal{y} \in \{1, 2, \dots, N_Y\}$, and considering the operating cost of PV generation is a negligible value, the revenue (i.e., equal to profit) of the solar system is calculated in (5-34):

$$R^{\mathcal{y}} = \sum_{t=1}^{N_T} \sum_{a=1}^{N_Y} P_{\mathcal{y},t}^{\mathcal{y}} \pi_t^{\mathcal{s},m} \tag{5-34}$$

5.2.2 Fuel-based distributed generation units

The model of the dispatchable fuel-based DGs is as follows [214]:

$$\mho_d^{\mathcal{Z}} U_{d,t}^{\mathcal{Z}} \leq P_{d,t}^{\mathcal{Z}} \leq \Omega_d^{\mathcal{Z}} U_{d,t}^{\mathcal{Z}} \qquad \forall d, \forall t \tag{5-35}$$

$$P_{d,t-1}^{\mathcal{Z}} - P_{d,t}^{\mathcal{Z}} > UR_d^{\mathcal{Z}} \quad \text{if} \quad P_{d,t-1}^{\mathcal{Z}} > P_{d,t}^{\mathcal{Z}} \qquad \forall d, \forall t \tag{5-36}$$

$$P_{d,t-1}^{\mathcal{Z}} - P_{d,t}^{\mathcal{Z}} > DR_d^{\mathcal{Z}} \quad \text{if} \quad P_{d,t-1}^{\mathcal{Z}} < P_{d,t}^{\mathcal{Z}} \qquad \forall d, \forall t \tag{5-37}$$

$$Q_{d,t}^{Z} = P_{d,t}^{Z}\sqrt{1-(f_d^{Z})^2}/f_d^{Z} \qquad \forall d, \forall t \qquad (5\text{-}38)$$

$$C_{d,t}^{Z} = \left(\alpha_d^{Z} {P_{d,t}^{Z}}^{2} + \beta_d^{Z} P_{d,t}^{Z} + \varsigma_d^{Z}\right) U_{d,t}^{Z} \qquad \forall d, \forall t \qquad (5\text{-}39)$$

$$R^{Z} = \sum_{t=1}^{N_T}\sum_{d=1}^{N_D}\left(P_{d,t}^{Z}\pi_t^{S,m} - C_{d,t}^{Z}\right) \qquad (5\text{-}40)$$

$$\mathcal{E}^{Z} = \sum_{t=1}^{N_T}\sum_{d=1}^{N_D} P_{d,t}^{Z} e_d^{Z} \qquad \forall d, \forall t \qquad (5\text{-}41)$$

where the active power $P_{d,t}^{Z}$ of generator $d \in \{1{:}\, N_D\}$ is limited by its maximum capacity Ω_d^{Z} and minimum capacity $\mho_d^{Z}$ in (5-35) when the fuel-based DG unit is operating (i.e., the binary variable $U_{d,t}^{Z} = 1$). Increasing and decreasing ramping constraints of DG units are modeled in (5-36) and (5-37) given the maximum increasing rate UR_d^{Z} and decreasing rate DR_d^{Z}. It is assumed that generators can provide reactive power $Q_{d,t}^{Z}$ based on (5-38) while operating at a constant power factor f_d^{Z}. Fuel consumption cost of DGs units $C_{d,t}^{Z}$ is calculated in (5-39) as a function of generating power of units where α_d^{Z}, β_d^{Z} and ς_d^{Z} are units fuel consumption coefficients. The total profit of units R^{Z} is calculated in (5-40) in which the first term refers to the revenue from selling power, and the second term refers to the fuel cost. Then, the total emission of the DG unit $\mathcal{E}^{Z}$ is determined in (5-41) by having $P_{d,t}^{Z}$ and fuel-to-emission rate e_d^{Z}.

5.3 Grid operation

The operation of the grid is subjected to several operational constraints as follows:

5.3.1 Distribution power flow:

Power flow equations for active and reactive powers are defined in (5-42) and (5-43):

$$P_i = \sum_{j=1}^{N_B} \Gamma_i \Gamma_j Y_{i,j} \cos\left(\Theta_{i,j} - \delta_i + \delta_j\right) \qquad \forall i \qquad (5\text{-}42)$$

$$Q_i = -\sum_{j=1}^{N_B} \Gamma_i \Gamma_j Y_{i,j} \sin\left(\Theta_{i,j} - \delta_i + \delta_j\right) \qquad \forall i \qquad (5\text{-}43)$$

where N_B is the number of buses, P_i, Q_i, Γ_i, and δ_i are the injected active power, injected reactive powers, voltage amplitude, and voltage angle at the bus i, respectively. $Y_{i,j}$ and $\Theta_{i,j}$ are the amplitude and angle of the $(i,j)^{th}$ entry of the bus admittance matrix [215].

5.3.2 Voltage limit of distribution buses:

$$\Gamma_{Min} \leq \Gamma_i \leq \Gamma_{Max} \qquad (5\text{-}44)$$

In order to reach a secure operation of the grid, the voltage of buses is limited to an acceptable operational voltage range $[\Gamma_{min}, \Gamma_{max}]$ for each bus i.

5.3.3 Power limit of distribution lines:

$$\left|P_{i,j}^{line}\right| \leq P_{i,j,Max}^{line} \qquad (5\text{-}45)$$

Similar to voltage limits, as stated in (5-45), the power flow of the line $P_{i,j}^{line}$ between bus i and j is limited to a maximum power $P_{i,j,Max}^{line}$ due to the thermal capacity of branches.

5.3.4 Power balance:

$$\sum_{y=1}^{N_Y} P_{y,t}^{\mathcal{Y}} + \sum_{d=1}^{N_D} P_{d,t}^{\mathcal{Z}} + \sum_{c \in C_B} \sum_{m=1}^{\bar{N}_{t,c}} P_{m,t,c}^{\mathcal{G},\mathcal{D}} + P_t^{\mathcal{S}} = P_t^{\mathcal{D}M} + P_t^{\mathcal{L}S} + \sum_{c \in C_B} \sum_{m=1}^{N_{M,c}} P_{m,t,c}^{\mathcal{G},\mathcal{C}} \qquad \forall t \qquad (5\text{-}46)$$

The hourly power balance equation between generation-demand of the network is modeled in (5-46), $P_t^{\mathcal{S}}$ is the amount of power provided by substation, $P_t^{\mathcal{D}M}$ is the hourly total load demand of the grid, and $P_t^{\mathcal{L}S}$ is hourly total power loss of the grid and is calculated in (5-47).

$$P_t^{\mathcal{LS}} = \sum_{i=1}^{N_B} \sum_{j>i}^{N_B} G_{i,j} \begin{bmatrix} \Gamma_{i,t}^2 + \Gamma_{j,t}^2 - \\ 2\Gamma_{i,t}\Gamma_{j,t} cos\left(\delta_{i,t} - \delta_{j,t}\right) \end{bmatrix} \quad (5\text{-}47)$$

where $G_{i,j}$ is the branch conductance between i^{th} and j^{th} buses. Using the distributed generators and storage system, the DSO aims to supply demands locally; however, the surplus/shortage powers are sold to/purchased from the upstream grid ($P_t^{\mathcal{S}}$) [212].

5.3.5 Distributed resources modeling:

In general, PV and PQ models are used for DG units in the grid operation [212]. This study considers DGs (both solar and fuel-based) as PQ nodes in which their generated powers are modeled as negative load in power flow formulations.

5.4 Objective functions

The objective functions Obj of this chapter include the total profit of DSO $R^{\mathcal{DSO}}$, total power loss $P^{\mathcal{LS}}$, total energy not supplied ENS, and voltage stability index VSI of the grid as follows:

$$Opt\{Obj\} = [\max R^{\mathcal{DSO}},\ \min P^{\mathcal{LS}}, \min ENS\,, \min VSI] \quad (5\text{-}48)$$

$$R^{\mathcal{DSO}} = R^{\mathcal{MG}} + R^{\mathcal{Y}} + R^{\mathcal{Z}} - \sum_{t=1}^{N_T} \left(P_t^{\mathcal{DM}} + P_t^{\mathcal{LS}}\right) \pi_t^{\mathcal{S},b} \quad (5\text{-}49)$$

$$P^{\mathcal{LS}} = \sum_{t=1}^{N_T} P_t^{\mathcal{LS}} \quad (5\text{-}50)$$

$$ENS = \sum_{t=1}^{N_T} \sum_{i=1}^{N_B - 1} \zeta_i\, L_i \left[\sum_{k \in \mathfrak{U}_i} Pd_{t,k}\, (r_k^s + r_k^r)\right] \quad (5\text{-}51)$$

$$VSI_t = \frac{1}{N_B} \sum_{j=1}^{N_B} VSI_{j,t} \quad (5\text{-}52)$$

DSO uses DGs and storage units to reduce the power loss and power purchase from the

upstream grid (5-49); otherwise, DSO needs to supply demands at the day-ahead market price $\pi_t^{s,b}$. The second objective is to minimize total power loss (5-50). In the *ENS* formulation (5-51), as the third objective, two terms of switching-time r_k^s and repair-time r_k^r are considered when the branch i is not available because of a failure, where $\mathfrak{U}_i$ denotes the set of buses not supplied when bus i is disconnected, and Pd_k is the amount of unsupplied load at buses $\mathfrak{U}_i$. A failure rate ζ_i and length L_i are assumed for each of the branches. Minimizing voltage stability index in (5-52) is the last objective function in which $VSI_{j,t} = SCC_{j,t}^{min}/SCC_{j,t}$. The Thevenin-equivalent circuit method in [216] is adopted to calculate the minimum short circuit current corresponding to marginal voltage stability index $SCC_{j,t}^{min}$, and the short circuit current at the location of each bus $SCC_{j,t}$. Finally, the value of objective function is $VSI = \max(\{VSI_1, VSI_2, \dots, VSI_t\})$.

5.5 Case study and results

In this study, the proposed methodology is applied to IEEE 33-bus and IEEE 136-bus DN to assess the effectiveness of utilizing MCAESs in the distribution grid in terms of given objectives. SRSR [131] is used as the optimization algorithm. Different scenarios of load variations are shown in Fig. 5-3 [7].

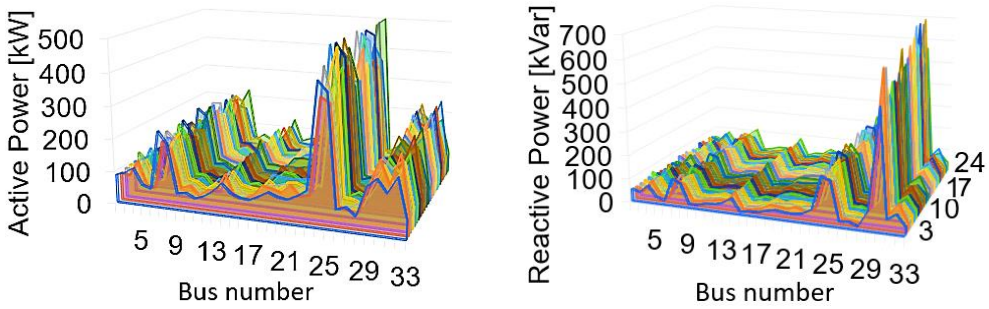

Fig. 5-3. Active and reactive load variations during 24h scheduling

The hourly price of the energy and realistic data of solar power production is based on the Australian electricity market, for 20th April of 2020 [217] (Fig. 5-4).

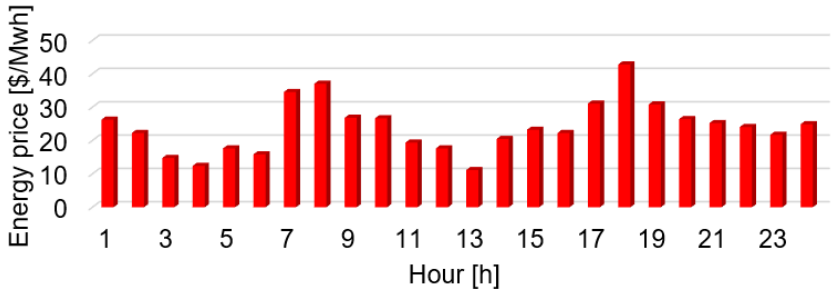

Fig. 5-4. Hourly energy price in the day-ahead market

The selling price is 10% lower than the purchasing price (i.e., due to transmission costs).

5.5.1 IEEE 33-bus system

- **Scenario 1: Solar and fuel-based DG units**

As the base case, this scenario investigates the involvement of solar and diesel units. Four solar units with a capacity of 400kW, 600kW, 800kW, and 1000kW are located at buses 10, 18, 26, and 32, respectively. The specifications of the DGs are presented in Table 5-1. A power factor of 0.9 is considered for all DGs (solar and fuel-based). In terms of ENS calculation, a failure rate ζ_i and length L_i are assumed for each of the branches (i.e., 0.05 and 1km for all lines). Two situations of single fault and double fault are considered for each hour.

Table 5-1. Specification of fuel-based DG units

Unit number	1	2	3	4
Min capacity [kW]	100	150	200	200
Max capacity [kW]	500	750	1000	1000
Location bus	16	18	31	33
Fuel factors α_d^Z [\$/kW^2], β_d^Z [\$/kW], ς_d^Z [\$]	5.8E-6, 0.21, 0	5.8E-6, 0.21, 0	5.3E-6, 0.20, 0	5E-6, 0.20, 0
Emission factor [g/kWh]	695	695	477	625

- **Scenario 2: Solar units, fuel-based DGs, and stationery CAESs**

In this scenario, the stationary form of CAESs is also added to the grid. Specifications of CAES units are detailed in Table 5-2. The proposed forward-backward approach has been employed in this case, though the location matrix formulation is not used for tanks as storage units are stationary in this scenario. The user-defined factors of energy mismatch e^g is 1kW and termination criterion e^3 is 50 in this study. The formulation and solution techniques in this scenario are the same as mobile ones, while there is no movement for tanks. The location of CAESs is considered as decision variables.

Table 5-2. Specification of CAES units

Parameter of motor-generator (MGs)	Value	Parameter of storage tanks	Value
Number of MGs	6	Number of tanks per MG	3
Maximum charging capacity of MGs [kW]	200	Capacity per tank [kWh]	200
Maximum discharging capacity of MGs [kW]	200	Initial idle hours of tanks	0
Charging/discharging stability rate of MGs	5%	Maximum depth of discharge	95%
Power factor	1	Mobile tanks speed [km/h]	65
Charging/discharging efficiency	0.85	Initial energy per tank [kWh]	100

- **Scenario 3: Solar units, fuel-based DGs, and MCAESs**

This scenario is an extended form of the previous scenario in which the location matrix of moving tanks is determined based on the proposed methodology. The fuel consumption of rigid trucks carrying tanks and the price of diesel fuel are assumed based on the Survey of Motor Vehicle Use, Australia [16].

- **Comparison of the results**

In the first scenario, fuel-based DGs need to compensate for the lack of energy produced

by solar units during the first and last hours of the day to improve the voltage of buses to the acceptable range. The results of this scenario for different objectives are detailed in Table 5-3.

Table 5-3. Optimum results for different objectives (Scenario 1)

Case num.	Objective	Operating profit [$]	Power loss [kWh]	ENS single; double fault/s [kWh]	VSI
1	$\max R^{DSO}$	-15,059.39	1372.9	-3,721.26; 512,200.26	0.7533
2	$\min P^{LS}$	-15,748.32	989.33	2,077.48; 559,425.95	0.7217
3	$\min ENS$	-15,415.25	1463.13	-6,328.27; 499,304.21	0.7927
4	$\min VSI$	-15,763.48	1346.82	5,509.76; 596,426.23	0.6685

A negative value for the ENS factor means that the total summation of generation during the 24h scheduling horizon is more than the corresponding load demand considering different scenarios of fault/failure. Similarly, operation profit has negative values since the DSO needs to buy energy from day-ahead markets. Although values of a specific objective for two or more cases are rather close (e.g., power loss in Case 1 and 4), they are very different in profit, ENS, and VSI.

In Scenario 2, stationary CAES units are added into the system. Scheduling results for the given configuration is detailed in Table 5-4.

Table 5-4. Optimum results for different objectives (Scenario 2)

Case num.	Objective	Operating profit [$]	Power loss [kWh]	ENS single; double fault/s [kWh]	VSI
1	$\max R^{DSO}$	-14,346.67	1,501.09	-5942.42; 505,850.66	0.7447
2	$\min P^{LS}$	-14,863.88	1,004.28	2,190.20; 71,943.27	0.7311
3	$\min ENS$	-14,975.01	1,578.68	-9,175.74; 473,740.43	0.6879
4	$\min VSI$	-15,490.74	1,326.02	3,301.22; 590,735.83	0.5983

As can be seen, compared to the results of the previous scenario, the value of objective functions is improved for different cases. Noteworthy, unlike fuel-based DG units that can generate energy, stationary storage systems can only take advantage of price changes, and

they could not be efficient in the case power loss. In terms of operating profit, CAES utilization can provide some benefit for the first three cases even though objectives are different for cases 2 and 3. However, the CAES unit offers a significant improvement in voltage stability in case 4, where stability index 0.5983 is achieved.

For Scenario 3, stationary CAESs are replaced with MCAES technology. The results of different cases for this scenario are presented in Table 5-5.

Table 5-5. Optimum results for different objectives (Scenario 3)

Case num.	Objective	Operating profit [$]	Power loss [kWh]	ENS single; double fault/s [kWh]	VSI
1	$\max R^{DSO}$	-14477.46	1,417.68	-2,940.04; 561,571.70	0.7176
2	$\min P^{LS}$	-15,067.08	970.92	1,732.26; 561,571.70	0.7136
3	$\min ENS$	-15,238.32	1,579.18	-9302.16; 473,828.68	0.6408
4	$\min VSI$	-15,603.11	1,318.05	2,309.82; 577,409.26	0.5641

As it is evident, MCAES technology could improve the operating condition of the grid in three terms of power loss, ENS, and VSI; however, operating profit in Scenario 3 could not reach a better value than for the Scenario 2. As a simple conclusion, DSO can operate the grid using stationary CAES technology in the normal condition with the objective of profit maximization. At the same time, to improve the reliability/ resilience or VSI correction of the grid after an event, DSO can simply switch from stationary to MCAES. Fig. 5-5 shows details of operating profits for Scenario 1 – Scenario 3. In this figure, the purchased energy includes base-load demand plus active power loss of the corresponding case. Besides, selling energy includes power generation of solar units, fuel-based DGs, and stationary/mobile CAESs. The primary pattern of power buying-selling is defined by solar and fuel-based DGs based on the hourly load profile, and the CAES units provide additional profit by reducing the expensive commitment of fuel-based DGs. Comparing two stationary and mobile modes of CAES, the

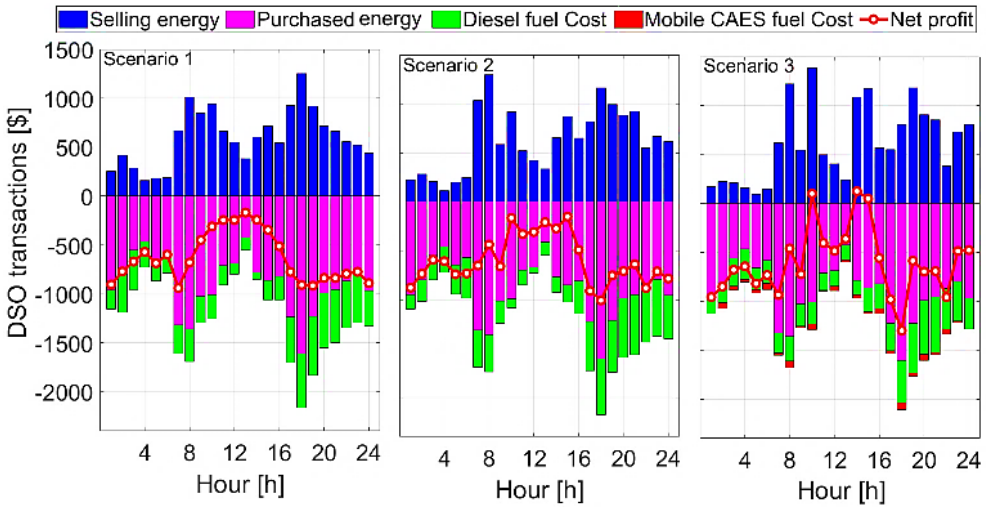

Fig. 5-5. Hourly financial transactions of DSO - Case 1 (Scenario 1 – 3)

lack of DLMP causes mobile technology not to be efficient to take advantage of price changes at the location of buses. Additionally, the fuel cost of MCAES is the reason to reduce the total profit in Scenario 3. In the case of power loss, compared to Scenario 1, MCAES provides a small improvement while offering a considerable profit improvement compared to Scenario 1. Similarly, as can be seen in Fig. 5-6, MCAESs are highly efficient for ENS improvement in comparison. Histogram for 24h voltage of the grid in Scenario 3 is shown in Fig. 5-7. It can be seen that Case 4 has the lowest divergence from the desired mean value of 1 p.u. This situation provides DSO with a safe zone against sudden changes (significant increase or decrease) of loads in the grid, although selecting this objective results in a higher operational

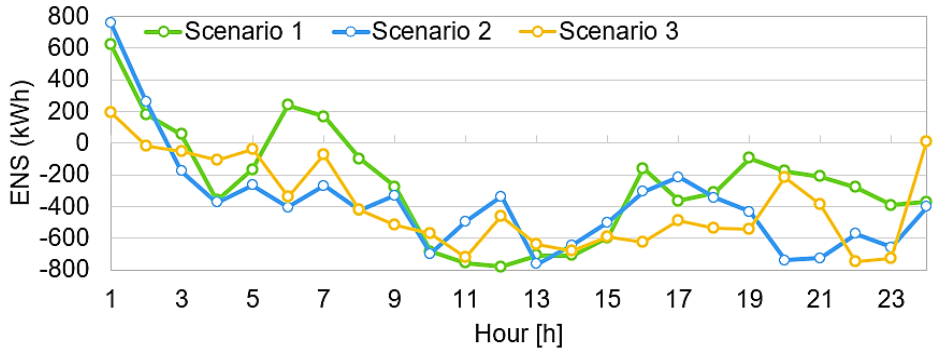

Fig. 5-6. Hourly single-fault ENS profile (Case 3) for Scenarios (1-3)

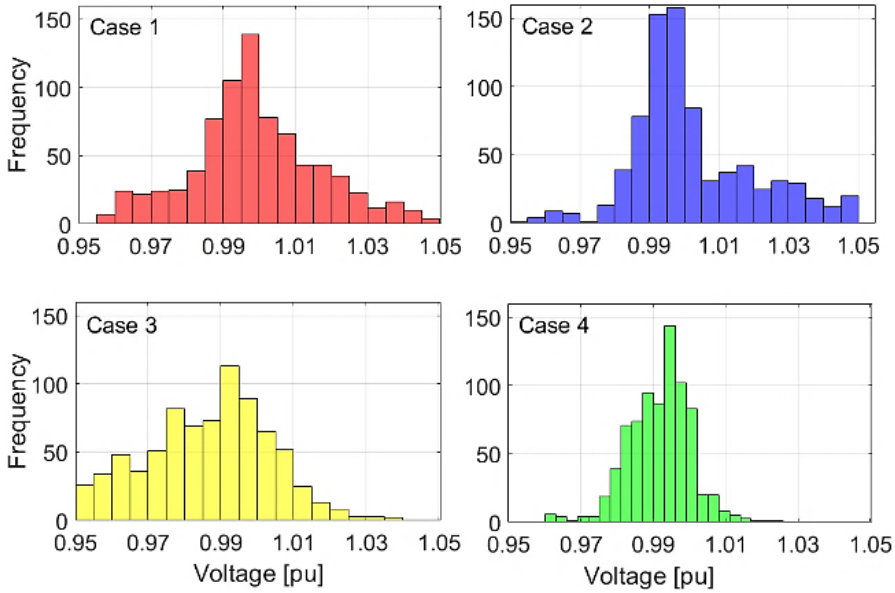

Fig. 5-7. Histogram for voltage profile of buses (different cases- Scenario 3)

cost based on Table 5-5. The total charge/discharge pattern of energy at the location of motor-generators of MCAES units are shown in Fig. 5-8.

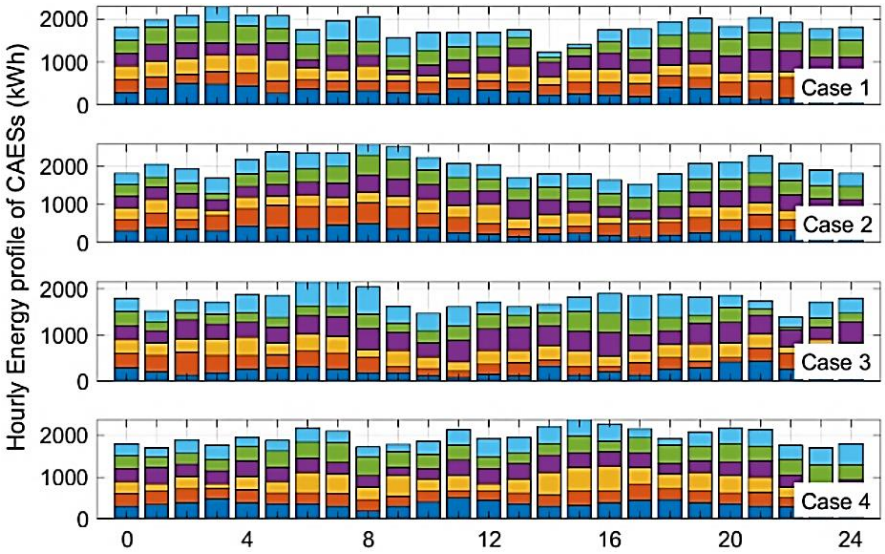

Fig. 5-8. The total hourly variations of energy for CAES units (Scenario 3)

Since there is no significant solar generation for hours in which the price of energy is high, fuel-based DGs and storage units are the only sources of power provision. In such a situation, the load will be supplied by CAES units if the energy price is around 35% higher than the

charging time (i.e., because 1/ ($\alpha_c^{\mathcal{G},\mathcal{C}} \times \alpha_c^{\mathcal{G},\mathcal{D}}$) where $\alpha_c^{\mathcal{G},\mathcal{C}} = \alpha_c^{\mathcal{G},\mathcal{D}} = 0.85$); otherwise, fuel-based DGs are the only option for the power supply. Hourly generation of fuel-based DGs in Scenario 3 is depicted in Fig. 5-9.

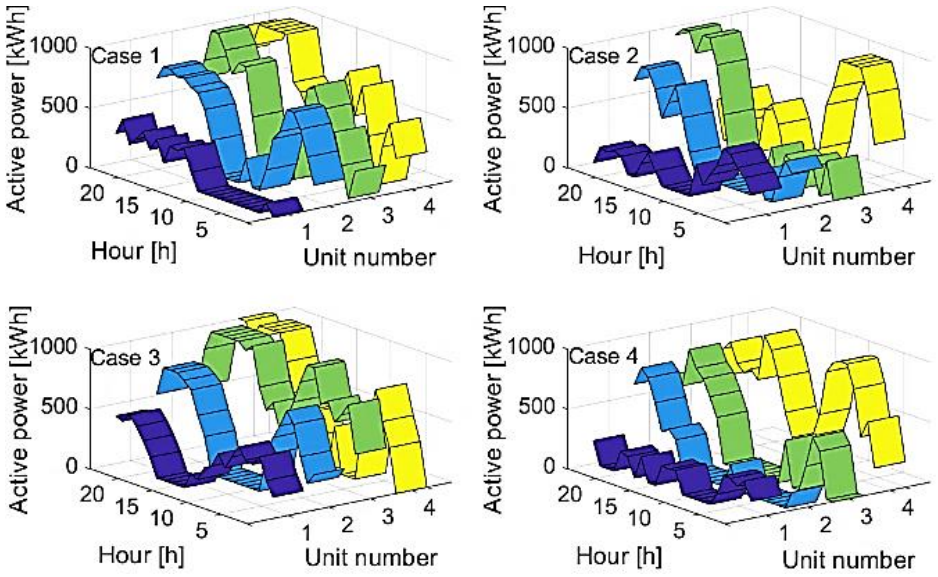

Fig. 5-9. Active generation of fuel-based DG units in different cases (Scenario 3)

The maximum total amount of fuel-based DGs generation happens in Case 3, where the energy provision of units directly affects the amount of ENS in the gird. For Case 2, fuel-based DGs are tending to maximize the profit by charging mobile tanks during the hours in which the price of energy is low and power injection during high energy prices. Therefore, the most expensive unit is the least involved.

5.5.2 IEEE 136-bus system

For this case study, the proposed methodology has been applied to the standard IEEE 136-bus system. The same scenarios and objective cases have been considered for this test system. The number of solar units, fuel-based DGs, and MCAES motor-generators have increased to 12, 9, and 11 units, respectively, while the number of tanks per MCAES unit has remained the

same. Results for the given scenarios are detailed in Table 5-6 - Table 5-8.

Table 5-6. Optimum results for different objectives (Scenario 1)

Case num.	Objective	Operating profit [$]	Power loss [kWh]	ENS single; double fault/s [kWh]	VSI
1	$\max R^{DSO}$	-83,622.45	4,469.43	93,036.74; 19,482,653	0.5661
2	$\min P^{LS}$	-86,444.44	4,155.87	95,380.70; 19,211,786	0.5237
3	$\min ENS$	-89,847.09	4,594.61	89,483.83; 19, 174,498	0.5785
4	$\min VSI$	-91,598.21	4,289.50	108,162.41; 19,956,241	0.4991

Table 5-7. Optimum results for different objectives (Scenario 2)

Case num.	Objective	Operating profit [$]	Power loss [kWh]	ENS single; double fault/s [kWh]	VSI
1	$\max R^{DSO}$	- 76,975.54	4,492.23	89,758.89; 19,117,132	0.5167
2	$\min P^{LS}$	-77,670.80	4,113.03	97,043.63; 19,351,856	0.5002
3	$\min ENS$	-78,908.34	4,565.98	67,794.97; 17,065,303	0.4716
4	$\min VSI$	-80,515.47	4,290.11	100,131.23; 19,749,275	0.4469

Table 5-8. Optimum results for different objectives (Scenario 3)

Case num.	Objective	Operating profit [$]	Power loss [kWh]	ENS single; double fault/s [kWh]	VSI
1	$\max R^{DSO}$	-78,012.28	4,419.09	91,736.19; 19,232,839	0.4518
2	$\min P^{LS}$	-79,328.02	3,969.87	94,185.46; 19,184,954	0.4159
3	$\min ENS$	-79,864.39	4,501.54	54,029.83; 16,212,038	0.3989
4	$\min VSI$	81,001,27	4,282.30	93,279.13; 19,635,249	0.3823

As can be seen, enlarging the grid-scale has made the impacts of MCAES technology utilization more highlighted in several cases. Especially considering the grid is geographically spread over a much larger area, the reliability factor ENS (case 3) is significantly decreased in Scenario 3 even compared to Scenario 2. Similarly, the notable applicability of MCAES for voltage stability enhancement (case 4) of the network in Scenario 3 is much more apparent in this test system compared to stationary CAES in Scenario 2. A lower mean value of VSI in different scenarios shows the IEEE 136-bus system is more stable than the IEEE 33-bus system. Evidently, the results demonstrate that the transportability of MCAES has more potential in

larger DNs to decrease the active power loss of the grid. In terms of the operating profit, even though MCAES could provide a substantial improvement compared to the base-case scenario, it still provides a lower profit than stationary CAES.

5.6 Summary

A novel detailed modeling of a TESS based on CAES technology has been presented in this chapter. Obtained results have demonstrated that how adding MCAES technology into the grid can significantly improve operating conditions of the grid while having different objectives (3.86% in net profit, 1.85% in power loss, 31.97% in single fault ENS, and 15.61% in VSI for the IEEE 33-bus system). Considering these values are better than the results of using stationary CAES (except the net profit), it can be inferred the high dispatchability of MCAES technology offered by employing several cheap mobile air storage tanks is the key factor in this regard, even though the number of motor-generators is much more limited. For the scenario of profit maximization, it also would be a potential option for DSO to switch between stationary and mobile modes to reach an extra 1.98% profit. Additionally, the IEEE 136-bus test system makes potential applications of MCAES more highlighted (6.75% in net profit, 4.47% in power loss, 39.62% in single fault ENS, 23.40% in VSI). Hence, the geographical dimensionality of the grid has a noticable effect on the applicability of the MCAES. Besides, for grids that heavily suffer from periodic voltage instability and critical events, MCAES has shown some significant performance improvements. Moreover, with the help of MCAESs, the lesser commitment of fuel-based DGs has been obtained, which also contributes to a lower amount of emission.

Additionally, the presented forward-backward approach for constraint handling of MCAES units along with the proposed solution coding has largely reduced the dimension, complexity,

and computational burden of the solution approach. Besides, using updated data of Google Maps API has removed the challenges related to mathematical modeling of route congestions and model linearization for optimal movements of storage units.

Chapter 6 Conclusions and Suggestions for Further Work

In this chapter, an overall review of the contributions of this thesis and the important possible areas for further research are reviewed and briefly summarized.

6.1 Summary and conclusions

This thesis firstly presents a literature review over the factors which have led traditional DNs toward the emergence of ADSs, and technical and regulatory requirements for the development of ADS, operating impacts of DERs and energy storages on optimal management of ADS, and the formation of decentralized MG during the recent years. Additionally, some studies related to day-ahead scheduling of the grid, the participation of DSO and DISCO in wholesale electricity markets, the aggregation concept of DERs and energy storage in ADSs are investigated. The impacts of two emerging energy storage technologies, including PEVs and CAES, on the operation of ADS are analyzed based on previous studies. Finally, the most important technical factors and technical modeling algorithms which have been utilized in the operation of restructured distribution grids are studied.

In Chapter 3, potential applications of a distribution size CAES for participation in the day-ahead market are investigated. At the same time, detailed thermal modeling has been added to the electrical formulations to provide an accurate model. As a result, a new thermal-electrical conversion rate suitable for SCAES is proposed that is lower than that of large-scale CAESs. Besides, considering several scenarios of energy storage involvement, the performance of SCAES is compared with EVCS. Then, a coordinated method is used to schedule both energy

storage technologies simultaneously. The results demonstrated that SCAES is highly capable of taking advantage of price differences during the operation period to maximize DSO's profit while improving operating factors like voltage profile and active power loss. The results of lifetime analysis and comparison of the CAES with battery units illustrates that SCAES is highly superior to battery systems in a longterm period due to their much lower construction cost and longer life-cycle. Comparing SCAES with EVCS, uncertainties related to arrival and departure of electric vehicles at a charging station as well as the high manufacturing cost of PEV batteries are factors which make SCAES a more reliable option.

In Chapter 4, modeling of an aggregator for privately owned CAES units is conducted. Based on the proposed two agent-structure, storage units are scheduled by CAES aggregator to reach maximum profit for CAES owners using the locational marginal price received from DSO. On the other hand, DSO as the second agent, is responsible for the scheduling of diesel generators and participating in the day-ahead market to maximize operating profit while securing the grid operation indices. The profit maximization problem for the CAES aggregator has been linearized and solved using a linear optimization toolbox, while the DSO modeling is accomplished through a multi-objective optimization approach to minimize emission and cost, and also maximize DSO profit in different scenarios. The comparison of results for scenarios with/without considering the SCAES aggregator is demonstrated so that implementation of such a market structure could potentially benefit both agents and encourage the private sector to invest in energy storage technologies.

In Chapter 5, a novel concept of mobile CAES is proposed. A new formulation suited to the proposed framework is presented to incorporate a high number of low construction cost mobile air tanks and a low number of motor-generators, which subsequently offers a larger

storage size compering to TESSs. For the constraint handling method, a novel heuristic approach is proposed, which maps the constrained solutions into their feasible ranges. Using the same matrix for both commitment and dispatch indication of MCAES was another novelty of this study. These could provide a significant improvement in terms of solution convergence and quality. Additionally, Google Maps API is used to calculate routes and avoid road congestions instead of modeling routes as an extra optimization problem. Results of simulations for two cases of 33-bus and 136-bus IEEE test systems demonstrated that mobile CAES units have very similar capabilities of the stationary storage system in terms of profit maximization and power loss reduction, while they can offer a substantial additional potential advantage for ENS/resilience and voltage stability improvement in DN.

Overall, this thesis has investigated three major technical studies. The first study models a DSO participation in wholesale electricity employing a SCAES with a detailed thermodynamic model. The second study presents a new double-agent based structure for the distribution market with the incorporation of SCAES aggregators. The last case study proposes the concept of mobile CAES along with a new constraint handing method to improve the operating conditions of the grid.

6.2 Future work

In this thesis, several operating methods for day-ahead scheduling of a DSO with the incorporation of solar DERs and SCAES units are presented. The current research can be extended in several ways, mainly:

- In this thesis, only solar power is modeled as DERs in different studies; however, the integration of other types of renewable energies with a different generation pattern can

significantly change the scheduling approach. For example, the integration of wind resources can provide inexpensive energy during the night, which can be highly suitable for charging stationary/mobile storage units during the very low load demand times.

- In chapter 3, a detailed accurate model for the thermodynamic modeling of CAES is proposed, which makes the obtained model non-linear and very complicated. However, applying some simplifications and linearization may offer a trade-off between accuracy and computational burden.
- In Chapter 4, the CAES aggregator needs to receive the DLMP from DSO to schedule SCAES units and maximize its profit. However, the calculation approach of DLMP is not modeled in this study. A novel approach for DLMP calculation considering the specifications of SCAES units and the configuration of the grid may offer a more accurate model that results in benefits for both agents.
- In Chapter 5, the application of MCAES for reliability improvement of the grid in terms of ENS factor is accomplished. However, ENS can be considered as a factor for the resilience of the grid; the application of MCAES can be specifically formulated and modeled for an extreme happening like bushfire and tornado. In such situations, MCAES can be very efficient for short-term supplying of the first responders and critical loads; or to be joined with other operating schemes like topology reconfiguration.

References

[1] Z. Hu and F. Li, "Cost-benefit analyses of active distribution network management, Part II: Investment reduction analysis," *IEEE Transactions on Smart Grid,* vol. 3, no. 3, pp. 1075-1081, 2012.

[2] H. Ghoreishi, H. Afrakhte, and M. J. Hhadi, "Optimal placement of tie points and sectionalizers in radial distribution network in presence of DGs considering load significance," in *Smart Grid Conference (SGC), 2013*, 2013, pp. 160-165: IEEE.

[3] J. Liu, H. Gao, Z. Ma, and Y. Li, "Review and prospect of active distribution system planning," *Journal of Modern Power Systems and Clean Energy,* vol. 3, no. 4, p. 457, 2015.

[4] M. H. Imani, K. Yousefpour, M. J. Ghadi, and M. T. Andani, "Simultaneous presence of wind farm and V2G in security constrained unit commitment problem considering uncertainty of wind generation," in *2018 IEEE Texas Power and Energy Conference (TPEC)*, 2018, pp. 1-6: IEEE.

[5] M. Faisal, M. A. Hannan, P. J. Ker, A. Hussain, M. B. Mansor, and F. Blaabjerg, "Review of energy storage system technologies in microgrid applications: Issues and challenges," *IEEE Access,* vol. 6, pp. 35143-35164, 2018.

[6] M. J. Ghadi, S. Ghavidel, A. Rajabi, A. Azizivahed, L. Li, and J. Zhang, "A review on economic and technical operation of active distribution systems," *Renewable and Sustainable Energy Reviews,* vol. 104, pp. 38-53, 2019.

[7] M. J. Ghadi *et al.*, "Day-Ahead Market Participation of an Active Distribution Network Equipped with Small-Scale Compressed Air Energy Storage Systems," *IEEE Transactions on Smart Grid,* 2020.

[8] M. Giberson and L. Kiesling, "The Need for Electricity Retail Market Reforms," *Regulation,* vol. 40, p. 34, 2017.

[9] A. Poullikkas, G. Kourtis, and I. Hadjipaschalis, "Parametric analysis for the installation of solar dish technologies in Mediterranean regions," *Renewable and Sustainable Energy Reviews,* vol. 14, no. 9, pp. 2772-2783, 2010.

[10] M. T. Islam, N. Huda, A. Abdullah, and R. Saidur, "A comprehensive review of state-of-the-art concentrating solar power (CSP) technologies: Current status and research trends," *Renewable and Sustainable Energy Reviews,* vol. 91, pp. 987-1018, 2018.

[11] S. H. Gilani, M. J. Ghadi, and H. Afrakhte, "Optimal allocation of wind turbines considering different costs for interruption aiming at power loss reduction and reliability improvement using imperialistic competitive algorithm," *International Review of Electrical Engineering,* vol. 8, no. 1, pp. 284-296, 2013.

[12] M. J. Ghadi, A. Rajabi, S. Ghavidel, A. Azizivahed, L. Li, and J. Zhang, "From active distribution systems to decentralized microgrids: A review on regulations and planning approaches based on operational factors," *Applied Energy,* vol. 253, p. 113543, 2019.

[13] M. F. Zia, E. Elbouchikhi, and M. Benbouzid, "Microgrids energy management systems: A critical review on methods, solutions, and prospects," *Applied energy,* 2018.

[14] A. Ehsan and Q. Yang, "State-of-the-art techniques for modelling of uncertainties in active distribution network planning: A review," *Applied Energy,* 2019.
[15] T. Gonen, *Electric power distribution engineering*. CRC press, 2016.
[16] V. N. Coelho, M. Weiss Cohen, I. M. Coelho, N. Liu, and F. G. Guimarães, "Multi-agent systems applied for energy systems integration: State-of-the-art applications and trends in microgrids," *Applied Energy,* vol. 187, pp. 820-832, 2017/02/01/ 2017.
[17] M. Stadler *et al.*, "Value streams in microgrids: A literature review," *Applied Energy,* vol. 162, pp. 980-989, 2016/01/15/ 2016.
[18] D. Trebolle, P. Hallberg, G. Lorenz, P. Mandatova, and J. T. Guijarro, "Active distribution system management," in *Electricity Distribution (CIRED 2013), 22nd International Conference and Exhibition on*, 2013, pp. 1-4: IET.
[19] P. Hallberg, "Active distribution system management a key tool for the smooth integration of distributed generation," *Eurelectric TF Active System Management,* vol. 2, no. 13, 2013.
[20] S. Ruester, S. Schwenen, C. Batlle, and I. Pérez-Arriaga, "From distribution networks to smart distribution systems: Rethinking the regulation of European electricity DSOs," *Utilities Policy,* vol. 31, pp. 229-237, 2014.
[21] M. Fan, Z. Zhang, A. Su, and J. Su, "Enabling technologies for active distribution systems," *Proceedings of the CSEE,* vol. 33, no. 22, pp. 12-18, 2013.
[22] V. A. Evangelopoulos, P. S. Georgilakis, and N. D. Hatziargyriou, "Optimal operation of smart distribution networks: A review of models, methods and future research," *Electric Power Systems Research,* vol. 140, pp. 95-106, 2016.
[23] D. Trebolle, P. Hallberg, G. Lorenz, P. Mandatova, and J. T. Guijarro, "Active distribution system management," in *Electricity Distribution (CIRED 2013), 22nd International Conference and Exhibition on*, 2014, pp. 1-4: IET.
[24] A. Gomez-Exposito, A. J. Conejo, and C. Canizares, *Electric energy systems: analysis and operation*. CRC press, 2018.
[25] G. Liu, R. Huang, T. Pu, and Z. Yang, "Design of energy management system for Active Distribution Network," in *Electricity Distribution (CICED), 2014 China International Conference on*, 2014, pp. 561-564: IEEE.
[26] A. Bernstein, L. Reyes-Chamorro, J.-Y. Le Boudec, and M. Paolone, "A composable method for real-time control of active distribution networks with explicit power setpoints. Part I: Framework," *Electric Power Systems Research,* vol. 125, pp. 254-264, 2015.
[27] K. Utkarsh, A. Trivedi, D. Srinivasan, and T. Reindl, "A consensus-based distributed computational intelligence technique for real-time optimal control in smart distribution grids," *IEEE Transactions on Emerging Topics in Computational Intelligence,* vol. 1, no. 1, pp. 51-60, 2017.
[28] S. Ruester, I. J. PÉREZ-ARRIAGA, S. Schwenen, C. Batlle, and J.-M. Glachant, "From distribution networks to smart distribution systems: Rethinking the regulation of European electricity DSOs," 9290841443, 2013.
[29] M. Vallés, J. Reneses, R. Cossent, and P. Frías, "Regulatory and market barriers to the realization of demand response in electricity distribution networks: a European perspective," *Electric Power Systems Research,* vol. 140, pp. 689-698, 2016.
[30] M. Vallés, J. Reneses, P. Frías, and C. Mateo, "Economic benefits of integrating

Active Demand in distribution network planning: A Spanish case study," *Electric Power Systems Research,* vol. 136, pp. 331-340, 2016.

[31] A. Rajabi, L. Li, J. Zhang, and J. Zhu, "Aggregation of small loads for demand response programs—Implementation and challenges: A review," in *Environment and Electrical Engineering and 2017 IEEE Industrial and Commercial Power Systems Europe (EEEIC/I&CPS Europe), 2017 IEEE International Conference on*, 2017, pp. 1-6: IEEE.

[32] A. Rajabi, L. Li, J. Zhang, J. Zhu, S. Ghavidel, and M. J. Ghadi, "A Review on Clustering of Residential Electricity Customers and Its Applications," presented at the The 20th International Conference on Electrical Machines and Systems, 2017 IEEE International Conference on, 2017.

[33] M. H. Abbasi, A. Rajabi, M. Taki, L. Li, S. Ghavidel, and M. J. Ghadi, "Risk-Constrained Offering Strategies for a Price-Maker DR Aggregator," presented at the Environment and Electrical Engineering and 2017 IEEE Industrial and Commercial Power Systems Europe (EEEIC/I&CPS Europe), 2017 IEEE International Conference on, 2017.

[34] N. G. Stewart, "Electrical power distribution system for enabling distributed energy generation," ed: Google Patents, 2017.

[35] A. Sharifian, M. J. Ghadi, S. Ghavidel, L. Li, and J. Zhang, "A new method based on Type-2 fuzzy neural network for accurate wind power forecasting under uncertain data," *Renewable energy,* vol. 120, pp. 220-230, 2018.

[36] M. J. Ghadi, S. H. Gilani, H. Afrakhte, and A. Baghramian, "Short-term and very short-term wind power forecasting using a hybrid ICA-NN method," *International Journal of Computing and Digital Systems,* vol. 3, no. 01, 2014.

[37] M. J. Ghadi, L. Li, J. Zhan, L. Chen, Q. Huang, and C. Li, "A Review on the development of concentrated solar power and its Integration in coal-fired power plants," in *2019 IEEE Innovative Smart Grid Technologies-Asia (ISGT Asia)*, 2019, pp. 1106-1111: IEEE.

[38] M. J. Ghadi, L. Li, and J. Zhang, "Optimal design of solar photovoltaic and concentrated solar power system for coal-fired power plants in NSW," 2020.

[39] M. Hosseini Imani, S. Zalzar, A. Mosavi, and S. Shamshirband, "Strategic behavior of retailers for risk reduction and profit increment via distributed generators and demand response programs," *Energies,* vol. 11, no. 6, p. 1602, 2018.

[40] S. Fan, T. Pu, L. Li, T. Yu, Z. Yang, and B. Gao, "Evaluation of impact of integrated distributed generation on distribution network based on time-series analysis," in *Electricity Distribution (CICED), 2016 China International Conference on*, 2016, pp. 1-5: IEEE.

[41] M. A. Zehir *et al.*, "Impacts of microgrids with renewables on secondary distribution networks," *Applied Energy,* 2017.

[42] A. Azizivahed, S. Ghavidel, M. J. Ghadi, L. Li, and J. Zhang, "New energy management approach in distribution systems considering energy storages," in *Electrical Machines and Systems (ICEMS), 2017 20th International Conference on*, 2017, pp. 1-6: IEEE.

[43] S. A. Kalogirou, "Solar thermal collectors and applications," *Progress in energy and combustion science,* vol. 30, no. 3, pp. 231-295, 2004.

[44] M. H. Imani, K. Yousefpour, M. T. Andani, and M. J. Ghadi, "Effect of Changes in Incentives and Penalties on Interruptible/Curtailable Demand Response Program in Microgrid Operation," in *2019 IEEE Texas Power and Energy Conference (TPEC)*, 2019, pp. 1-6: IEEE.

[45] A. Alhamali, M. E. Farrag, G. Bevan, and D. M. Hepburn, "Review of Energy Storage Systems in electric grid and their potential in distribution networks," in *Power Systems Conference (MEPCON), 2016 Eighteenth International Middle East*, 2016, pp. 546-551: IEEE.

[46] P. Lombardi *et al.*, "An A-CAES pilot installation in the distribution system: A technical study for RES integration," *Energy Science & Engineering,* vol. 2, no. 3, pp. 116-127, 2014.

[47] X. Luo, J. Wang, M. Dooner, and J. Clarke, "Overview of current development in electrical energy storage technologies and the application potential in power system operation," *Applied Energy,* vol. 137, pp. 511-536, 2015.

[48] A. Bizuayehu, P. Medina, J. P. Catalao, E. Rodrigues, and J. Contreras, "Analysis of electrical energy storage technologies' state-of-the-art and applications on islanded grid systems," in *T&D Conference and Exposition, 2014 IEEE PES*, 2014, pp. 1-5: IEEE.

[49] A. K. Marvasti, Y. Fu, S. DorMohammadi, and M. Rais-Rohani, "Optimal operation of active distribution grids: A system of systems framework," *IEEE Transactions on Smart Grid,* vol. 5, no. 3, pp. 1228-1237, 2014.

[50] A. Mishra *et al.*, "Integrating energy storage in electricity distribution networks," in *Proceedings of the 2015 ACM Sixth International Conference on Future Energy Systems*, 2015, pp. 37-46: ACM.

[51] F. Pilo *et al.*, "Planning and optimisation of active distribution systems-An overview of CIGRE Working Group C6. 19 activities," 2012.

[52] C. Sun *et al.*, "Sustainability evaluation in power system related applications—A review," in *Power System Technology (POWERCON), 2016 IEEE International Conference on*, 2016, pp. 1-6: IEEE.

[53] G. Celli, F. Pilo, G. Pisano, and G. G. Soma, "Reference scenarios for Active Distribution System according to ATLANTIDE project planning models," in *Energy Conference (ENERGYCON), 2014 IEEE International*, 2014, pp. 1190-1196: IEEE.

[54] L. Shao, X. Zhou, J. Li, H. Liu, and X. Chen, "Microgrids as Flexible and Network-Connected Grid Assets in Active Distribution Systems," *Journal of Electrical and Computer Engineering,* vol. 2018, 2018.

[55] K. S. A. Sedzro, A. J. Lamadrid, and L. F. Zuluaga, "Allocation of Resources Using a Microgrid Formation Approach for Resilient Electric Grids," *IEEE Transactions on Power Systems,* vol. 33, no. 3, pp. 2633-2643, 2018.

[56] S. Chowdhury and P. Crossley, *Microgrids and active distribution networks*. The Institution of Engineering and Technology, 2009.

[57] A. Kargarian and Y. Fu, "System of systems based security-constrained unit commitment incorporating active distribution grids," *IEEE Trans. Power Syst,* vol. 29, no. 5, pp. 2489-2498, 2014.

[58] A. Sinha, A. Basu, R. Lahiri, S. Chowdhury, S. Chowdhury, and P. A. Crossley, "Setting of market clearing price (MCP) in microgrid power scenario," in *Power and*

Energy Society General Meeting-Conversion and Delivery of Electrical Energy in the 21st Century, 2008 IEEE, 2008, pp. 1-8: IEEE.

[59] A. L. Dimeas and N. D. Hatziargyriou, "Operation of a multiagent system for microgrid control," *IEEE Transactions on Power systems,* vol. 20, no. 3, pp. 1447-1455, 2005.

[60] M. H. Imani, P. Niknejad, and M. Barzegaran, "The impact of customers' participation level and various incentive values on implementing emergency demand response program in microgrid operation," *International Journal of Electrical Power & Energy Systems,* vol. 96, pp. 114-125, 2018.

[61] G. Celli, F. Pilo, G. Pisano, and G. Soma, "Optimal participation of a microgrid to the energy market with an intelligent EMS," in *Power Engineering Conference, 2005. IPEC 2005. The 7th International*, 2005, pp. 663-668: IEEE.

[62] H. A. Gil and G. Joos, "Models for quantifying the economic benefits of distributed generation," *IEEE Transactions on power systems,* vol. 23, no. 2, pp. 327-335, 2008.

[63] S. N. Singh and I. Erlich, "Strategies for wind power trading in competitive electricity markets," *IEEE transactions on energy conversion,* vol. 23, no. 1, pp. 249-256, 2008.

[64] D. E. Olivares, C. A. Cañizares, and M. Kazerani, "A centralized energy management system for isolated microgrids," *IEEE Trans. Smart Grid,* vol. 5, no. 4, pp. 1864-1875, 2014.

[65] S. A. Arefifar, Y. A.-R. I. Mohamed, and T. H. El-Fouly, "Supply-adequacy-based optimal construction of microgrids in smart distribution systems," *IEEE transactions on smart grid,* vol. 3, no. 3, pp. 1491-1502, 2012.

[66] S. A. Arefifar and Y. A.-R. I. Mohamed, "DG mix, reactive sources and energy storage units for optimizing microgrid reliability and supply security," *IEEE Transactions on Smart Grid,* vol. 5, no. 4, pp. 1835-1844, 2014.

[67] X. Zhao, Q. Chen, Q. Xia, C. Kang, and H. Wang, "Multi-period coordinated active-reactive scheduling of active distribution system," in *Power and Energy Society General Meeting (PES), 2013 IEEE*, 2013, pp. 1-5: IEEE.

[68] A. A. Ibrahim, B. Kazemtabrizi, and C. Dent, "Operational planning and optimisation in active distribution networks using modern intelligent power flow controllers," in *PES Innovative Smart Grid Technologies Conference Europe (ISGT-Europe), 2016 IEEE*, 2016, pp. 1-6: IEEE.

[69] A. Azizivahed, H. Lotfi, M. J. Ghadi, S. Ghavidel, L. Li, and J. Zhang, "Dynamic feeder reconfiguration in automated distribution network integrated with renewable energy sources with respect to the economic aspect," in *2019 IEEE Innovative Smart Grid Technologies-Asia (ISGT Asia)*, 2019, pp. 2666-2671: IEEE.

[70] H. Gao, J. Liu, and L. Wang, "Robust Coordinated Optimization of Active and Reactive Power in Active Distribution Systems," *IEEE Transactions on Smart Grid,* 2017.

[71] J. Duan, T. Mu, F. Yan, L. Chen, K. Wang, and Y. Lei, "Optimization schedule of active distribution system based on improved harmony search algorithm," in *Electric Utility Deregulation and Restructuring and Power Technologies (DRPT), 2015 5th International Conference on*, 2015, pp. 2678-2683: IEEE.

[72] A. Borghetti *et al.*, "Short-term scheduling and control of active distribution systems with high penetration of renewable resources," *IEEE Systems Journal,* vol. 4, no. 3,

pp. 313-322, 2010.
[73] A. Saint-Pierre and P. Mancarella, "Active distribution system management: a dual-horizon scheduling framework for DSO/TSO interface under uncertainty," *IEEE Transactions on Smart Grid,* 2016.
[74] A. Azizivahed, S. Ghavidel, M. J. Ghadi, L. Li, and J. Zhang, "Multi-area economic emission dispatch considering load uncertainty," in *2017 20th International Conference on Electrical Machines and Systems (ICEMS)*, 2017, pp. 1-6: IEEE.
[75] M. H. Abbasi *et al.*, "Risk-constrained offering strategies for a price-maker demand response aggregator," in *2017 20th international conference on electrical machines and systems (ICEMS)*, 2017, pp. 1-6: IEEE.
[76] S. Ghavidel, M. Barani, A. Azizivahed, M. J. Ghadi, L. Li, and J. Zhang, "Hybrid power plant offering strategy to deal with the stochastic nature and outage of wind generators," in *2017 20th International Conference on Electrical Machines and Systems (ICEMS)*, 2017, pp. 1-6: IEEE.
[77] S. Ghavidel *et al.*, "Hybrid power plant bidding strategy including a commercial compressed air energy storage aggregator and a wind power producer," in *2017 Australasian Universities Power Engineering Conference (AUPEC)*, 2017, pp. 1-6: IEEE.
[78] S. Ghavidel, A. Rajabi, M. Jabbari Ghadi, A. Azizivahed, L. Li, and J. Zhang, "Hybrid power plant bidding strategy for voltage stability improvement, electricity market profit maximization, and congestion management," *IET Energy Systems Integration,* vol. 3, no. 2, pp. 130-141, 2021.
[79] S. Sekizaki, I. Nishizaki, and T. Hayashida, "Electricity retail market model with flexible price settings and elastic price-based demand responses by consumers in distribution network," *International Journal of Electrical Power & Energy Systems,* vol. 81, pp. 371-386, 2016.
[80] H. H. Abdeltawab and Y. A.-R. I. Mohamed, "Mobile Energy Storage Scheduling and Operation in Active Distribution Systems," *IEEE Transactions on Industrial Electronics,* 2017.
[81] A. Zakariazadeh, S. Jadid, and P. Siano, "Multi-objective scheduling of electric vehicles in smart distribution system," *Energy Conversion and Management,* vol. 79, pp. 43-53, 2014.
[82] Y. Xiang, J. Liu, and Y. Liu, "Optimal active distribution system management considering aggregated plug-in electric vehicles," *Electric Power Systems Research,* vol. 131, pp. 105-115, 2016.
[83] A. Rajabi, M. Eskandari, M. J. Ghadi, L. Li, J. Zhang, and P. Siano, "A comparative study of clustering techniques for electrical load pattern segmentation," *Renewable and Sustainable Energy Reviews,* vol. 120, p. 109628, 2020.
[84] A. Azizivahed, S. Ghavidel, M. J. Ghadi, L. Li, and J. Zhang, "Multi-Objective Energy Management Approach Considering Energy Storages in Distribution Networks with Respect to Voltage Security," in *2019 IEEE International Conference on Industrial Technology (ICIT)*, 2019, pp. 661-666: IEEE.
[85] M. Nasouri Gilvaei, M. Hosseini Imani, M. J. Ghadi, L. Li, and A. Golrang, "Profit-Based Unit Commitment for a GENCO Equipped with Compressed Air Energy Storage and Concentrating Solar Power Units," *Energies,* vol. 14, no. 3, p. 576, 2021.

[86] M. Farrokhifar, "Optimal operation of energy storage devices with RESs to improve efficiency of distribution grids; technical and economical assessment," *International Journal of Electrical Power & Energy Systems,* vol. 74, pp. 153-161, 2016.
[87] M. Koller, T. Borsche, A. Ulbig, and G. Andersson, "Review of grid applications with the Zurich 1MW battery energy storage system," *Electric Power Systems Research,* vol. 120, pp. 128-135, 2015.
[88] E. Reihani, S. Sepasi, L. R. Roose, and M. Matsuura, "Energy management at the distribution grid using a Battery Energy Storage System (BESS)," *International Journal of Electrical Power & Energy Systems,* vol. 77, pp. 337-344, 2016.
[89] H. Saboori and H. Abdi, "Application of a grid scale energy storage system to reduce distribution network losses," in *Electrical Power Distribution Networks (EPDC), 2013 18th Conference on*, 2013, pp. 1-5: IEEE.
[90] A. Azizivahed *et al.*, "Risk-Oriented Multi-Area Economic Dispatch Solution with High Penetration of Wind Power Generation and Compressed Air Energy Storage System," *IEEE Transactions on Sustainable Energy,* 2019.
[91] G. Venkataramani, P. Parankusam, V. Ramalingam, and J. Wang, "A review on compressed air energy storage–A pathway for smart grid and polygeneration," *Renewable and Sustainable energy reviews,* vol. 62, pp. 895-907, 2016.
[92] M. J. Ghadi *et al.*, "Application of Small-Scale Compressed Air Energy Storage in the Daily Operation of an Active Distribution System," *Energy,* p. 120961, 2021.
[93] S. G. Jirsaraie, M. J. Ghadi, A. A. Vahed, J. Aghaei, L. Li, and J. Zhang, "Risk-Constrained Bidding Strategy for a Joint Operation of Wind Power and Compressed Air Energy Storage Aggregators," *IEEE Transactions on Sustainable Energy,* 2019.
[94] S. Shafiee, H. Zareipour, A. M. Knight, N. Amjady, and B. Mohammadi-Ivatloo, "Risk-constrained bidding and offering strategy for a merchant compressed air energy storage plant," *IEEE Transactions on Power Systems,* vol. 32, no. 2, pp. 946-957, 2016.
[95] A. Attarha, N. Amjady, S. Dehghan, and B. Vatani, "Adaptive robust self-scheduling for a wind producer with compressed air energy storage," *IEEE Transactions on Sustainable Energy,* vol. 9, no. 4, pp. 1659-1671, 2018.
[96] S. Shafiee, H. Zareipour, and A. Knight, "Considering thermodynamic characteristics of a CAES facility in self-scheduling in energy and reserve markets," *IEEE Transactions on Smart Grid,* 2016.
[97] H. S. de Boer, L. Grond, H. Moll, and R. Benders, "The application of power-to-gas, pumped hydro storage and compressed air energy storage in an electricity system at different wind power penetration levels," *Energy,* vol. 72, pp. 360-370, 2014.
[98] P. Denholm and R. Sioshansi, "The value of compressed air energy storage with wind in transmission-constrained electric power systems," *Energy Policy,* vol. 37, no. 8, pp. 3149-3158, 2009.
[99] S. Shafiee, H. Zareipour, A. M. Knight, N. Amjady, and B. Mohammadi-Ivatloo, "Risk-constrained bidding and offering strategy for a merchant compressed air energy storage plant," *IEEE Transactions on Power Systems,* vol. 32, no. 2, pp. 946-957, 2017.
[100] X. Wang, C. Yang, M. Huang, and X. Ma, "Multi-objective optimization of a gas turbine-based CCHP combined with solar and compressed air energy storage system,"

Energy conversion and management, vol. 164, pp. 93-101, 2018.
[101] B. Cleary, A. Duffy, A. OConnor, M. Conlon, and V. Fthenakis, "Assessing the economic benefits of compressed air energy storage for mitigating wind curtailment," *IEEE Transactions on Sustainable Energy,* vol. 6, no. 3, pp. 1021-1028, 2015.
[102] H. Lund, G. Salgi, B. Elmegaard, and A. N. Andersen, "Optimal operation strategies of compressed air energy storage (CAES) on electricity spot markets with fluctuating prices," *Applied thermal engineering,* vol. 29, no. 5-6, pp. 799-806, 2009.
[103] M. Jadidbonab *et al.*, "Risk-constrained energy management of PV integrated smart energy hub in the presence of DR and compressed air energy storage," *IET Renewable Power Generation,* vol. 13, no. 6, 2019.
[104] Z. Guo *et al.*, "Operation of Distribution Network Considering Compressed Air Energy Storage Unit and Its Reactive Power Support Capability," *IEEE Transactions on Smart Grid,* vol. 11, no. 4, 2020.
[105] J. Cheng *et al.*, "Dispatchable Generation of a Novel Compressed-Air Assisted Wind Turbine and Its Operation Mechanism," *IEEE Transactions on Sustainable Energy,* vol. 10, no. 4, pp. 2201-2210, 2018.
[106] J. Zhang *et al.*, "A bi-level program for the planning of an islanded microgrid including CAES," *IEEE Transactions on Industry Applications,* vol. 52, no. 4, pp. 2768-2777, 2016.
[107] M. H. Imani, K. Yousefpour, M. J. Ghadi, and M. T. Andani, "Simultaneous presence of wind farm and V2G in security constrained unit commitment problem considering uncertainty of wind generation," in *Texas Power and Energy Conference (TPEC), 2018 IEEE*, 2018, pp. 1-6: IEEE.
[108] G. Bharati and S. Paudyal, "Coordinated control of distribution grid and electric vehicle loads," *Electric Power Systems Research,* vol. 140, pp. 761-768, 2016.
[109] S. Faddel, A. A. Mohamed, and O. A. Mohammed, "Fuzzy logic-based autonomous controller for electric vehicles charging under different conditions in residential distribution systems," *Electric Power Systems Research,* vol. 148, pp. 48-58, 2017.
[110] N. O'Connell, Q. Wu, J. Østergaard, A. H. Nielsen, S. T. Cha, and Y. Ding, "Day-ahead tariffs for the alleviation of distribution grid congestion from electric vehicles," *Electric Power Systems Research,* vol. 92, pp. 106-114, 2012.
[111] I. G. Unda, P. Papadopoulos, S. Skarvelis-Kazakos, L. M. Cipcigan, N. Jenkins, and E. Zabala, "Management of electric vehicle battery charging in distribution networks with multi-agent systems," *Electric Power Systems Research,* vol. 110, pp. 172-179, 2014.
[112] V. T. Bina and D. Ahmadi, "Stochastic modeling for scheduling the charging demand of EV in distribution systems using copulas," *International Journal of Electrical Power & Energy Systems,* vol. 71, pp. 15-25, 2015.
[113] A. Azizivahed, S. Ghavidel, M. J. Ghadi, L. Li, and J. Zhang, "A novel reliability oriented bi-objective unit commitment problem," in *2017 Australasian Universities Power Engineering Conference (AUPEC)*, 2017, pp. 1-6: IEEE.
[114] J. Zhang, H. Cheng, and C. Wang, "Technical and economic impacts of active management on distribution network," *International Journal of Electrical Power & Energy Systems,* vol. 31, no. 2-3, pp. 130-138, 2009.
[115] F. Zhao, J. Si, and J. Wang, "Research on optimal schedule strategy for active

distribution network using particle swarm optimization combined with bacterial foraging algorithm," *International Journal of Electrical Power & Energy Systems,* vol. 78, pp. 637-646, 2016.
[116] M. Degefa, M. Lehtonen, R. Millar, A. Alahäivälä, and E. Saarijärvi, "Optimal voltage control strategies for day-ahead active distribution network operation," *Electric Power Systems Research,* vol. 127, pp. 41-52, 2015.
[117] M. A. Ghasemi and M. Parniani, "Prevention of distribution network overvoltage by adaptive droop-based active and reactive power control of PV systems," *Electric Power Systems Research,* vol. 133, pp. 313-327, 2016.
[118] M. Bahramipanah, R. Cherkaoui, and M. Paolone, "Decentralized voltage control of clustered active distribution network by means of energy storage systems," *Electric Power Systems Research,* vol. 136, pp. 370-382, 2016.
[119] S. Abapour, E. Babaei, and B. Y. Khanghah, "Application of active management on distribution network with considering technical issues," in *Smart Grids (ICSG), 2012 2nd Iranian Conference on*, 2012, pp. 1-6: IEEE.
[120] X. Dai, "Study on Reactive Power Optimization of Active Distribution Network Based on Bifurcation Theory," 2015.
[121] M. N. Gilvaei, H. Jafari, M. J. Ghadi, and L. Li, "A novel hybrid optimization approach for reactive power dispatch problem considering voltage stability index," *Engineering Applications of Artificial Intelligence,* vol. 96, p. 103963, 2020.
[122] Y. Feng, Y. Li, Y. Cao, and Y. Zhou, "Automatic voltage control based on adaptive zone-division for active distribution system," in *Power and Energy Engineering Conference (APPEEC), 2016 IEEE PES Asia-Pacific*, 2016, pp. 278-282: IEEE.
[123] T. Zhao, J. Zhang, and P. Wang, "Flexible active distribution system management considering interaction with transmission networks using information-gap decision theory," *CSEE Journal of Power and Energy Systems,* vol. 2, no. 4, pp. 76-86, 2016.
[124] L. Mokgonyana, J. Zhang, L. Zhang, and X. Xia, "Coordinated two-stage volt/var management in distribution networks," *Electric Power Systems Research,* vol. 141, pp. 157-164, 2016.
[125] M. McGranaghan and F. Goodman, "Technical and system requirements for advanced distribution automation," in *18th International Conference and Exhibition on Electricity Distribution*, 2005, vol. 5, p. 93: IET.
[126] F. Capitanescu, I. Bilibin, and E. R. Ramos, "A comprehensive centralized approach for voltage constraints management in active distribution grid," *IEEE Transactions on Power Systems,* vol. 29, no. 2, pp. 933-942, 2014.
[127] W. Zheng, W. Wu, B. Zhang, H. Sun, and Y. Liu, "A fully distributed reactive power optimization and control method for active distribution networks," *IEEE Transactions on Smart Grid,* vol. 7, no. 2, pp. 1021-1033, 2016.
[128] Y. Wang, W. Wu, B. Zhang, Z. Li, and W. Zheng, "Robust voltage control model for active distribution network considering PVs and loads uncertainties," in *Power & Energy Society General Meeting, 2015 IEEE*, 2015, pp. 1-5: IEEE.
[129] Q. Zhu, J. Zhang, P. W. Sauer, A. Domínguez-García, and T. Başar, "A game-theoretic framework for control of distributed renewable-based energy resources in smart grids," in *American Control Conference (ACC), 2012*, 2012, pp. 3623-3628: IEEE.

[130] M. J. Ghadi, S. H. Gilani, H. Afrakhte, and A. Baghramian, "A novel heuristic method for wind farm power prediction: A case study," *International Journal of Electrical Power & Energy Systems,* vol. 63, pp. 962-970, 2014.
[131] M. Bakhshipour, M. J. Ghadi, and F. Namdari, "Swarm robotics search & rescue: A novel artificial intelligence-inspired optimization approach," *Applied Soft Computing,* vol. 57, pp. 708-726, 2017.
[132] M. J. Ghadi, S. H. Gilani, A. Sharifiyan, and H. Afrakhteh, "A new method for short-term wind power forecasting," in *Electrical Power Distribution Networks (EPDC), 2012 Proceedings of 17th Conference on*, 2012, pp. 1-6: IEEE.
[133] A. Rajabi, L. Li, J. Zhang, J. Zhu, S. Ghavidel, and M. J. Ghadi, "A review on clustering of residential electricity customers and its applications," in *Electrical Machines and Systems (ICEMS), 2017 20th International Conference on*, 2017, pp. 1-6: IEEE.
[134] M. Hosseini Imani, M. Jabbari Ghadi, S. Shamshirband, and M. M. Balas, "Impact Evaluation of Electric Vehicle Parking on Solving Security-Constrained Unit Commitment Problem," *Mathematical and Computational Applications,* vol. 23, no. 1, p. 13, 2018.
[135] M. H. Imani, M. J. Ghadi, S. Ghavidel, and L. Li, "Demand Response Modeling in Microgrid Operation: a Review and Application for Incentive-Based and Time-Based Programs," *Renewable and Sustainable Energy Reviews,* vol. 94, pp. 486-499, 2018.
[136] A. Sharifian, S. F. Sasansara, M. J. Ghadi, S. Ghavidel, L. Li, and J. Zhang, "Dynamic performance improvement of an ultra-lift Luo DC–DC converter by using a type-2 fuzzy neural controller," *Computers & Electrical Engineering,* vol. 69, pp. 171-182, 2018.
[137] H. Li *et al.*, "Reliability evaluation of active distribution systems considering energy storage and real-time electricity pricing," in *Probabilistic Methods Applied to Power Systems (PMAPS), 2016 International Conference on*, 2016, pp. 1-5: IEEE.
[138] A. González, J. A. Saavedra, J. Tello-Guijarro, D. Trebolle, and M. Casas, "PRICE-GDI: A pilot experience for the integration of Distributed Generation in active distribution systems," in *Smart Electric Distribution Systems and Technologies (EDST), 2015 International Symposium on*, 2015, pp. 183-188: IEEE.
[139] S. A. Arefifar, M. Ordonez, and Y. Mohamed, "Voltage and current controllability in multi-microgrid smart distribution systems," *IEEE Transactions on Smart Grid,* 2016.
[140] S. Ge, L. Xu, H. Liu, and M. Zhao, "Reliability assessment of active distribution system using Monte Carlo simulation method," *Journal of Applied Mathematics,* vol. 2014, 2014.
[141] X. Zheng, B. Zeng, G. Wu, J. Zhang, M. Zeng, and J. Shi, "Capacity credit assessment of renewable distributed generation in active distribution systems considering demand response impact," in *Electric Utility Deregulation and Restructuring and Power Technologies (DRPT), 2015 5th International Conference on*, 2015, pp. 108-113: IEEE.
[142] G. Petretto *et al.*, "Representative distribution network models for assessing the role of active distribution systems in bulk ancillary services markets," in *Power Systems Computation Conference (PSCC), 2016*, 2016, pp. 1-7: IEEE.
[143] L. Hu, K.-Y. Liu, Y. Diao, X. Meng, and W. Sheng, "Operational Reliability

Evaluation Method Based on Big Data Technology," in *Cyber-Enabled Distributed Computing and Knowledge Discovery (CyberC), 2016 International Conference on*, 2016, pp. 341-344: IEEE.

[144] Y. Ju, W. Wu, B. Zhang, and H. Sun, "An extension of FBS three-phase power flow for handling PV nodes in active distribution networks," *IEEE Transactions on Smart Grid,* vol. 5, no. 4, pp. 1547-1555, 2014.

[145] E. Grover-Silva, R. Girard, and G. Kariniotakis, "Multi-temporal optimal power flow for assessing the renewable generation hosting capacity of an active distribution system," in *Transmission and Distribution Conference and Exposition (T&D), 2016 IEEE/PES*, 2016, pp. 1-5: IEEE.

[146] S. Syafii and K. Nor, "Unbalanced Active Distribution Analysis with Renewable Distributed Energy Resources," *TELKOMNIKA (Telecommunication Computing Electronics and Control),* vol. 13, no. 1, pp. 21-31, 2015.

[147] S. Bolognani and S. Zampieri, "On the existence and linear approximation of the power flow solution in power distribution networks," *IEEE Transactions on Power Systems,* vol. 31, no. 1, pp. 163-172, 2016.

[148] J. Olamaei, M. A. Ghasemabadi, and M. H. Kapourchali, "An efficient method for load flow analysis of distribution networks including PV nodes," in *Electric Power and Energy Conversion Systems (EPECS), 2011 2nd International Conference on*, 2011, pp. 1-6: IEEE.

[149] M. J. Ghadi, A. Baghramian, and M. H. Imani, "An ICA based approach for solving profit based unit commitment problem market," *Applied Soft Computing,* vol. 38, pp. 487-500, 2016.

[150] H. Gao, J. Liu, L. Wang, and Y. Liu, "Cutting planes based relaxed optimal power flow in active distribution systems," *Electric Power Systems Research,* vol. 143, pp. 272-280, 2017.

[151] S. Ghavidel, M. J. Ghadi, A. Azizivahed, J. Aghaei, L. Li, and J. Zhang, "Risk-constrained bidding strategy for a joint operation of wind power and CAES aggregators," *IEEE Transactions on Sustainable Energy,* vol. 11, no. 1, pp. 457-466, 2019.

[152] E. Barbour, D. Mignard, Y. Ding, and Y. Li, "Adiabatic compressed air energy storage with packed bed thermal energy storage," *Applied energy,* vol. 155, pp. 804-815, 2015.

[153] M. J. Tessier, M. C. Floros, L. Bouzidi, and S. S. Narine, "Exergy analysis of an adiabatic compressed air energy storage system using a cascade of phase change materials," *Energy,* vol. 106, pp. 528-534, 2016.

[154] S. Mei *et al.*, "Paving the way to smart micro energy grid: concepts, design principles, and engineering practices," *CSEE Journal of Power and Energy Systems,* vol. 3, no. 4, pp. 440-449, 2017.

[155] S. Ghavidel, A. Rajabi, M. J. Ghadi, A. Azizivahed, L. Li, and J. Zhang, "Risk-constrained demand response and wind energy systems integration to handle stochastic nature and wind power outage," *IET Energy Systems Integration,* vol. 1, no. 2, pp. 114-120, 2019.

[156] A. Rajabi *et al.*, "A pattern recognition methodology for analyzing residential customers load data and targeting demand response applications," *Energy and*

Buildings, vol. 203, p. 109455, 2019.
[157] J. Cheng, R. Li, F. Choobineh, Q. Hu, and S. Mei, "Dispatchable Generation of a Novel Compressed-Air Assisted Wind Turbine and its Operation Mechanism," *IEEE Transactions on Sustainable Energy,* 2018.
[158] S. H. Gilani, H. Afrakhte, and M. J. Ghadi, "Probabilistic method for optimal placement of wind-based distributed generation with considering reliability improvement and power loss reduction," in *The 4th Conference on Thermal Power Plants*, 2012, pp. 1-6: IEEE.
[159] A. H. Alami, "Experimental assessment of compressed air energy storage (CAES) system and buoyancy work energy storage (BWES) as cellular wind energy storage options," *Journal of Energy Storage,* vol. 1, pp. 38-43, 2015.
[160] G. Venkataramani and V. Ramalingam, "Performance analysis of a small capacity compressed air energy storage system for renewable energy generation using TRNSYS," *Journal of Renewable and Sustainable Energy,* vol. 9, no. 4, p. 044106, 2017.
[161] S. Wang, X. Zhang, L. Yang, Y. Zhou, and J. Wang, "Experimental study of compressed air energy storage system with thermal energy storage," *Energy,* vol. 103, pp. 182-191, 2016.
[162] J. Cheng and F. Choobineh, "Microgrid expansion through a compressed air assisted wind energy system," in *2016 IEEE Power & Energy Society Innovative Smart Grid Technologies Conference (ISGT)*, 2016, pp. 1-5: IEEE.
[163] C. Fang, L. Chen, Y. Zhang, C. Wang, and S. Mei, "Operation of low-carbon-emission microgrid considering wind power generation and compressed air energy storage," in *Proceedings of the 33rd Chinese Control Conference*, 2014, pp. 7472-7477: IEEE.
[164] A. Gheiratmand, E. Ayoubi, and M. Sarlak, "Optimal operation of micro-grid in presence of renewable resources and compressed air energy storage," in *2017 Conference on Electrical Power Distribution Networks Conference (EPDC)*, 2017, pp. 131-136: IEEE.
[165] R. Latha, S. Palanivel, and J. Kanakaraj, "Frequency control of microgrid based on compressed air energy storage system," *Distributed Generation & Alternative Energy Journal,* vol. 27, no. 4, pp. 8-19, 2012.
[166] H. Ibrahim, K. Belmokhtar, and M. Ghandour, "Investigation of usage of compressed air energy storage for power generation system improving-application in a microgrid integrating wind energy," *Energy Procedia,* vol. 73, pp. 305-316, 2015.
[167] H. Ibrahim, A. Bourji, M. Ghandour, and A. Merabet, "Optimization of compressed air storage's volume for a stand-alone wind-diesel hybrid system," in *2013 IEEE Electrical Power & Energy Conference*, 2013, pp. 1-7: IEEE.
[168] J. Cheng and F. Choobineh, "Microgrid expansion through a compressed air assisted wind energy system," in *Innovative Smart Grid Technologies Conference (ISGT), 2016 IEEE Power & Energy Society*, 2016, pp. 1-5: IEEE.
[169] M. Diekerhof, S. Hecker, and A. Monti, "Modeling and optimization of industrial compressed-air energy systems for Demand Response," in *Energy Conference (ENERGYCON), 2016 IEEE International*, 2016, pp. 1-6: IEEE.
[170] E. Jannelli, M. Minutillo, A. L. Lavadera, and G. Falcucci, "A small-scale CAES (compressed air energy storage) system for stand-alone renewable energy power plant

for a radio base station: A sizing-design methodology," *Energy,* vol. 78, pp. 313-322, 2014.
[171] A. Setiawan, A. Priyadi, M. Pujiantara, and M. Purnomo, "Sizing compressed-air energy storage tanks for solar home systems," in *Computational Intelligence and Virtual Environments for Measurement Systems and Applications (CIVEMSA), 2015 IEEE International Conference on*, 2015, pp. 1-4: IEEE.
[172] L. Rui, C. Laijun, Y. Tiejiang, and L. Chunlai, "Optimal dispatch of zero-carbon-emission micro Energy Internet integrated with non-supplementary fired compressed air energy storage system," *Journal of Modern Power Systems and Clean Energy,* vol. 4, no. 4, pp. 566-580, 2016.
[173] S. Habib, M. Kamran, and U. Rashid, "Impact analysis of vehicle-to-grid technology and charging strategies of electric vehicles on distribution networks–a review," *Journal of Power Sources,* vol. 277, pp. 205-214, 2015.
[174] Z. Min, C. Qiuyu, X. Jiajia, Y. Weiwei, and N. Shu, "Study on influence of large-scale electric vehicle charging and discharging load on distribution system," in *2016 China International Conference on Electricity Distribution (CICED)*, 2016, pp. 1-4: IEEE.
[175] W. Su and K. Zhang, "Investigating the impact of plug-in electric vehicle charging on power distribution systems with the integrated modeling and simulation of transportation network," in *2014 IEEE transportation electrification conference and expo (Asia-Pacific), Beijing, China*, 2014, vol. 31.
[176] F. Jozi, K. Mazlumi, and H. Hosseini, "Charging and discharging coordination of electric vehicles in a parking lot considering the limitation of power exchange with the distribution system," in *2017 IEEE 4th International Conference on Knowledge-Based Engineering and Innovation (KBEI)*, 2017, pp. 0937-0941: IEEE.
[177] J. Hu, S. You, M. Lind, and J. Østergaard, "Coordinated charging of electric vehicles for congestion prevention in the distribution grid," *IEEE Transactions on Smart Grid,* vol. 5, no. 2, pp. 703-711, 2013.
[178] M. R. Sarker, H. Pandžić, and M. A. Ortega-Vazquez, "Optimal operation and services scheduling for an electric vehicle battery swapping station," *IEEE transactions on power systems,* vol. 30, no. 2, pp. 901-910, 2014.
[179] Y. Song, Y. Zheng, and D. J. Hill, "Optimal scheduling for ev charging stations in distribution networks: A convexified model," *IEEE Transactions on Power Systems,* vol. 32, no. 2, pp. 1574-1575, 2016.
[180] Z. Moghaddam, I. Ahmad, D. Habibi, and Q. V. Phung, "Smart charging strategy for electric vehicle charging stations," *IEEE Transactions on Transportation Electrification,* vol. 4, no. 1, pp. 76-88, 2017.
[181] Y. Zhang, P. You, and L. Cai, "Optimal charging scheduling by pricing for ev charging station with dual charging modes," *IEEE Transactions on Intelligent Transportation Systems,* 2018.
[182] M. Hosseini Imani, M. Jabbari Ghadi, S. Shamshirband, and M. Balas, "Impact evaluation of electric vehicle parking on solving security-constrained unit commitment problem," *Mathematical and Computational Applications,* vol. 23, no. 1, p. 13, 2018.
[183] J. I. Pérez-Díaz, M. Chazarra, J. García-González, G. Cavazzini, and A. Stoppato, "Trends and challenges in the operation of pumped-storage hydropower plants,"

Renewable and Sustainable Energy Reviews, vol. 44, pp. 767-784, 2015.
[184] A. Poullikkas, "A comparative overview of large-scale battery systems for electricity storage," *Renewable and Sustainable energy reviews,* vol. 27, pp. 778-788, 2013.
[185] B. Liu, Q. Lin, T. Zheng, L. Chen, and S. Mei, "Low carbon economic dispatch for multi-energy distribution network with compressed air energy storage system as energy hub," in *2017 36th Chinese Control Conference (CCC)*, 2017, pp. 3083-3088: IEEE.
[186] M. Moazzami, M. Ghanbari, H. Shahinzadeh, J. Moradi, and G. B. Gharehpetian, "Application of multi-objective grey wolf algorithm on energy management of microgrids with techno-economic and environmental considerations," in *2018 3rd Conference on Swarm Intelligence and Evolutionary Computation (CSIEC)*, 2018, pp. 1-9: IEEE.
[187] H. H. Abdeltawab and Y. A.-R. I. Mohamed, "Mobile energy storage scheduling and operation in active distribution systems," *IEEE Transactions on Industrial Electronics,* vol. 64, no. 9, 2017.
[188] H. Abdeltawab and Y. A.-R. I. Mohamed, "Mobile Energy Storage Sizing and Allocation for Multi-Services in Power Distribution Systems," *IEEE Access,* vol. 7, pp. 176613-176623, 2019.
[189] A. Srivastava *et al.*, "Minimizing Cost of Smart Grid Operations by Scheduling Mobile Energy Storage Systems," *IEEE Letters of the Computer Society,* vol. 2, no. 3, 2019.
[190] Y. Song *et al.*, "Multi-objective configuration optimization for isolated microgrid with mobile energy storage and shiftable load," in *2018 IEEE Conference on Energy System Integration* 2018, pp. 1-7: IEEE.
[191] S. Yao, P. Wang, and T. Zhao, "Transportable energy storage for more resilient distribution systems with multiple microgrids," *IEEE Transactions on Smart Grid,* vol. 10, no. 3, pp. 3331-3341, 2018.
[192] J. Kim and Y. Dvorkin, "Enhancing distribution system resilience with mobile energy storage and microgrids," *IEEE Transactions on Smart Grid,* vol. 10, no. 5, pp. 4996-5006, 2018.
[193] D. K. Mishra, M. J. Ghadi, L. Li, and J. Zhang, "Proposing a Framework for Resilient Active Distribution Systems using Withstand, Respond, Adapt, and Prevent Element," in *2019 29th Australasian Universities Power Engineering Conference (AUPEC)*, 2019, pp. 1-6: IEEE.
[194] D. K. Mishra, M. J. Ghadi, A. Azizivahed, L. Li, and J. Zhang, "A review on resilience studies in active distribution systems," *Renewable and Sustainable Energy Reviews,* vol. 135, p. 110201, 2021.
[195] Y. Chen, Y. Zheng, F. Luo, J. Wen, and Z. Xu, "Reliability evaluation of distribution systems with mobile energy storage systems," *IET Renewable Power Generation,* vol. 10, no. 10, pp. 1562-1569, 2016.
[196] S. Yao *et al.*, "Two-stage stochastic scheduling of transportable energy storage systems for resilient distribution systems," in *2018 IEEE International Conference on PMAPS*, 2018, pp. 1-6: IEEE.
[197] P. Prabawa and D.-H. Choi, "Multi-Agent Framework for Service Restoration in Distribution Systems With Distributed Generators and Static/Mobile Energy Storage

Systems," *IEEE Access,* vol. 8, 2020.
[198] H. Saboori and S. Jadid, "Optimal scheduling of mobile utility-scale battery energy storage systems in electric power distribution networks," *Journal of Energy Storage,* vol. 31, p. 101615, 2020.
[199] S.-Y. Kwon *et al.*, "Optimal V2G and Route Scheduling of Mobile Energy Storage Devices Using a Linear Transit Model " *IEEE Transactions on Industry Applications,* vol. 56, no. 1, pp. 34-47, 2019.
[200] J. P. Coutier and E. Farber, "Two applications of a numerical approach of heat transfer process within rock beds," *Solar Energy,* vol. 29, no. 6, pp. 451-462, 1982.
[201] S. Ergun, "Fluid flow through packed columns," *Chem. Eng. Prog.,* vol. 48, pp. 89-94, 1952.
[202] M.-A. Rostami, A. Kavousi-Fard, and T. Niknam, "Expected cost minimization of smart grids with plug-in hybrid electric vehicles using optimal distribution feeder reconfiguration," *IEEE Transactions on Industrial Informatics,* vol. 11, no. 2, pp. 388-397, 2015.
[203] J.-H. Teng, "A direct approach for distribution system load flow solutions," *IEEE Transactions on power delivery,* vol. 18, no. 3, pp. 882-887, 2003.
[204] L. P. Fernandez, T. G. San Román, R. Cossent, C. M. Domingo, and P. Frias, "Assessment of the impact of plug-in electric vehicles on distribution networks," *network,* vol. 16, p. 21, 2011.
[205] M. J. Ghadi and A. Baghramian, "A new heuristic method for solving unit commitment problem in competitive environment," *International Journal of Soft Computing and Engineering,* vol. 2, no. 6, pp. 2231-2307, 2013.
[206] M. J. Ghadi, A. I. Karin, A. Baghramian, and M. H. Imani, "Optimal power scheduling of thermal units considering emission constraint for GENCOs' profit maximization," *International Journal of Electrical Power & Energy Systems,* vol. 82, pp. 124-135, 2016.
[207] K. Miettinen, M. M. Mäkelä, and J. Toivanen, "Numerical comparison of some penalty-based constraint handling techniques in genetic algorithms," *Journal of Global Optimization,* vol. 27, no. 4, pp. 427-446, 2003.
[208] M. Kashem, V. Ganapathy, G. Jasmon, and M. Buhari, "A novel method for loss minimization in distribution networks," in *DRPT2000. International Conference on Electric Utility Deregulation and Restructuring and Power Technologies. Proceedings (Cat. No. 00EX382)*, 2000, pp. 251-256: IEEE.
[209] S. Rezaee, E. Farjah, and B. Khorramdel, "Probabilistic analysis of plug-in electric vehicles impact on electrical grid through homes and parking lots," *IEEE Transactions on Sustainable Energy,* vol. 4, no. 4, pp. 1024-1033, 2013.
[210] Y. Wang, "Renewable electricity in Sweden: an analysis of policy and regulations," *Energy policy,* vol. 34, no. 10, pp. 1209-1220, 2006.
[211] A. Askarzadeh, "Distribution generation by photovoltaic and diesel generator systems: Energy management and size optimization by a new approach for a stand-alone application," *Energy,* vol. 122, pp. 542-551, 2017.
[212] A. Azizivahed, S. Ghavidel, M. J. Ghadi, L. Li, and J. Zhang, "New energy management approach in distribution systems considering energy storages," in *2017 20th International Conference on Electrical Machines and Systems (ICEMS)*, 2017,

pp. 1-6: IEEE.
[213] H. Ghoreishi, H. Afrakhte, and M. J. ghadi, "Optimal placement of tie points and sectionalizers in radial distribution network in presence of DGs considering load significance," in *2013 Smart Grid Conference (SGC)*, 2013, pp. 160-165.
[214] E. A. Farsani, H. A. Abyaneh, M. Abedi, and S. Hosseinian, "A novel policy for LMP calculation in distribution networks based on loss and emission reduction allocation using nucleolus theory," *IEEE Transactions on Power Systems,* vol. 31, no. 1, pp. 143-152, 2015.
[215] H. H. Abdeltawab and Y. A.-R. I. Mohamed, "Mobile energy storage scheduling and operation in active distribution systems," *IEEE Transactions on Industrial Electronics,* vol. 64, no. 9, pp. 6828-6840, 2017.
[216] A. Azizivahed, H. Narimani, E. Naderi, M. Fathi, and M. R. Narimani, "A hybrid evolutionary algorithm for secure multi-objective distribution feeder reconfiguration," *Energy,* vol. 138, pp. 355-373, 2017.
[217] "Market Data National Energy Market (NEM) Web," ed, 2020.